Dissertation zur Erlangung des Doktorgrades
der Fakultät für Chemie und Pharmazie
der Ludwig-Maximilians-Universität München

Characterization of new chemosensitizing agents: spongistatin 1 and T8

Lilianna Schyschka

aus Pyskowice

2009

Erklärung

Diese Dissertation wurde im Sinne von § 13 Abs. 3 bzw. 4 der Promotionsordnung vom 29. Januar 1998 von Frau Prof. Dr. A. M. Vollmar betreut.

Ehrenwörtliche Versicherung

Diese Dissertation wurde selbständig, ohne unerlaubte Hilfe erarbeitet.

München, am 19.01.2009

Lilianna Schyschka

Dissertation eingereicht am: 19.01.2009

1. Gutachter: Frau Prof. Dr. A. M. Vollmar

2. Gutachter: Herr Prof. Dr. F. Böckler

Mündliche Prüfung am: 13.02.2009

Table of contents

I   Introduction

1   Background

Cancer, together with cardiovascular and infectious diseases, belongs to the three leading causes of death in the world [1]. Thus, anti-cancer strategies are of high scientific interest. The idea of treating cancer with drugs is about 500 years old, when first mixtures of zinc, silver and mercury were used. Certainly, the first documented treatment of cancer with chemotherapeutics refers to the German doctor Lissauer, who had treated leukemia patients in 1865 with potassium arsenite [2]. Although better understanding of cancer pathophysiology and the development of new agents caused therapeutic progress in cancer treatment, resistence to established agents has been described. Thus, new drugs and the development of more effective strategies to treat cancer and to overcome chemoresistance are still urgently required.

Natural products play a pivotal role as a source of new drugs. After analyzing the available anticancer drugs of the last 25 years it is obvious that the majority of the new approved drugs are natural or natural-related compounds (see Figure I.1) [3]. Such natural products as the vinca alkaloids vinblastine and vincristine, isolated from the Madagascar periwinkle (*Catharanthus roseus*), or paclitaxel originally isolated from the bark of the pacific yew tree, *Taxus brevifolia*, significantly contribute to the successful treatment of many cancers.

The screening program of the U. S. National Cancer Institute (NCI) identified many compounds from natural sources that show anti-cancer activity. Currently, the screen consists of 60 different tumor cell lines which are treated with compounds to assess selective growth inhibition or cell killing. This screen is unique in its complexity since the effectiveness of a compound on a large number of different cancer types (e.g. leukemia, breast cancer, lung cancer, melanoma, ovary cancer) can be tested which leads to characteristic profile generation. NCI-founded groups collected e.g. marine organisms, mostly invertebrates, isolated new compounds out of them and subsequently tested the substances in the *in vitro* screening program [4]. This search led to the discovery of such active compounds as dolastatin, halichondrine B or bryostatin 1, which are now evaluated in clinical trials.

The large number of natural products and the huge amount of information about their structural and biological activities makes it difficult to handle with this data. On the other hand the progress in understanding the fundamental principles of protein-ligand interactions and targets in the anti-cancer therapy provides new possibilities for rationalized drug discovery. The computational approaches, like virtual screening experiments, have already successfully been applied to find new target-specific drugs [5, 6]. The common idea of these approaches, the *in silico* selection of a limited number of potential agents which are proposed

to have biological activity, results in time- and cost- reduction in the discovery of new drug. Thus, applying computational approaches within the early drug discovery process can have great benefits for the search of new active anti-cancer drugs.
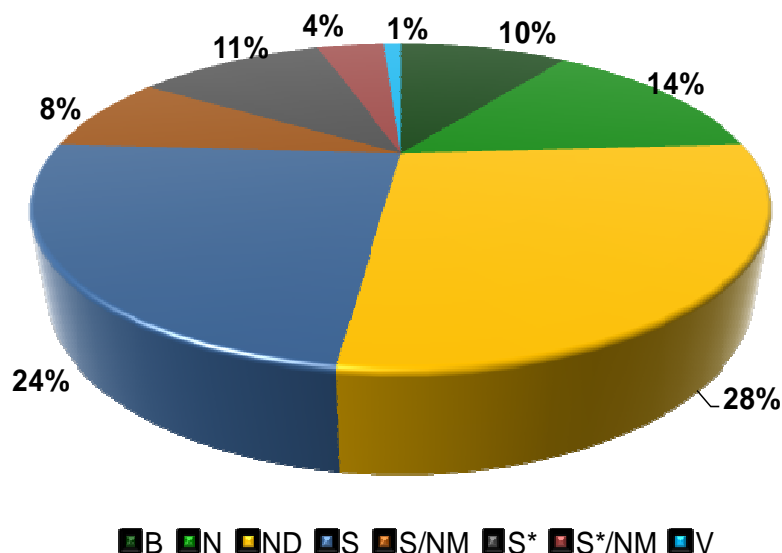
Figure I.1 Classification of all available anticancer drugs (from 1940 to 2006) by source (from [3])

The analyses of all available anticancer drugs show that natural products play a dominant role in the discovery of leads for the development of drugs for cancer treatment. The chart shows the sources of anticancer drugs: natural products (N); biological, usually large peptides or proteins (B); derived from a natural product, usually with semisynthetic modifications (ND); total synthetic drugs (S); made by total synthesis, but the pharmacophore was from a natural product (S*); vaccine (V); natural product mimic (NM).

2   Aim of the study

Chemoresistance is a major difficulty in successful cancer treatment. It is related to deregulation and alterations in proteins involved in apoptosis, a form of programmed cell death. In many types of cancer, proapoptotic proteins have inactivating mutations as well as antiapoptotic proteins are often upregulated [7, 8], resulting in ineffective therapy outcome. Thus, new effective compounds that target multiple signaling pathways and restore the programmed cell death in cancer cells are still urgently required.

Therefore, the aim of this work was:

1   the characterization of apoptotic potential of spongistatin 1 in chemoresistant leukemia cells

2   the identification and pharmacological evaluation of new compounds selected from pharmacophore-based virtual screening on its ability to inhibit anti-apoptotic XIAP-Bir3 protein and restore programmed cell death in cancer cells.

3   Spongistatin 1

Spongistatin 1 (Figure I.2) was isolated from the Eastern Indian Ocean (Republic of Maladives) sponge *Hyrtios erecta*. The group of G. R. Pettit (Arizona State University, USA) found this marine Porifera during its expedition in 1988 [9]. Only 5 mg of this macrocyclic lactone were isolated from the 400 kg of wet sponge.

In the same time the group of Kobayashi found an identical structure in the Okinawan marine sponge *Hyrtios altum* (Figure I.2C) [10] and named it Altohyrtin A.
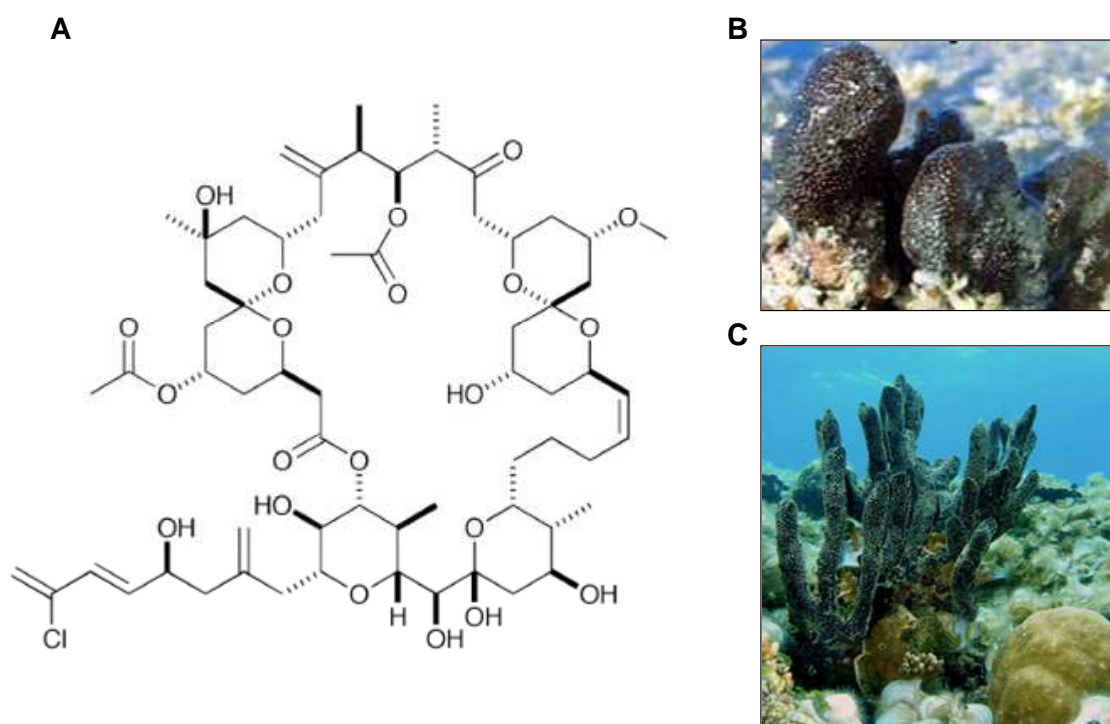
Figure I.2 Chemical structure of spongistatin 1 (A), *Hyrtios erecta* (B) and *Hyrtios altum* (C)

Spongistatin 1 belongs to the macrocyclic lactones (A) and was isolated from (B) *Hyrtios erecta* [11] and (C) *Hyrtios altum* [12].

Spongistatin 1 was tested in the NCI panel of 60 human cancer cell lines (see Figure I.3) and identified to be extraordinary potent against twenty of them. The analysis of the data from NCI screen using the computerized, pattern-recognition algorithm COMPARE shows profile similarities between spongistatin 1 and such antimitotic agents as vincristine, vinblastine, taxol or podophyllotoxin [13]. Indeed, this correlation could be validated by experiments of Bai et al. [14], that show that spongistatin 1 binds to the same pocket of tubulin as vinblastine and GTP. Thereby, spongistatin 1 hinders interactions of tubulin interdimers and contributes to depolimerization of tubulin. Spongistatin 1, for the first time introduced as a broad spectrum antifungal compound [15], was also tested in a pancreas KCI-MOH1 cell line-

derived SCID mouse xenograft model and showed synergistic antitumor effects in combination with gemcitabine [16].

Panel/Cell Line	Log$_{10}$ GI50	GI50
Leukemia		
CCRF-CEM	-10.37	
HL-60(TB)	-10.49	
K-562	-10.52	
MOLT-4	-10.12	
RPMI-8226	-10.31	
SR	-10.75	
Non-Small Cell Lung Cancer		
A549/ATCC	-10.04	
EKVX	-9.74	
HOP-62	-10.02	
HOP-92	> -9.00	
NCI-H23	-10.00	
NCI-H322M	-9.55	
NCI-H522	-10.59	
Colon Cancer		
COLO 205	-10.67	
HCC-2998	-9.90	
HCT-116	-10.43	
HCT-15	-9.59	
HT29	-10.56	
SW-620	-10.35	
CNS Cancer		
SF-268	-10.18	
SF-295	-10.60	
SF-539	-10.46	
SNB-19	-9.17	
SNB-75	-10.67	
U251	-9.87	
Melanoma		
MALME-3M	-10.42	
M14	-10.37	
SK-MEL-28	-10.13	
SK-MEL-5	-10.60	
UACC-257	-10.06	
UACC-62	-10.52	
Ovarian Cancer		
IGROV1	-10.01	
OVCAR-3	-10.22	
OVCAR-4	> -9.00	
OVCAR-8	-9.73	
SK-OV-3	-10.35	
Renal Cancer		
786-0	-9.90	
A498	-10.22	
ACHN	-9.60	
CAKI-1	-9.84	
SN12C	-9.76	
UO-31	-9.51	
Prostate Cancer		
PC-3	-10.50	
DU-145	-9.81	
Breast Cancer		
MCF7	-10.23	
MCF7/ADR-RES	-9.60	
MDA-MB-231/ATCC	-9.68	
MDA-MB-435	-11.12	
MDA-N	-10.96	
BT-549	-9.06	
T-47D	-9.35	
MG MID	-10.09	
Delta	1.03	
Range	2.12	

Figure I.3 The cytotoxic profile of spongistatin 1 evaluated by the NCI in vitro assay [13]

The zero value represents the mean of all cell lines tested. The bars indicate the deviation of the mean data obtained from the individual cell line from the overall mean and mark the sensitivity of the cell lines for spongistatin 1 (the negative bars represent more sensitive cell lines than the calculated average; the positive bars represent the less sensitive ones). GI$_{50}$: 50 % growth inhibition after the 48 hrs cytotoxicity assay.

4 Pharmacophore-based virtual screening for the discovery of target-specific compounds

The continuously increasing amount of relevant molecular targets in cancer therapy and the progress in understanding of the molecular processes within cells allow searching for target-specific compounds. These are characterized by selectivity for cancer cells and therefore show fewer side effects on healthy cells. In this searching process various *in silico* tools can provide help to rational discovery of bioactive anti-cancer compounds.

A pharmacophore is the ensemble of steric and electronic features that is necessary to ensure the optimal supramolecular interactions with a specific biological target structure and to trigger (or to block) its biological response [17]. Thus, pharmacophore models are useful tools for drug discovery. There exist two approaches for developing pharmacophore models: either by analyzing the known structure of the target molecule (structure-based design) or by starting from a set of ligands which are supposed to bind to the same area within the target (ligand-based design). For structure-based model generation (Figure I.4) the information about 3D structure of a ligand conformation, combined with the exact binding site of the target to ligand is needed [18]. This information can be obtained from the Brookhaven Protein Data Bank (PDB) [19], an unique platform containing 3D coordinates of ligand and target structures from NMR and co-crystal experiments. The use of software tools such as LigandScout [20] automates the modeling process. It incorporates the data from 3D interaction structure including such chemical features as hydrogen bond donors, acceptors, lipophilic areas or positively and negatively ionizable chemical groups into the structure-based pharmacophore model [20]. This tool is ideally used for virtual screening of large databases and to make predictions about the biological activity of chemical compounds.

The application of pharmacophore models in virtual screening of large databases allows the selection of a limited number of agent-candidates proposed to have biological activity. Moreover, the molecules that do not possess the essential features of ligand-target interaction quickly get eliminated and fewer *in vitro* experiments have to be performed [21]. Hence, the structure-based pharmacophore model used as a filter can hugely enrich the hit rate of bioactive compounds in comparison to random screening.
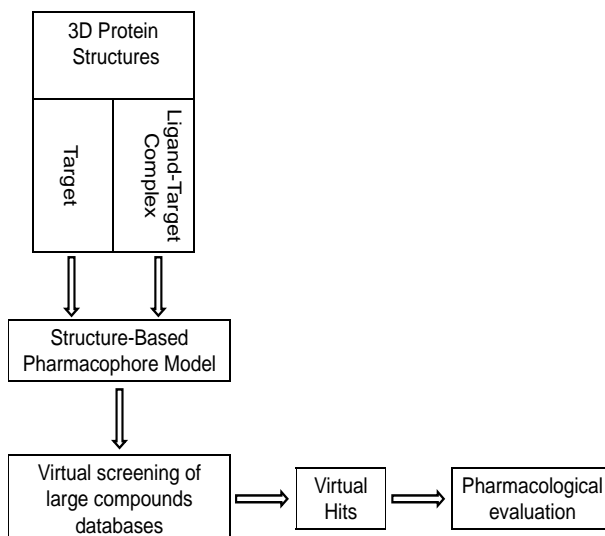
Figure I.4 Identification of new bioactive compounds by pharmacophore-based virtual screening

The information from 3D structures of proteins and their targets is used as a starting point for structure-based pharmacophore model generation. As the next step, virtual screening of large compound databases can be prepared and the hits can be validated via its biological activity in pharmacological tests.

5 Classification of cell death

The rapid development of new techniques in molecular biology makes it difficult to clearly classify the different cell death modalities. Based on the Nomenclature Committee on Cell Death (NCCD) proposal a cell is regarded as dead if any of the following molecular or morphological events can be detected: (i) the cell membrane is not intact any longer, (ii) the cell is fragmented into "apoptotic bodies" and (iii) its fragments have been engulfed by a neighboring cell (*in vivo*) [22].

There are two distinct ways by which cells can die. The first one is the so called programmed cell death (PCD), which is characterized by the activation of genetically encoded biochemical processes and by saving the tissue from inflammation (Figure I.5). The PCD classification includes different cell death forms such as apoptosis and autophagy.

The second way by which cells can die is necrosis, it ends in the uncontrolled destruction of the cell body and causes tissue inflammation. A characteristic sign of necrosis is the increased cell volume (oncosis) and the swelling of organelles, finally leading to plasma membrane rupture and inflammation of neighbor tissue. Initially, necrosis was defined as a completely accidental process of cell death but recent research has figured out that it can be a regulated process as well, mediated through a set of cellular pathways involving death domain- and Toll-like- receptors.
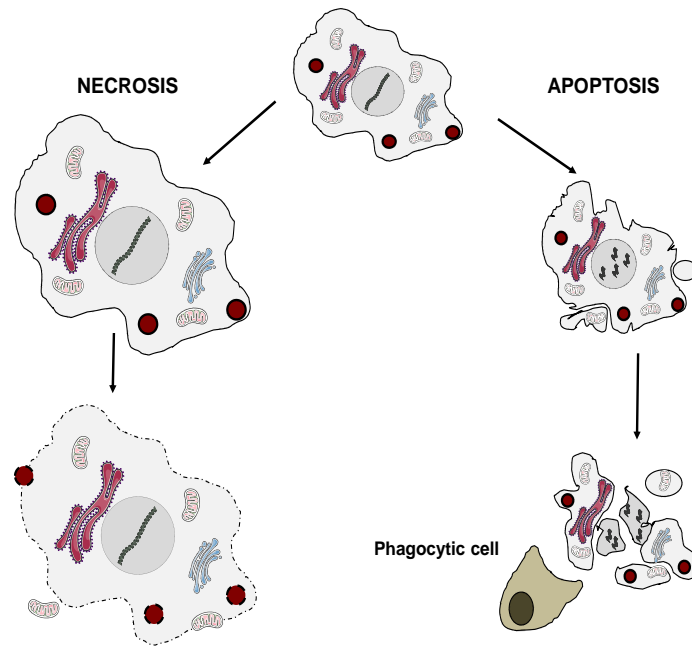
Figure I.5 Overview of necrosis and apoptosis

Necrosis is characterized through cell swelling and membrane rapture. The cellular content is released into the surrounding tissue, resulting in inflammation. In apoptosis the cell volume decreases, the chromatin is condensed and fragmented; cell organelles are enclosed in apoptotic bodies which are later phagocyted through macrophages.

6 Apoptosis

Apoptosis is an important cell death program that occurs both, in the developing and in the adult organism. The balance between proliferation and cell death is necessary for tissue homeostasis. Thus, an increase, a decrease or defects in the apoptotic process cause many pathological disorders such as autoimmune diseases, neurodegenerative diseases or cancer [23]. Apoptosis can be trigged by a variety of extrinsic and intrinsic pathway-induced signals. In both cases caspases are the essential players in the cell death process.

6.2 Caspases

Caspases are an evolutionary conserved family of cysteinyl-aspartate specific proteases which are involved in the cleavage of key protein substrates finally leading to apoptosis. Caspase-1 was identified in 1992 [24, 25] as the interleukin-1β-converting enzyme (ICE) which cleaves the precursor interleukin-1β after Asp^{116}, thereby producing the active cytokine. At that time nothing was known about a role of ICE in apoptosis. Not before 1993, the group of Horvitz cloned the C. elegans gene ced-3 and showed the similarity to human ICE and the mouse nedd-2 gene [26]. They also proposed that the CED-3 protein acts as a cysteine protease in the

initiation of PCD in C. elegans and those cysteine proteases may have the same role in mammals. At least 14 caspases are identified up to now.

6.2.1 Caspase structure and classification

Caspases involved in apoptosis are divided into two groups: the initiator caspases (caspase-2, -8, -9, and -10) and effector caspases (caspase-3, -6, and -7).

All caspases are produced as inactive zymogens, which are activated either by autocleavage (initiator caspases) or cleavage by other caspases (effector caspases). The cleavage occurs at a specific internal aspartic acid residue (see Figure I.6) and produces two subunits: a large (20 kDa) and a small one (10 kDa).
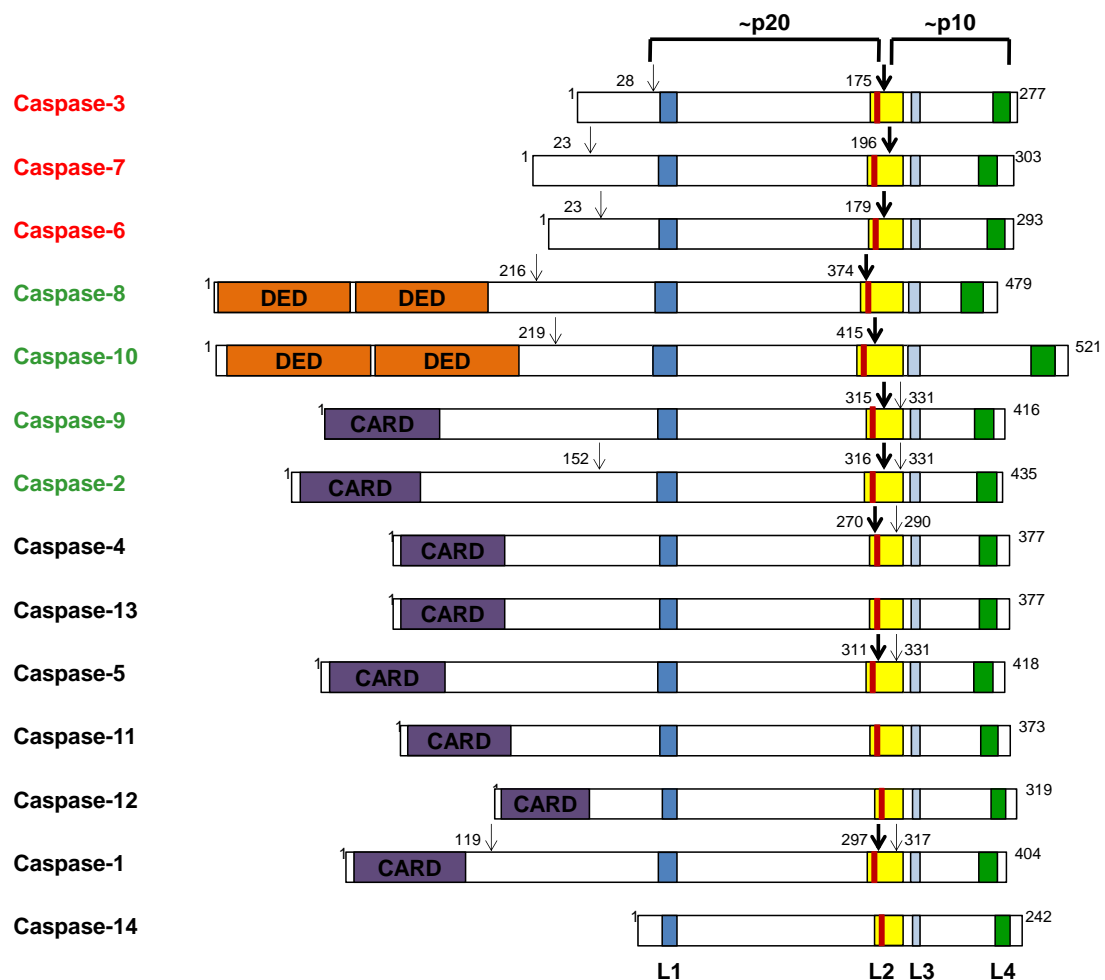
Figure I.6 Schematic diagram of the different caspase structures (adopted from [27])

Structure of human caspases (except caspase-11, -12 [mouse] and -13 [bovine]). The initiator and effector caspases are labeled in red and green, respectively. The bold arrows show the first activation cleavage, small arrows indicate additional sites of cleavage. The L1-L4 indicates the four surface loops that shape the catalytic groove. The red line at the beginning of L2 loop shows catalytic Cys.

6.2.2 Caspase activation

Caspases (see chapter 6.2.1) play an important role in mammalian apoptosis. The activating cleavage takes place within a short peptide fragment which connects the large and small subunit of the zymogen and usually occurs at the highly conserved Asp-297 (caspase-1 numbering convention) (see Figure I.6). In this way, the most activated caspase can process itself and other caspase zymogens (see Figure I.7) [28].

Initiator caspases are characterized by one or more N-terminal adapter motifs (CARD= caspase recruitment domain or DED= death effector domain). These adapter motifs interact with similar motifs of the adapter proteins within activation platforms (apoptosome, PIDDosome and death inducing signaling complex- DISC). Two theories concerning the activation of the initiator caspases are discussed: the induced proximity model and the proximity-driven dimerization model [28, 29]. Generally, the initiator caspases get autoactivated when caspases are brought very close to each other (e.g. as by the DISC complex). For caspase-9 activation the induced conformation model was proposed. The apoptosome directly activates monomeric caspase-9 by modification of its active site conformation in an unknown process [30, 31]. All models are not mutually exclusive; there are several possibilities leading to initiator caspase activation. Once activated, initiator caspases can initiate the caspase cascade by proteolytic processing of effector caspases.
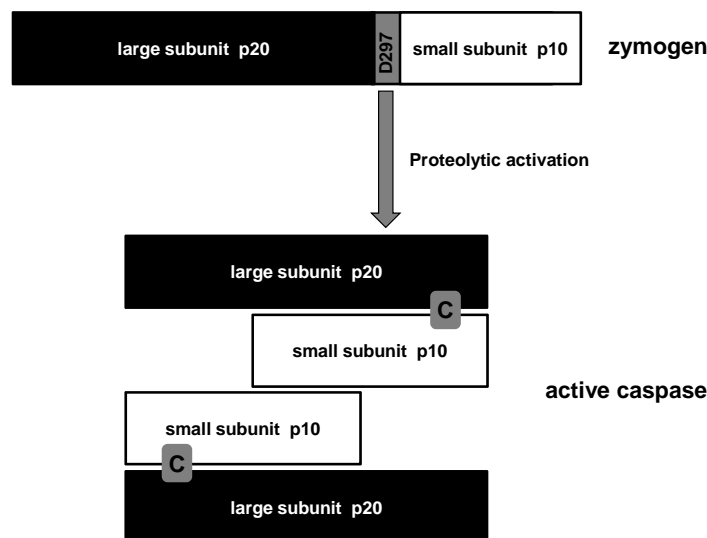
Figure I.7 Caspase activation by proteolysis (modified from [28])

Caspases are synthesized as single chain zymogens. Activation usually occurs by cleavage at the conserved D297 (caspase-1 numbering convention). The active caspase is a tetramer of two heterodimers, each comprising a large and a small subunit and an active site (grey circle).

6.2.3 Caspase substrates

As mentioned above, the apoptotic process is executed by the caspase-mediated cleavage of numerous cellular proteins. As the consequence of this cleavage the caspase substrates are activated or inactivated. As the name cysteine-dependent aspartate specific protease implies, caspases use their conserved Cys side chain as a nucleophile to hydrolyze peptide bonds and they have a primary specificity for Asp. The catalytic cleft of a caspase is responsible for its specifity and is formed by the strictly conserved residues Arg179, Arg314 and Gln283 (caspase-1 numbering convention) and is almost identical for all caspases [32, 33]. Caspases recognize 4 specific amino acids residues of their substrates (P_1-P_4) and have a cleavage preference to the position prior first Asp (see Table 1). This feature makes the protelolytic cleavage more specific.

Table 1 Cleavage sites of caspases substrates (from [32])

Caspase	P_5	P_4	P_3	P_2	P_1	$P_{1'}$
1, 4, 5, 14		W/Y	E	X	**D**	Φ
8, 9, 10		I/L	E	X	**D**	Φ
3, 7		D	E	X	**D**	Φ
6		V	E	X	**D**	Φ
2	V/L	D	E	X	**D**	Φ

Φ means that G, A, T, S or N is preferred in position $P_{1'}$; **D** the cleavage position

The cleavage by a caspase can activate the substrate, e.g. effector caspases or proapoptotic Bid [34]. On the other hand, cleavage can result in a loss of function as in case for the poly(ADP-ribose) polymerase (PARP). This enzyme is responsible for the repair of DNA-strand breaks. After degradation through caspase it loses the ability to restore the DNA entireness [35].

7 Extrinsic apoptotic pathway

Apoptosis can be initiated in mammalian cells by two different pathways: (i) by the extrinsic way which implicates the activation of death receptors of the tumor necrosis factor (TNF) receptor superfamily, or (ii) by the intrinsic way which involves mitochondria and release of proapoptotic proteins out of them. There exists a crosslink between these two pathways which results in amplification loop.

The extrinsic pathway is crucial for the proper function of the immune system. Up to date, six different death receptors are identified. CD95 (APO1/Fas), TNFRI (tumor necrosis factor receptor I) and TRAIL (TNF-related apoptosis-inducing ligand) receptors are the best known. They are characterized by the intracellular death domain (DD) which is essential for the apoptotic signal transduction [36]. Stimulation of the receptors (e.g. CD95) by binding to their ligands (e.g. CD95L) results in the trimerization of the receptors and the recruitment of

adaptor molecules like FADD (Fas-associated death domain) which is mediated by its interaction with the DD (see Figure I.8). In the following, FADD recruits caspase-8 or -10 proforms, forming a complex called DISC (death-inducing signaling complex). The oligomerization of the caspase zymogens in turn drives their activation by autocleavage (see also chapter I.6.2.2). Active caspases then activate effector caspases (e.g. caspase-3) [37]. In type I cells, large amounts of caspase-8 are activated leading to the rapid cleavage of caspase-3. In comparison, in the type II cells the relative amount of activated caspase-8 is insufficient for full caspase-3 activation. In this case caspase-8 cleaves Bid protein into truncated Bid (t-Bid) which in turn induces mitochondria outer membrane permeabilization (MOMP) and the activation of effector caspases [34].
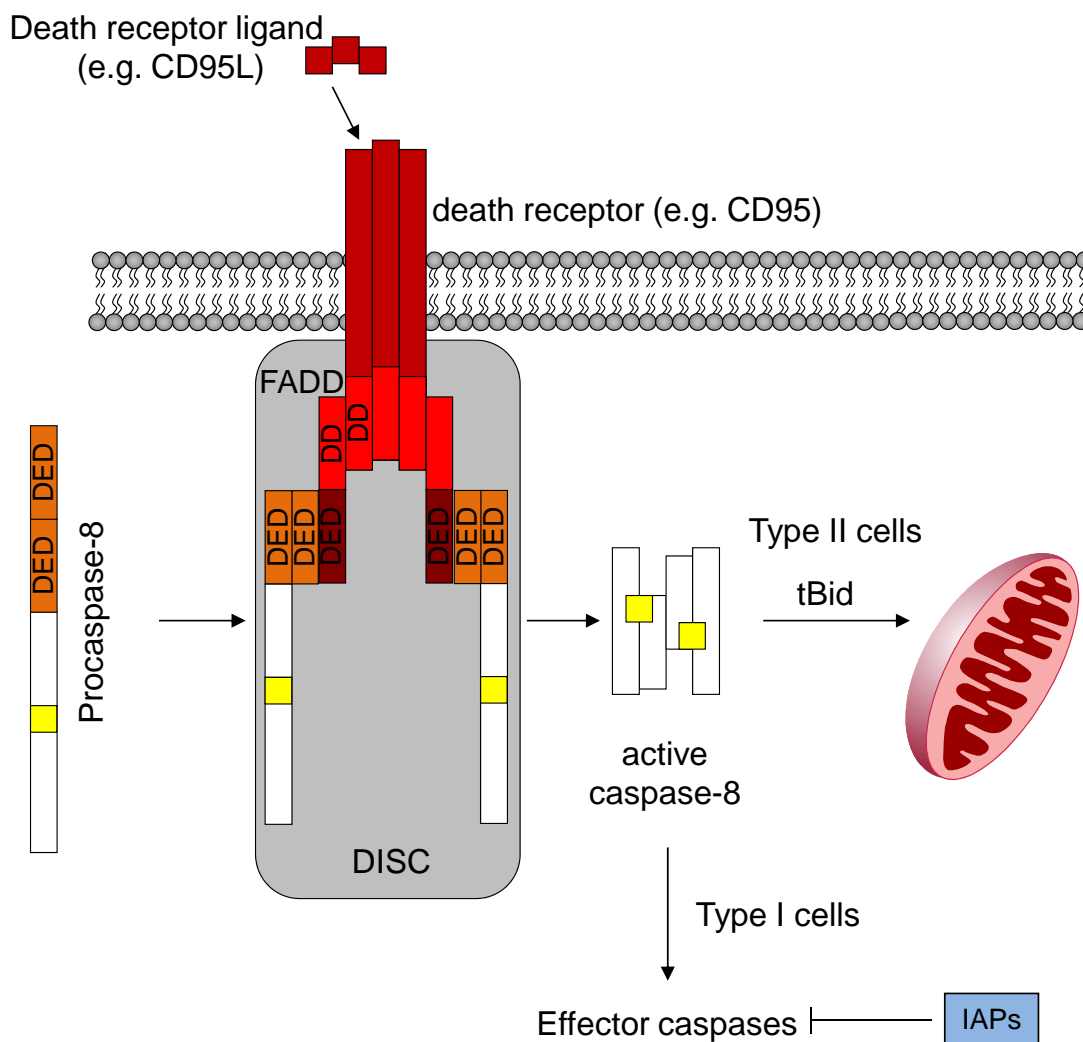
Figure I.8 Extrinsic apoptotic pathway

Binding of the ligand on its receptor leads to receptor trimerization in the membrane and FADD recruitment to the complex. Caspase-8 binds to the assembly by its DED domain and the death inducing signaling complex (DISC) is formed. On this platform caspase-8 is autoactivated. The initiator caspase-8 activates downstream effector caspases (type I cells), or cleaves Bid and leads to an amplification of apoptosis by involving the mitochondria (type II cells).

8 Intrinsic apoptotic pathway

Mitochondria represent the central elements of the intrinsic apoptotic pathway. Besides their function as energy supplier for the cells, mitochondria contain, between the double-membrane, important proteins for the initiation of apoptosis.

Activated by cell death stimuli (e. g. oxidative stress, DNA-damage or signals induced by chemotherapeutic drugs) proapoptotic proteins, the cytosolic Bax and mitochondria bound Bak form pores in the outer mitochondria membrane (OMM) [38, 39] (see Figure I.9). This leads to a decrease of the membrane potential ($\Delta\Psi$) and to the release of proapoptotic proteins such as cytochrome c, second mitochondria-derived activator of caspase/direct IAP-binding protein with low PI (smac/DIABLO), high-temperature requirement protein A2 (Omi/HtrA2), apoptosis-inducing factor (AIF) and endonuclease G (endoG) into the cytosol [40]. Once released, EndoG and AIF translocate to the nucleus where they are able to induce DNA fragmentation in a caspase-independent manner [41, 42].

In contrast, in the presence of ATP cytochrome c interacts with Apaf-1 and forms a large (about 1.4 kDa) complex- the apoptosome, leading to caspase activation. By its CARD domain, caspase-9 is recruited to the CARD domain of Apaf-1 [29, 43]. Caspase-9 gets activated and in turn mobilizes activation of caspase-3 and initiates the apoptotic cascade which finally causes DNA fragmentation and cell death.

The proapoptotic proteins smac/DIABLO and Omi/HtrA2 counteract inhibitors of apoptosis proteins (IAPs), a conserved family of antiapoptotic proteins responsible for the regulation of caspase activity (for detailed description see chapter 10).

I Introduction
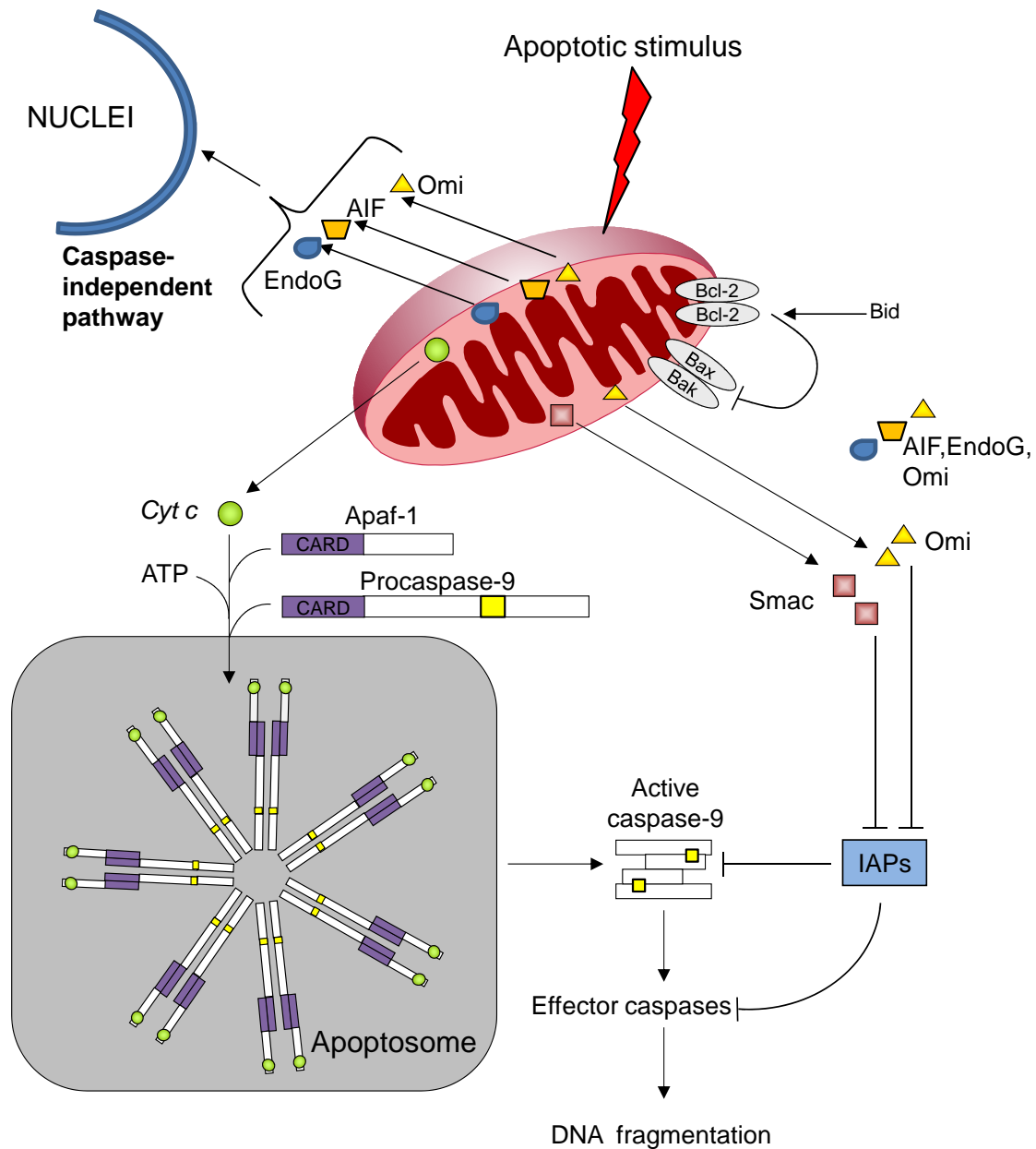
Figure I.9 Intrinsic apoptotic pathway

Apoptotic stimuli induce the release of intermembrane proteins from mitochondria into the cytosol. Cytochrome c together with Apaf-1, ATP and caspase-9 forms the apoptosome complex that leads to caspase-9 activation and results in the activation of effector caspases. The IAPs are able to inhibit both the initiator and effector caspases. Smac/DIABLO and Omi/HtrA2 antagonize the IAPs and facilitate caspase activation. After release from mitochondria, Omi/HtrA2, AIF and endoG translocate to the nucleus and induce caspase independent cell death.

9 Bcl-2 protein family

In mammals, there exist at least 12 Bcl-2 family proteins which either has pro- or anti-apoptotic properties. The Bcl-2 homology (BH) domain is a conserved region among all family members and up to date four BH domains could be identified: BH1-BH4. Bcl-2 family members have been grouped into three classes [38, 44].

First anti-apoptotic class (e. g. Bcl-2 or Bcl-xl) can suppress cell death induction. Most proteins belonging to this class possess a hydrophobic tail, which allows the attachment to membranes of organelles like mitochondria. They prevent the release of apoptogenic factors from mitochondria and therefore protect against outer membrane permeabilization by a not fully understood mechanism.

The second group includes proapoptotic multidomain proteins which share several regions of sequence homology (e.g. Bax, Bak or Bok). Bax is loosely attached to the outer membrane of mitochondria or is sequestered in cytosol, whereas Bak has an anchor that attaches it to the mitochondrial outer membrane. Upon a death stimulus Bak and Bax undergo a conformational change, oligomerize and induce the formation of a pore in the OMM leading to the release of e.g. cytochrome c and smac/DIABLO.

The last group, also known as BH3-only proteins, has many members whose common feature is the presence of a single BH3 domain. The BH3 domain serves as ligand for Bcl-2 and Bcl-xl suppression or for Bax and Bak activation. Bid for example is thought to induce the conformational change of Bax/Bak, which leads to insertion in the OMM.

10 IAP family

The mammalian IAP family consists of eight proteins, that all have at least one Bir domain (baculoviral IAP repeat) (see also Figure I.10). The IAPs were discovered in insect cells from *Spodoptera frugiperda* infected with the virus *Autographa californica* which lacks p35 [45]. P35 acts by inhibiting the activity of members of the ICE family of cysteine proteases [46, 47]. Later the first IAP protein, NAIP was found in mammals [48] and in 1996 the group of Thompson showed that IAP can also prevent cell death in mammalian cells [49]. This data suggested IAPs to be an evolutionary conserved family involved in apoptosis. It is now known that the IAPs are involved in many other cellular functions e.g. protein degradation and stabilization, cellular morphogenesis, mitotic chromosome segregation, cell motility or copper homeostasis [50-53].

The Bir domain of IAP proteins consists of ~70 amino acids with the signature sequence $CX_2CX_{16}HX_6C$ (C= cysteine, H= histidine, and X= any amino acid). The central zinc ion is coordinated via histidine and cysteine residues. The Bir domains mediate the protein-protein interactions, and although there is high similarity between them they have high specificity for

binding partners. It implicates, that the composition of the interaction is completely different among the Bir domains.
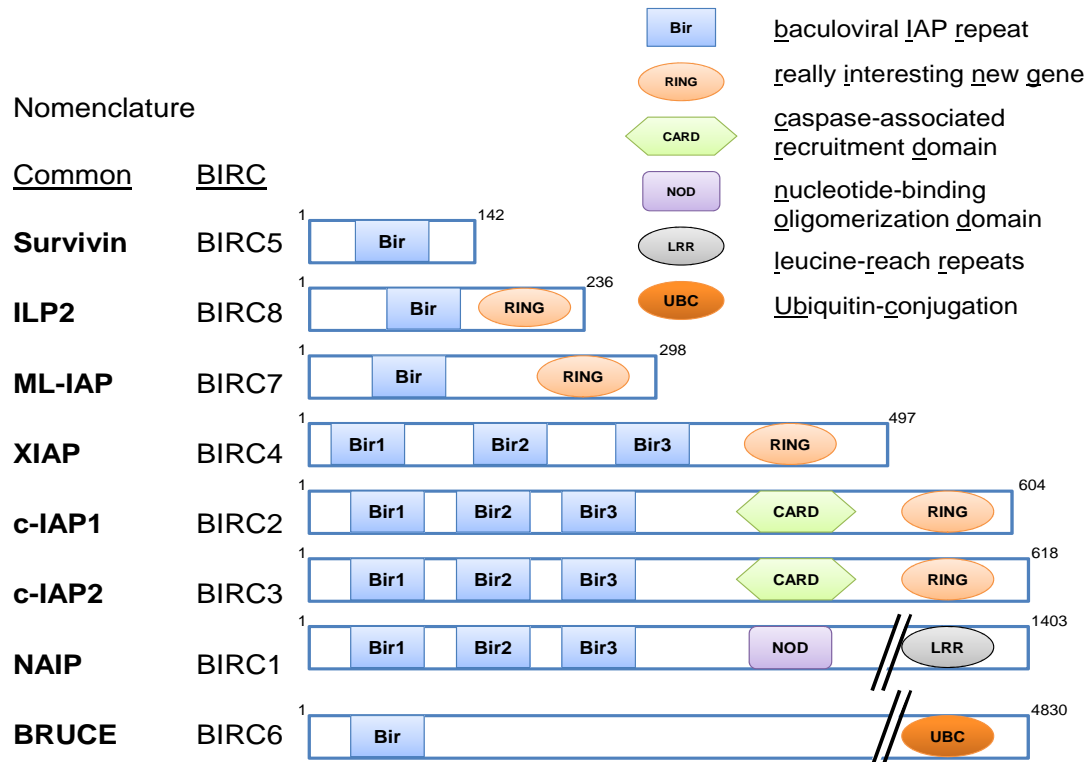
Figure I.10 Schematic structure of the inhibitor of apoptosis protein family (from [54])

IAPs have at least one baculoviral IAP repeat (Bir) domain. Additionally, most IAPs have other distinct functional domains such as the nucleotide-binding oligomerization domain (NOD), the leucine-rich repeats (LRRs) and the really interesting new gene domain (RING), an E3 ligase that presumably directs targets to the ubiquitin-proteasome degradation system. Bruce has an ubiquitin-conjugation (UBC) domain that is found in many ubiquitin-conjugating enzymes. (cIAP, cellular IAP; IAP, inhibitor of apoptosis protein; ILP, IAP-like protein; ML-IAP, melanoma IAP; NAIP, neuronal apoptosis inhibitory protein; XIAP, X-chromosome-linked IAP).

Although the IAPs were originally discovered as inhibitors of apoptosis, not all of them inhibit caspases with the same efficiency (see Table 2). The most potent caspase inhibitor is XIAP (X-linked inhibitor of apoptosis proteins), which prevents both, the activation of the initiator caspase-9 as well as of the effector caspases-3 and -7.

Table 2 IAP proteins inhibits various caspases with different inhibitory constants (K_i) (adopted from [55-60])

IAP member	Inhibited caspase	K_i (nM)
XIAP	3	0.7
	7	0.2
	9	Not defined
c-IAP1	3	108
	7	42
c-IAP2	3	35
	7	29
NAIP	3,7	Not defined
Survivin	3	20.9
Livin	3,7,9	Not defined
ILP-2	9	Not defined
BRUCE	3	Not defined

10.2 X-linked Inhibitor of Apoptosis Protein

XIAP (also known as MIHA/hILP/BIRC4) is a key member of the family of intrinsic inhibitors of apoptosis proteins (IAP). This 57 kDa protein contains three baculoviral IAP repeat (Bir) domains and a C-terminal really interesting new gene domain (RING). XIAP was shown to directly bind and inhibit caspases-3, -7 and -9 [61-63]. The structures of XIAP Bir2 and Bir3 domains have been determined by nuclear magnetic resonance [64, 65] and were found to be very similar. However, different sets of amino acids residues were found to be responsible for the inhibition of distinct caspases.

XIAP is involved in many regulatory mechanisms in cells: it is a potent caspase inhibitor [61]. It is involved in ubiquitination and proteasomal degradation of many proteins [66] and in the activation of NF-κB [66, 67] (Figure I.11).

The IAP mediated inhibition of caspases is antagonized by a family of proteins that contain an IAP-binding motif (IBM). After getting released from mitochondria, smac/DIABLO forms homodimers and binds simultaneously to Bir2 and Bir3 domains of XIAP [68] via the IBM and restores the caspase activity. Moreover, the mitochondrial protease Omi/HtrA2 binds to the Bir domains of XIAP and additionally degrades XIAP [69, 70].

The XIAP associated factor 1 (XAF1) negatively regulates XIAP by initiating XIAP translocation from cytoplasm into nuclei [71]. Furthermore, calpains mediated XIAP degradation [72] and also caspases are able to cleave the XIAP into different fragments [73].
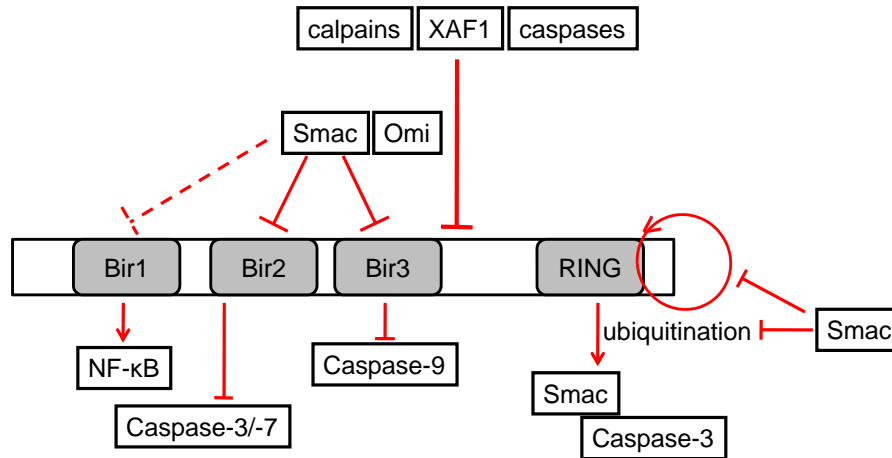
Figure I.11 XIAP protein-protein interactions in the cell

XIAP directly inhibits caspase-3, -7 and -9, promotes proteasomal degradation of smac/DIABLO and caspase-3 and is able to activate NF-κB pathways. Negative regulators of XIAP are smac/DIABLO, Omi/HtrA2, calpains, XAF1 and caspases. XIAP is also able to initiate its self-degradation in autoubiquitination process.

XIAP translation is regulated by a unique cap-independent mechanism which allows the production of new proteins if the majority of cap-dependent translation initiation is aborted. XIAP mRNA contains an internal ribosome entry site (IRES) in its 5'-untranslated region (5'-UTR) which directly recruits ribosomes to mRNA [74].

Interestingly, XIAP deficient mice are viable and show no phenotype. An explanation may be the elevated levels of c-IAP1 and c-IAP2 possibly compensating the lack of XIAP [75].

10.2.1 Bir1 domain of XIAP

The Bir1 domain of XIAP, in contrast to Bir2 and Bir3, does not bind the proteins with IBM motif, but is indirectly involved in apoptotic events via activation of TAK1 and NF-κB pathway [76].

The Bir1 and RING domain induce XIAP dimerization (see Figure I.12), stimulating the interaction between Bir1 and TGF-β-activated kinase 1-binding protein 1 (TAB1). This complex activates TGF-β-activated kinase 1 (TAK1) which in turn activates NF-κB. Smac/DIABLO is able to disrupt the Bir1 dimerization and consequently inhibits NF-κB activation [67]. After TNFα stimulation, XIAP enhances a second wave of NF-κB nuclear translocation by interaction and ubiquitination of MEKK2 [77].
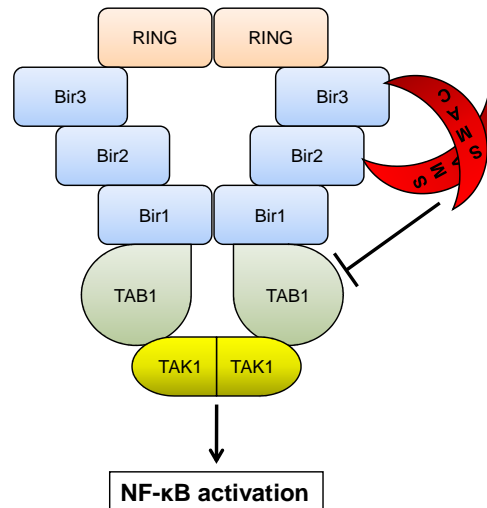
Figure I.12 Bir1 dimerization and NF-κB activation (adopted from [67])

The Bir1 and RING domain induce XIAP dimerization and interaction between Bir1 and TGF-β-activated kinase 1-binding protein 1 (TAB1), the upstream activator of TAK1. Subsequently TAK1 stimulates the NF-κB pathway activation. This activation process can be disrupted by smac/DIABLO.

10.2.2 Bir2 and Bir3 domains of XIAP

The conserved amino acids within the linker region between the Bir1 and the Bir2 domains were found to be critical for inhibition of caspase-3 and -7 [64]. This side linker peptide forms together with the Bir2 domain a tight complex with effector caspase and inhibits their catalytic activity [62].

The Bir3 domain was identified as region of XIAP that specifically inhibits caspase-9 [73]. Upon processing of caspase-9 into p12 subunit at Asp315, the four amino-terminal residues (Ala-Thr-Pro-Phe) are exposed. These residues interact with XIAP-Bir3 domain and form XIAP-caspase-9 heterodimers [78]. The same conserved tetrapeptide sequence of caspase-9 is responsible for caspase homodimerization and activation on the apoptosome platform. Thus, XIAP sequesters caspase-9 in an inactive monomeric state [63].

10.2.3 RING domain of XIAP

The C-terminal RING (really interesting new gene) domain of XIAP regulates the (auto)ubiquitination of target proteins [50, 66]. The RING domain coordinates Zn^{2+} via three cysteine and histidine amino acids. This motif is the basis of the E3 ubiquitin ligase activity of XIAP and the platform for binding the E2 ubiquitin-conjugating enzymes. The autoubiquitination sites of XIAP are located in the Bir3 domain at Lys322 and Lys328 [66]. The RING domain promotes ubiquitination and proteasomal degradation of active caspase-3 [79] and smac/DIABLO [80] and thus regulates caspase activity at a post-translational level.

II Materials and Methods

1 Materials
1.1 Compounds

Spongistatin 1 was kindly provided by G. R. Pettit (Tempe, Arizona, USA) [14]. The T substances were purchased from Asinex Ltd. (Moscow, Russland) (see Figure III.20). T8 was furthermore synthesized and kindly provided by the group of Prof. K. T. Wanner from Department of Pharmacy at the Ludwig Maximilians University in Munich, Germany. The ABT-11 compound [81] was kindly provided by Abbott Laboratories (Abbott Park, Illinois, USA).

1.2 Reagents

Complete^{TM}	Roche, Mannheim, Germany
FCSgold	PAN Biotech, Aidenbach, Germany
zVADfmk	Calbiochem, Schwalbach, Germany
Endothelial Growth Medium	PromoCell, Heidelberg, Germany
Hoechst 33342	Sigma, Taufkirchen, Germany
MTT	Sigma, Taufkirchen, Germany
Propidium iodide	Sigma, Taufkirchen, Germany
Pyruvate	Sigma, Taufkirchen, Germany
Paclitaxel	Sigma, Taufkirchen, Germany
Etoposide	Calbiochem, Schwalbach, Germany
Doxorubicin HCl	Sigma, Taufkirchen, Germany
Staurosporine	Cayman Chemical, Ann Arbor, USA
G418 sulfate	PAA Laboratories, Cölbe, Germany
DMSO	AppliChem, Darmstadt, Germany
Puromycin	PAA Laboratories, Cölbe, Germany
RPMI1640	PAA Laboratories, Cölbe, Germany
DMEM	PAA Laboratories, Cölbe, Germany
Ac-DEVD-AFC	Bachem, Bubendorf, Germany
Ac-LEHD-AFC	Bachem, Bubendorf, Germany
TNFα	Sigma, Taufkirchen, Germany
*Killer*TRAIL	Axxora Deutschland GmbH, Lörrach, Germany

1.3 Equipment

ViCELL^{TM}	Beckman Coulter, Krefeld, Germany
FACS Calibur	Beckton Dickinson, Heidelberg, Germany
Tecan Sunrise^{TM}	Tecan, Crailsheim, Germany
Luminometer	Berthols Detection Systems, Pforzheim, Germany
Curix 60	AGFA, Cologne, Germany
Li-Cor	LI-COR Bioscence GmbH, Bad Homburg, Germany
Thermoshake THO 500	Gerhard, Königswinter, Germany

2 Pharmacophore-based virtual screening for XIAP inhibitors

The pharmacophore modeling and virtual screening was performed by the group of Prof. Hermann Stuppner from the Institute of Pharmacy, Pharmacognosy at the University of Innsbruck, Austria.

A NMR-structure of an antagonist of the XIAP-caspase-9-interaction complex to the BIR3 domain of XIAP (PDB entry 1TFQ) (Figure II.1) served as primary information for the pharmacophore model generation [81]. The data together with the information from structure-activity relationship (SAR) studies [82, 83] were implemented into the pharmacophore model using the Catalyst Software 4.9 (Accelrys Inc., San Diego, USA). To make the pharmacophore model more precisely, the side chains of the protein, which could disturb the ligand-target interaction, were tagged with exclusion spheres.

II Materials and Methods
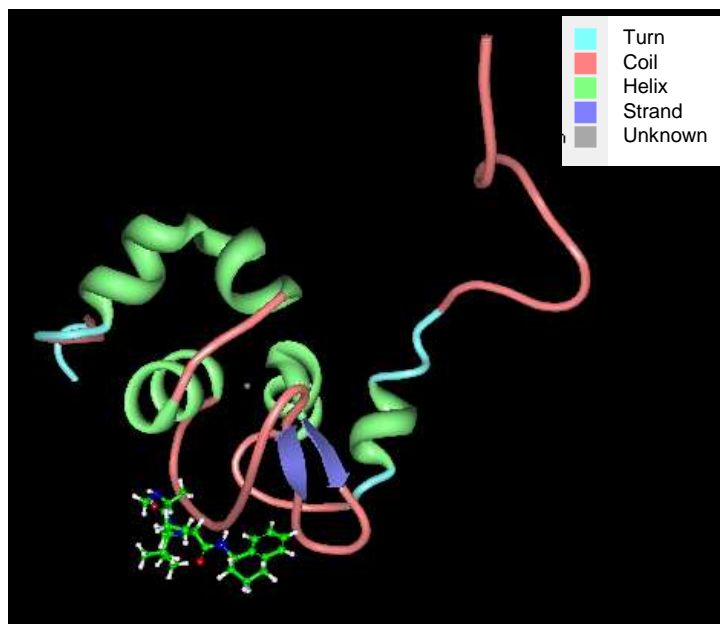
Figure II.1 Model of an antagonist of the XIAP-caspase-9-interaction complex to the BIR3 domain of XIAP (PDB entry 1TFQ)

Before initiation of the large virtual screening, the pharmacophore model (Hypo2-1TFQexcludvolumes7) was validated in a self made database of 30 compounds which are well known to inhibit XIAP-Bir3 interaction.

To retrieve a limited number of virtual hits, a consensus screening was applied using the GRID-based pharmacophore model [43, 84]. The resulting hypothesis was incorporated into Hypo2-1TFQexcludvolumes7 model. The virtual screening of commercial available databases (Asinex Platinum 1104, Asinex Gold 1104, Specs 110, Maybridge 2004 Derwent WDI_2003 and NCI) was performed by Catalyst Software.

Test compounds were selected from the virtual screening hits according to the (i) best fit values derived from consensus screening, (ii) compound availability, (iii) fulfilment of the Lipinski "rule of five" and (iv) experience based on toxicity prediction.

3 Cell culture
3.2 Cell lines

Human leukemia Jurkat T cells (wild type Jurkat clone J16, S-Jurkat), empty vector (Neo-Jurkat), Bcl-2 overexpressing Jurkat cells (Bcl-2 Jurkat), Bcl-xl overexpressing Jurkat cells (Bcl-xl Jurkat), CD95-deficient Jurkat cells (R-Jurkat) [85] wild type A3-Jurkat cells, FADD deficient A3 (FADD-/- Jurkat) and caspase-8 deficient Jurkat cells (8-/-) [86] were obtained from H. Walczak and P. H. Krammer (Heidelberg, Germany). Caspase-9 deficient Jurkat cells

(9-/-) were kindly provided by K. Schulze-Osthoff, Düsseldorf, Germany. Empty vector Jurkat cells (pBabe), XIAP overexpressing Jurkat cells (XIAP-Jurkat), and Bir3/RING overexpressing Jurkat cells were kindly provided by C. Duckett (Ann Arbor, Michigan, USA). LNCAP cells were provided by I. Jeremias (Munich, Germany) and MDA-MB-231 cells were a kind gift from B. Bachmeier (Munich, Germany), PancTu1 cells were obtained from S. Fulda (Ulm, Germany) [87] and L3.6pl cells were obtained from C. Bruns (Munich-Großhadern, Germany) [88]. Human embryonic kidney-293 cells (HEK-293) were obtained from DSMZ.

3.3 Primary cell isolation

Human peripheral mononuclear blood cells (PMBCs) were freshly isolated from the blood of healthy human donors. Blood, anticoagulated with EDTA (1mg EDTA/ml blood), was diluted with an equal volume of PBS$^+$ and layered without mixing over Ficoll Paque PLUS (Amersham Pharmacia Biotech, Uppsala, Sweden) in a 50 ml falcon. After 0.5 hrs of centrifugation at 400 x g, the top layer containing plasma was carefully removed and the PMBCs were harvested into a new tube. Cells were washed twice with PBS$^+$ to remove rests of Ficoll solution and recovered in fresh medium.

Primary leukemic blasts were obtained from children treated for acute leukemia at the Ludwig Maximilians University children's hospitals in 2006/2007. Blasts were isolated by bone marrow puncture at initial diagnosis or diagnosis of relapse and isolated using Ficoll Isopaque (Amersham Pharmacia Biotech, Uppsala, Sweden).

Human umbilical vein cells (HUVECs) were prepared by digestion of umbilical veins with 0.1 g/l of collagenase A [89].

3.4 Cell culture

All cell lines were cultivated at 37°C, in 5 % CO$_2$ atmosphere in media complemented with serum and additional supplements (see Table 3). The suspension cell lines were maintained at the density below 1 x 10^6. All adherent cell lines were passaged after reaching 80-90 % confluency. Primary leukemia cells and fresh isolated PMBCs were used for experiments immediately after isolation, whereas HUVECs were used up to passage number 3. L3.6pl cell line was used up to passage number 30 as this cell line was established first after passage number 14 [88]. All other cell lines were used up to passage 20 to avoid mutations.

Table 3 Cell lines and maintaining medium

Cell line	Medium	Serum	Supplements	Antibiotics
S-Jurkat (J16)	RPMI 1640	10 % FCS gold	1 % pyruvate	
R-Jurkat	RPMI 1640	10 % FCS gold	1 % pyruvate	
FADD -/-Jurkat	RPMI 1640	10 % FCS gold	1 % pyruvate	
Caspase-8 -/- Jurkat	RPMI 1640	10 % FCS gold	1 % pyruvate	
Caspase-9 -/- Jurkat	RPMI 1640	10 % FCS gold heat inactivated	1 % pyruvate	
pBabe-Jurkat	RPMI 1640	10 % FCS gold heat inactivated	1 % pyruvate	1µg/ml puromycin every 3rd passage
XIAP-Jurkat	RPMI 1640	10 % FCS gold heat inactivated	1 % pyruvate	1µg/ml puromycin every 3rd passage
Bir3/Ring-Jurkat	RPMI 1640	10 % FCS gold heat inactivated	1 % pyruvate	1µg/ml puromycin every 3rd passage
Neo-Jurkat	RPMI 1640	10 % FCS gold	1 % pyruvate	1mg/ml G418 every 5th passage
Bcl-xl Jurkat	RPMI 1640	10 % FCS gold	1 % pyruvate	1mg/ml G418 every 5th passage
Bcl-2 Jurkat	RPMI 1640	10 % FCS gold	1 % pyruvate	1mg/ml G418 every 5th passage
MDA-MB-231	DMEM with high glucose	10 % FCS gold heat inactivated		
LNCAP	RPMI 1640	15 % FCS gold heat inactivated		
PancTu1	DMEM with high glucose	10 % FCS gold heat inactivated		1 % P/S
L3.6pl	DMEM with high glucose	10 % FCS gold heat inactivated	1 % pyruvate 1 % nonessential amino acids	
PMBC	RPMI 1640	10 % FCS gold	1 % pyruvate	1 % P/S
HUVEC	Endothelial growth medium	10 % FCS gold heat inactivated	Supplement®	1 % P/S; 1 % Amphotericin B
HEK-239	DMEM without phenol red	10 % FCS gold heat inactivated	1 % glutamine	1 % P/S

3.5 Splitting and seeding for experiments

Suspensions cells were splitted every three days to a concentration 0.5 - 0.8 x 10^5 cells/ml. For experiments, cells were seeded in 96- or 24-well plates at a cell number of 5 x 10^5 cells/ml and stimulated the next day. In some cases, cells were seeded at cell number of 7 x 10^6 cells /ml and stimulated after 4-5 hrs.

Adherent cell lines were grown as monolayer in 75 cm^2 flasks coated with 0.001 % collagen G (Biochrom AG, Berlin, Germany). Cells were splitted after reaching 70-80 % confluency. For experiments, cells were seeded at a cell number of 5 x 10^4 – 8 x 10^4 cells/cm^2 and left over night for attaching to the surface. The Trypsin/EDTA (T/E) solution was used to detach the cells from the plastic surface. Briefly, the medium was removed from the flask or well plate, cells were washed with PBS to eliminate the rest of the old medium and a sufficient amount of T/E was added. Cells were shortly incubated in the cell culture incubator and the enzymatic reaction was stopped by adding new medium.

The cell density and viability was determinate using ViCELL^{TM} cell viability analyzer (Beckman Coulter, Krefeld, Germany).

Trypsin-EDTA (T/E)	
Trypsin	0.5 g
Na$_2$EDTA	0.2 g
PBS	ad 1,000 ml

PBS$^+$	
NaCl	8.0 g
KCl	0.2 g
Na$_2$HPO$_4$	1.15 g
KH$_2$PO$_4$	0.2 g
MgCl$_2$x6H$_2$O	0.1 g
CaCl$_2$x2H$_2$O	0.1 g
H$_2$O	ad 1,000 ml

PBS	
NaCl	7.2 g
Na$_2$HPO$_4$	1.48 g
KH$_2$PO$_4$	0.43 g
H$_2$O	ad 1,000 ml

3.6 Freezing and thawing

From all cell lines nitrogen stocks were prepared. After centrifugation for 10 min. at 180 x g, 4$^°$C the pellet was resuspended using freezing medium (70 % normal medium for each cell line, 10 % DMSO and 20 % additional/FCSgold) to a concentration of 2-3x10^6 cells/ml. 1.5 ml of the cell suspension were transferred into cryovials and stored overnight at -20$^°$C. Afterwards, cells were stored at -85$^°$C or transferred into liquid nitrogen for long time storage.

For thawing, cells were quickly defrozen in the water bath and diluted with 10-15ml pre-warmed medium. Subsequently, cells were centrifuged for 10 min. at 180 x g to remove the DMSO and transferred into new medium. Cells were cultivated at least for 4-5 days before they were used for experiments.

4 Cytotoxicity measurement (MTT assay)

The MTT assay is a colorimetric method to measure cell survival and cytotoxicity of tested substances. In healthy cells, the mitochondrial dehydrogenase converts the yellow tetrazolium salt (MTT) into violet formazan. This reaction is proportional to the cell number and viability of the cells in the sample [90].

Cells were seeded into 96-well plates (100µl/well) as described in 3.5 and stimulated for the indicated times with the indicated compounds. Afterwards, 10µl MTT solution (5mg/ml in PBS) per well was added and cells were incubated for 1-2 hours. To dissolve the formazan crystals in the cells, 190µl DMSO were added per well and cells were incubated at room temperature under gentle agitation for one hour. The absorption was measured in the Tecan microplate reader (Sunrise^{TM}, Crailsheim, Germany) at 550 nm. Untreated cells were set at 100 % viability.

5 Proliferation measurement

The crystal violet assay is a quantitative method to measure the cell number and proliferation. The crystal violet dye is absorbed in the nuclei of cells and the amount is proportional to the cell number.

Cells were seeded into 96-well plates (100µl/well) as described in 3.5 and stimulated for the indicated times. Afterwards, medium was discarded and 100µl crystal violet solution (0.5 % crystal violet in 20 % methanol) per well was added. Cells were incubated for 10 min under agitation. The dye was removed by washing with H$_2$O and subsequently the plate was air dried. The crystal violet was dissolved from nuclei with destaining solution (0.1 M sodium citrate in 50 % ethanol or with 0.1 % SDS). The absorption was measured on the Tecan at 550 nm. The untreated cells were set at 100 % viability.

6 Light and fluorescence microscopy

Light microscopy is a convenient method for detecting morphological changes in the dying cell, such as cell shrinkage as well as cell blebbing and cellular swelling. Other features of the apoptotic cell like chromatin condensation can be detected after Hoechst 33342 application in the fluorescence microscope. Hoechst 33342 is a cell permeable, vital dye which intercalates into the DNA. In contrast to healthy cells, nuclei from apoptotic cells are fragmented and DNA is strongly condensed resulting in the emission of intense blue signals.

Cells were seeded as described and stimulated for the indicated time. Afterwards, cells were monitored with a Zeiss Axiovert 200 microscope (Zeiss, Oberkochen, Germany)

connected to a Imago-QE camera system (Till Photonics, Gräfelfing, Germany) with or without Hoechst 33342 (5µg/ml) staining.

7 Flow cytometry

Flow cytometry allows multiparameter analysis of single particles suspended in a stream of liquid in a very short time. Each particle (e.g. cell) individually passes a laser beam, gets illuminated and can be characterized due to its physical properties such as size, granularity and fluorescence.

To move cells through a laser beam one after another, the principle of hydrodynamic focusing is applied (see Figure II.2). The sample is injected into a stream of sheath fluid within the flow chamber, where the sheath fluid accelerates the particles and restricts them to the center of the sample core.
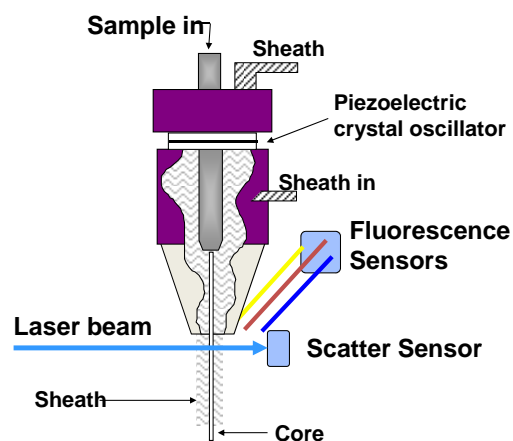
Figure II.2 Principles of the hydrodynamic focusing (from [91])

In the flow chamber the suspension of single cells emerges from the sample needle into a surrounding sheath fluid moving with greater velocity. The sheath fluid accelerates the particles, restricts them to the center of the sample core and forces them to travel one by one in the central portion of the fluid.

When particles pass the laser beam the light is scattered and the forward scatter (FSC) is measured in line with the laser beam and is proportional to the cell size. The sideward scatter (SSC) is measured from perpendicular light scattering and is proportional to the amount of inclusion within particles. Beyond these properties, fluorescence can be measured. Simultaneously, if the particles e.g. cells have their own fluorescence source (e.g. cells transfected with GFP) or were stained with fluorochromes (e.g. propidium iodide) fluorescence occurs. The scattered and fluorescence light is collected by lenses and forwarded to the appropriate detectors.

All measurements were performed on a FACSCalibur (Beckton Dickinson, Heidelberg, Germany) with a 488nm argon laser.

The PMBCs and primary leukemic blasts were stimulated as indicated directly after isolation and examined for cell death by forward/side scatter analysis in FACscan after 48 hours. Apoptotic cells were defined as smaller and more granular cells in comparison to control cells.

Sheath fluid	
NaCl	8.12 g
KH_2PO_4	0.26 g
Na_2HPO_4	2.35 g
KCl	0.28 g
Na_2EDTA	0.36 g
LiCl	0.43 g
Na-azide	0.20 g
H_2O	ad 1,000 ml
pH 7.37	

7.1 Nicoletti assay

The Nicoletti assay is a rapid method to evaluate changes of cellular DNA amount and integrity. Besides, the method allows monitoring of the cell size and granularity changes within a cell population. Originally, the method was introduced by Nicoletti et al. [92]. Cells get permeabilized with Triton-X-100 and incubated with propidium iodide.

Cells were seeded as described in 3.5 and stimulated for the indicated times. Afterwards, cells were harvested and centrifuged for 10 min. at 600 x g, 4°C. The supernatant was discarded and the cell pellet was washed with ice cold PBS, the centrifugation procedure was repeated and the pellet was resuspended in hypotonic fluorescence solution (0.1 % sodium citrate, 0.1 % Triton-X-100) containing 50µg/ml propidium iodide. After 2 hrs or overnight incubation at 4°C the cells were analyzed in FACS with CellQuest Pro software. The cells left to the G_0/G_1 peak were considered as apoptotic cells (sub.G_0/G_1, see also Figure II.3).
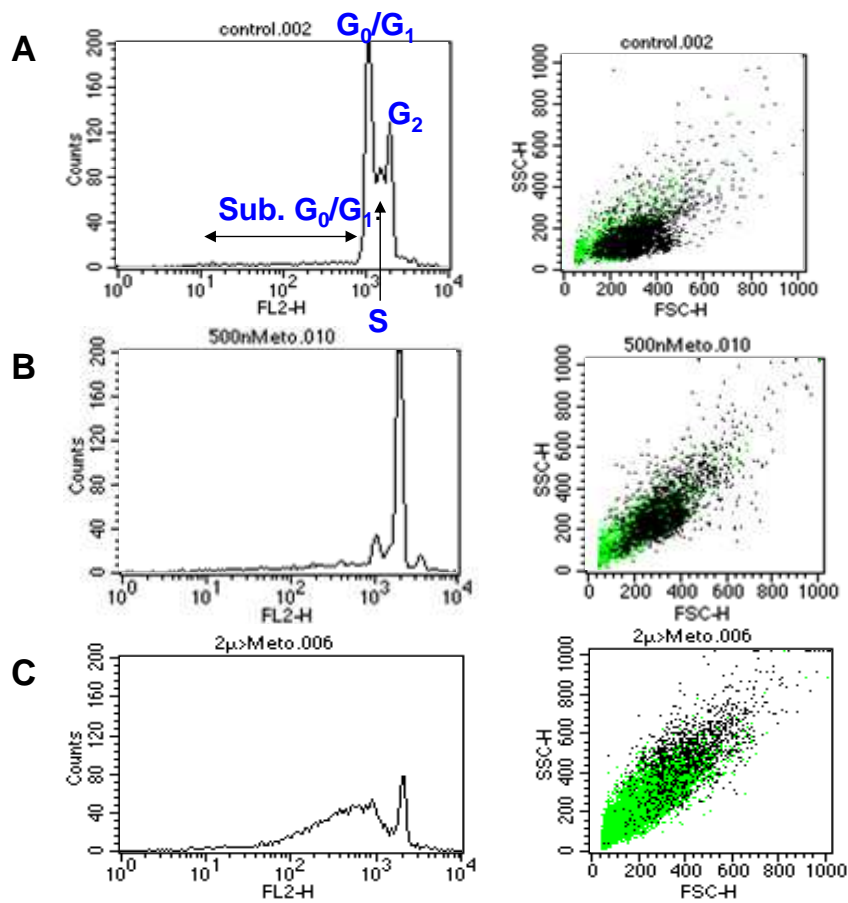
Figure II.3 Data analysis of the Nicoletti assay with CellQest Pro software

Histogram plot (left insert) or dot plot (right insert) from untreated control cells (A), cells stimulated for 24 hrs with 500nM etoposide (B) or 2μM etoposide (C). The sub G_0/G_1 area is defined as apoptotic.

8 Western blot

Western blot is a common method to analyze the proteins in a cell lysate. Proteins are solubilized and boiled at 95°C in the presence of SDS (for denaturation) and DTT or 2-mercaptoethanol (for reduction of disulfide bounds). So prepared samples are loaded on polyacrylamide gels were proteins are separated towards their molecular weight in the electric field. Afterwards, proteins are transferred onto a membrane and the protein of the interest is detected with a specific antibody.

8.2 Preparation of samples

8.2.1 Whole lysate preparation

Lysis buffer	
30 mM	Tris-HCl, pH 7.5
150 mM	NaCl
2 mM	EDTA
1 %	Triton X-100
	Complete™

Lysis buffer for phosphorylated proteins
50 mM Hepes
50 mM NaCl
5 mM Na_2EDTA
10 mM $Na_4P_2O_7$
50 mM NaF
1 mM Na_3VO_4
1 % Triton-X-100
PMSF
Complete™

For experiments, cells were prepared as described (see 3.5). At least 3ml of the cell suspension were pooled and centrifuged for 10 min. at 400 x g, $4°$C. The pellet was washed with 1ml ice cold PBS and incubated for 0.5 hrs with the appropriate lysis buffer. Afterwards, the suspension was centrifuged for 10 min. at 10,000 x g, $4°$C and the supernatant was collected in new tubes. One part was used for determination of protein concentration (see chapter 8.4); the rest was diluted with Laemmli buffer (4 parts of the lysate, 1 part of the buffer) and boiled for 5 min at $95°$C. Samples were used immediately or stored at $-20°$C.

Sample buffer (5 x)	
3.125 M Tris-HCl, pH 6.8	100 µl
Glycerol	500 µl
SDS 20 %	250 µl
DTT 16 %	125 µl
Pyronin Y 5 %	5 µl
H_2O	ad 1,000 µl

8.3 Preparation of cytosolic and mitochondrial fractions

In the apoptotic process the compartmentation of mitochondrial proteins such as cytochrome c, smac/DIABLO, Omi/HtrA2 and others plays a pivotal role. After mitochondria permeabilization, these proteins are release into the cytosol and induce the apoptotic cascade. To investigate the release of proteins from mitochondria, cells were permeabilized using buffer containing digitonin. Digitonin binds to cholesterol and

forms micropores in the membranes. Thus, the hypotonic buffer cytosol fraction is eluted, whereas organelles remain within the cell.

Permeabilization buffer (pH 7.2)	
Mannitol	210 mM
Sucrose	70 mM
Hepes pH 7.2	10 mM
Na_2EGTA	0.2 mM
Succinate	5 mM
BSA	0.15 % (w/v)
Digitonin	60 µg/ml

For experiments, cells were prepared as described (see 3.5). At least 3ml of the cell suspension were pooled and centrifuged for 10 min. at 360 x g at 4°C. The pellet was washed with 1ml ice cold PBS and incubated for 20 min with 100µl of permeabilization buffer. The cytosolic fraction was obtained by centrifugation of the cell suspension at 360 x g (4°C, 10 min) and the supernatant was cleared from any remaining cell fragments at 13,000 x g (4°C, 10 min). The pellet of the first centrifugation after permeabilization contains mitochondria, other organelles and membranes were resuspended in 0.1% Triton-X 100 in PBS (100µl) and lysed for 15 min on ice. The supernatant of a subsequent centrifugation step (13,000 x g, 4°C, 10 min) constitutes the mitochondria-enriched fraction. A part of the lysate was used for determination of protein concentration (see chapter 8.4) and the rest was diluted with Laemmli buffer (4 parts of the lysate, 1 part of the buffer) and boiled for 5 min at 95°C. Probes were used immediately or stored at -20°C.

8.4 Protein quantification

The Bradford method [93] was used for protein quantification. This method is based on the binding of the dye Coomassie Brilliant-Blue to proteins. The dye absorption maximum shifts from 465 nm to 595 nm after protein binding and the absorption is measured at 595 nm. To determine the protein concentration, samples with known BSA content are used as calibration curve.

Briefly, the protein samples were diluted 1:10 in water, 10µl of this dilution and from BSA calibration curve were pipetted in a 96-well plate and incubated for 5 min with 190µl of 5 times diluted Roti[R]-Quant (Roth, Karlsruhe, Germany). Absorbance was measured at 592 nm in a microplate absorbance reader (Sunrice[TM], Tecan, Crailsheim, Germany).

8.5 SDS-PAGE

Stacking gel	
PAA solution 30 %	1.7 ml
1.25 M Tris-HCl pH 6.8	1 ml
SDS 10 %	100 µl
H_2O	7 ml
TEMED	20 µl
APS	100 µl

Separating gel (10 %)	
PAA solution 30 %	5 ml
1.5 M Tris-HCl pH 8.8	3.75 ml
SDS 10 %	150 µl
H_2O	6.1 ml
TEMED	15 µl
APS	75 µl

Equal amounts of the protein lysates were separated by discontinuous denaturizing SDS-PAGE according to the method introduced by Laemmli [94]. Sodium dodecyl sulphate (SDS) is used to solubilize the proteins upon binding to hydrophobic parts. Thereby protein secondary and tertiary structures are destroyed. Further unfolding is achieved by the reducing agent dithiothreitol (DTT), which cleaves disulfide bonds. Proteins get highly negative charged by SDS and are though drawn towards the anode in an electric field. Therefore, the proteins are separated solely by their size in the polyacrylamide gel. This discontinuous electrophoresis system consists out of two layers: the stacking gel, where the proteins are concentrated and the separating gel, where the proteins are separated. The polyacrylamide (Rotiphorese^{TM} Gel 30, Roth, Karlsruhe, Germany) concentration in separating gel varies depending on the molecular weight of the proteins of interest.

Acrylamid concentration	Proteins
7.5 %	60-120 kDa
10 %	70-30 kDa
12 %	50-20 kDa
15 %	10-45 kDa

Electrophoresis buffer	
Tris base	3 g
Glycine	14.4 g
SDS	1 g
H_2O	ad 1,000 ml

To determine the molecular weight, samples were compared with prestained broad range molecular weight marker (MBI-Fermentas, St. Leon-Rot, Germany). Electrophoresis was performed using the vertical Mini Protean III system (BioRad, Munich, Germany). Electrophoresis was run at 100 V for 21 min for stacking of proteins and at 200 V for 35-40 min for the separation of proteins in the electrophoresis buffer.

8.6 Western blotting and detection

Tank buffer (5 x)	
Tris base	15.2 g
Glycine	72.9 g
H_2O	ad 1,000 ml

Tank buffer (1 x)	
Tank buffer (5 x)	200 ml
Methanol	200 ml
H_2O	ad 1,000 ml

Tank blot technique was used for protein transfer from gels onto nitrocellulose blotting membranes (Hybond™-ECL™, Amersham Biosciences, Freiburg, Germany) or PVDF blotting membranes (Immobilion-P, Millipore, Schwalbach, Germany). Membranes were activated in 1 x blotting buffer for 10 min and transfer sandwiches were assembled as follows:

sandwich holder cathode side
wetted pad
blotting paper
gel
membrane
blotting paper
wetted pad
sandwich holder anode side

Sandwiches were inserted into a transfer device (Mini Trans-Blot®, BioRad, Munich, Germany) and transfer was performed in electrophoresis chamber filled up with 1 x transfer buffer at 4°C at 100V for 60-90 min or at 23 V overnight.

After transfer membranes were incubated with 5 % non fat milk (BioRad, Munich, Germany) in TBS-T and subsequently with diluted antibody of interest for 2 hrs at RT or over night at 4°C under gentle shaking.

TBS-T	
Tris base	3 g
NaCl	11.1 g
Tween 20	1 ml
H_2O	ad 1,000 ml

Afterwards, membranes were washed 3 times for 10 min with TBS-T and incubated with secondary antibody conjugated to horseradish peroxidase for 1 hour. The membrane was washed 3 times for 10 min with TBS-T, all steps concerning membrane incubation were prepared upon gentle agitation. Proteins were visualized using the ECL solution. The enzyme horseradish peroxidase (HRP) catalyzes the oxidation of luminol in the presence of H_2O_2. After 1 min of incubation of membranes with ECL solution luminescence was detected by exposure of membranes to an X-ray film and developed with a Curix 60 Developing system (Agfa-Gevaert AG, Cologne, Germany).

II Materials and Methods

Table 4 Primary antibodies

Antibody	Isotype	Dilution	Company	Order number
Actin	Mouse IgG	1:1,000	Milipore	MAB1501R
Caspase 2	Mouse IgG$_1$	1:1,000	Transduct.Lab/BD	611022
Caspase 3	Rabbit IgG	1:1,000	Santa Cruz	sc-7148
Caspase 8	Mouse IgG$_{2b}$	1:1,000	Upstate	05-477
Caspase 9	Rabbit IgG	1:1,000	Cell Signaling	9502
Cytochrome c	Rabbit IgG	1:1,000	Cell Signaling	4272
Cytochrome c oxidase	Mouse IgG$_{2a}$	1:1,000	Molecular Probes	A6403
HtrA2/Omi	Rabbit IgG	1:1,000	RD Systems	AF1458
PARP	Mouse IgG$_1$	1:100	Oncogene	AM30
Smac/DIABLO	Rabbit IgG	1:500	Biozol	BZL 00676
XIAP	mouse IgG$_1$	1:250	Transduct.Lab/BD	610717

Table 5 Secondary antibodies

Antibody	Dilution	Company	Order number
Goat anti-mouse IgG$_1$: HRP	1:1,000	Biozol	BZL04266
Goat anti-mouse IgG: HRP	1:1,000	Santa Cruz	sc-2005
Goat anti-mouse IgG$_{2a}$: HRP	1:1,000	Southern Biotech Assoc.	1080-05
Goat anti-rabbit: HRP	1:10,000	BioRad	172-1013
Alexa Fluor® 680 Goat anti-mouse IgG	1:10,000	Molecular Probes	A-21057

Alexa Fluor® 680 Goat anti-mouse IgG is directly labeled with infrared (IR) fluorophore with emission at 700 nm. Proteins of interest were detected using Odyssey imaging system (Li-COR Biosciences GmbH, Bad Homburg, Germany).

ECL solution	
Tris HCl, pH 8.5	1 ml
1M Luminol	50 µl
1M p-coumaric acid	22 µl
H_2O_2	3 µl
H_2O	9ml

8.7 Membrane stripping

In certain cases the PVDF membrane was reprobed with other antibodies which have approximately the same molecular weight as the first detected antibody. In this case membrane was incubated for 10 min at room temperature with 0.5 % NaOH or for 30 min at 50°C in the stripping buffer. Subsequently membrane was blocked with 5 % non-fat milk for one hour and incubated with the next antibody of interest.

Stripping buffer	
Tris-HCl pH 6.8	62.5 mM
SDS	2 %
2-mercaptoethanol	100 mM

8.8 Staining of gels and membranes

For the visual control of the Western Blot procedure the gels were stained for 10 min with Coomassie Blue solution and subsequently bleached with destaining solution. The membranes were stained with 0.2 % Ponceau S (Sigma, Taufkirchen, Germany) solution and destained with TBS-T.

Coomassie staining solution			Coomassie destaining solution	
Coomassie Blue	3 g		Glacial acetic acid	100 ml
Glacial acetic acid	100 ml		Ethanol	333.3 ml
Ethanol	450 ml		H_2O ad	1,000 ml
H_2O	ad 1,000 ml			

9 Caspase activity assay

Caspase activity can be analyzed in Western blot analysis by the detection of active cleavage products (see chapter 8). Another method to assess the caspase activity is based on the ability of caspases to specifically cleave their substrates. The peptide-based small substrates with a tetrapeptide sequence carrying the preferred caspase consensus sequence (see chapter I.6.2.3) are coupled to a fluorogenic reporter, which produces a fluorescence signal upon cleavage.

Cells were prepared as described in 3.5 and stimulated with compounds. Cells were collected by centrifugation, washed with ice cold PBS and stored with 70µl/sample lysis buffer at -85°C over night. Afterwards, lysate were centrifuged (10,000 x g, 4°C), supernants were collected and incubated with caspase substrate (Bachem, Bubendorf, Germany) in a 96-well plate. The reading was performed in a plate-reading multifunction photometer (Spectrafluor PLUS, Tecan, Crailsheim, Germany). The

activity was calculated from the difference between fluorescence in the 0 point and after 1 or 3 hrs of substrate incubation for caspase-3 and-9, respectively. Protein concentration of the samples was used for normalization.

Lysis buffer for caspase activity	
5 mM	$MgCl_2$
1 mM	Na_2EGTA
0.1 %	Triton-X-100
25 mM	HEPES, pH 7.5

10 Clonogenic survival assay

The clonogenic survival or colony formation assay is an *in vitro* method to investigate the long term effects of drugs on cell survival. Moreover, it can be examined in this test if the substances are able to kill the whole cell population, what is of high interest for the anti-cancer therapy.

Suspension cells were seeded in 24-well plates as described in 3.5 and stimulated for 1-4 hrs. Afterwards, cells were washed with PBS, replaced in new medium, counted and diluted to a concentration of 5×10^5/ml. 0.1 ml of this suspension was diluted with 0.9 ml of clonogenic assay medium (20 % methocult, 40 % FCSgold, 40 % normal medium). Cells were seeded in 96-well plates (100µl cell suspension/well) and kept under normal growth conditions. After seven days a picture of each well was taken and colony number was counted (at least 5 cells in each colony).

Adherent cells were seeded in 6-well plates (2×10^4 cells/well) and stimulated as indicated for 24 hrs. Afterwards, cells were washed two times with PBS^+, supported with new medium and allowed to grow for six days. Afterwards, cells were stained with crystal violet (0.5 % crystal violet in 20 % methanol) for 10 min., the unbound crystal violet was subsequently removed by washing with water and the plates were air dried. Intracellular crystal violet was solved and absorption at 550 nm was measured. The untreated cells were set at 100 % viability.

11 Reporter gene assay

Firefly luciferase is widely used as a reporter to study gene expression. Light is produced by converting the chemical energy of luciferin oxidation through an electron transition, forming the product oxyluciferin. The enzyme catalyzes the luciferin oxidation using ATP and Mg^{2+} as co-substrates. The generated flash of light can be measured on a luminometer.

II Materials and Methods

HEK-293 cells were seeded at a concentration of 4 x 10^6 cells/100 mm dish. The next day, Ca^{2+}-phosphate transfection was performed. Cells were co-transfected with 2.8 µg of a plasmid containing 5.7 kB of the human NF-κB promoter driving a firefly luciferase gene (pNF-κB-Luc, Stratagene, LaJolla, CA, USA) and 90 µg of a β-galactosidase plasmid (pβ-Gal, 6.82 kB, Promega, Mannheim, Germany). Transfection efficiency was controlled by transfecting pEGFP (Clontech, Mountain View, USA). After 6 hrs cells were washed with PBS^+ and allowed to grow over night to grow. Cells were seeded in 24-well plates at the concentration of 1 x 10^5 cells/well and allowed to attach over night. Cells were stimulated with increasing concentrations of T8 or with 50 µM pyrrolidine dithiocarbamate (PDTC) for 0.5 hour following stimulation with 1ng/ml TNFα for the next 5.5 hrs. Afterwards, cells were washed with PBS^+, 100µl lysis buffer (Promega, Mannheim, Germany) per well was added and samples were frozen at -85°C over night.

Lysate were incubated for 15 min under gentle agitation and subsequently, 50µl of lysate/sample were transferred into white 96-well plates. Luciferase activity was measured on Orion II Microplate Luminometer (Berthold Detection Systems, Pforzheim, Germany) using luciferase assay buffer.

As a control, β-galactosidase activity measurement was performed in a plate-reading multifunction photometer (Spectrafluor PLUS, Tecan, Crailsheim, Germany) at 505 nm. Briefly, 20µl of cell lysate from luciferase assay was transferred into 96-well plates and 180 µl of substrate buffer was added (200µl of 50nM CPRG, 20 µl β-mercaptoethanol in 20ml Z-buffer). The enzyme activity was calculated as the difference between fluorescence in the 0 point and after 16 hrs and was used for luciferase activity normalization.

Luciferase assay buffer		Z-buffer	
D-Luciferin	470 µM	Na_2HPO_4 x2H_2O	60 mM
Coenzym A	270 µM	NaH_2PO_4 x H_2O	40 mM
DTT	33.3 mM	KCl	10 mM
ATP	530 µM	$MgCl_2$ x 6H_2O	10 mM
$MgSO_4$	2.67 mM	H_2O	ad 500ml
Tricine	20 mM		
EDTA	0.1 mM		

12 TaqMan reverse-transcriptase-polymerase chain reaction

RNA was isolated from Jurkat leukemia cells with the RNeasy Mini Kit (Qiagen, Hilden, Germany) following the manufacturer´s protocol. RNA purity was confirmed by the 260/280 nm ratio and its integrity was visualized by agarose gels. Total RNA (2 µg) was reverse-transcribed using TaqMan® Reverse Transcriptase Reagents (Applied Biosystems, Foster City, USA). Experiments were performed employing the ABI 7300 Real-Time PCR System (Applied Biosystems, Foster City, USA) using the TaqMan® Universal PCR Master Mix Reagents Kit as recommended by the manufacturer. Ribosomal RNA (18S rRNA) was used as endogenous control. XIAP and 18s rRNA primer and probes were purchased as pre-designed TaqMan® Gene Expression Assays by ABI (Applied Biosystems, Foster City, USA).

13 Transformation of bacteria and plasmid purification

The Bir2 domain (residues 124-237 with Fesik mutation C202A C213G [64])with N-term 8 x His-tag and the Bir3 domain of XIAP (residues 252-348) with N-term 6 x His-tag plasmids, both in pET-15b Vector (Novagen, Darmstad, Germany) were kindly provided by Guy Salvesen (Burnham Institute for Medical Research, La Jolla, CA, USA).

For transformation, 100µl of a solution containing the competent *E.coli* DHα5 strain were incubated for 30 min on ice with 5µl of each plasmid, followed by incubation at 42°C for 30 sec. Subsequently, bacteria were placed on ice for 1-2 min and cell suspension was diluted with 900µl LB Medium (20g Lennox L Broth Base (Invitrogen)/l H_2O) and incubated for 2 hrs on the Thermomixer comfort (Eppendorf, Hamburg, Germany). 50µl of bacteria suspension were spread onto agar plates (15 g Lennox Agar (Invitrogen)/l H_2O) and incubated over night at 37°C. LB medium and agar plates were supplemented with 100 mg/ml ampicillin (Calbiochem).

Colonies were picked from the agar plates, inoculated into 2-3 ml of LB medium and grown in a thermoshaker over night. Plasmids were isolated with EndoFree QIAprep Spin Miniprep Kit (Qiagen, Hilden, Germany) according to provided instruction. The quality of the plasmid purification was analyzed by agarose gel electrophoresis. Subsequently, bacteria cultures were expanded in 100 ml of LB medium and plasmid purification was prepared using EndFree Plasmid Maxi Kit (Qiagen). The plasmids were dissolved in endotoxin free H_2O and the DNA concentration was determined with NanoDrop ND-1000 Spectrophotometer (PeqLab Biotechnologie GmbH, Erlangen, Germany). Plasmids were stored at -20°C.

From bacteria a glycerol stock was prepared as following: 750µl bacteria suspension was diluted in 250µl glycerol and shock frozen in liquid nitrogen. The prepared stocks were stored at -85°C.

14 Fluorescence polarization assay

Fluorescence polarization experiments were performed in collaboration with Martin Gräber in the group of Dr. Thorsten Berg from the Department of Molecular Biology at the Max Planck Institute of Biochemistry, Martinsried, Germany.
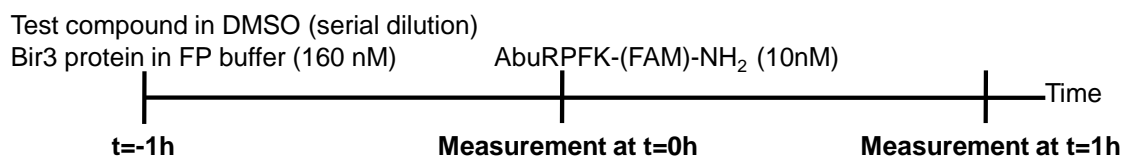
The fluorescence polarization assay is a fast and sensitive method for the screening of large chemical libraries in the search for binding partners to the targets of interest. For this reason the method is widely used in drug discovery. It based on the molecular weight which affects the polarization of fluorescence emission. The fluorescence polarization is relatively low when the fluorescence labeled molecule is small and high when fluorescence label is attached to large molecules. This increase in the polarization of the emitted fluorescence could also be observed after binding of small, fluorescence labeled molecules (e.g. peptides) to a large binding partner (e.g. protein domain) [95, 96]. The competition binding assay allows the detection of inhibitors (competitors) of the fluorescence labeled ligand and its binding partner. In our case it was used for pharmacophore modeling hypothesis validation.

XIAP-Bir3 (aa 238-353; based on NCBI GenBank entry U45880) in pET28a (Novagen Darmstad, Germany) and artificial smac-derived peptide AbuRPFK-(FAM)-NH$_2$ (published by Nikolovska-Coleska *et al.* [97]) were used in the assay. Binding experiments were performed in 384-well, black flat bottom plates (Corning, Lowell, USA) using an Ultra Evolution reader (Tecan, Crailsheim, Germany) as described by Schust and Berg [96].

FP assay buffer	
Hepes pH 7.5	10 mM
EDTA	1 mM
NaCl	50 mM
NP-40	0.1 %
DTT	1 mM

Test compounds were prediluted in DMSO and incubated with 160 nM XIAP-Bir3 protein for 1 hour at room temperature. Afterwards, fluorescence-labeled peptide (AbuRPFK-(FAM)-NH$_2$) at a final concentration of 10 nM in fluorescence polarization (FP) assay buffer was added. The final concentration of DMSO in the assay was 10 %. Binding curves were fitted with SigmaPlot (SPSS Science Software GmbH). Measurements were taken at point 0 and after 1h (see Figure II.4).

Test compound in DMSO (serial dilution)
Bir3 protein in FP buffer (160 nM)   AbuRPFK-(FAM)-NH$_2$ (10nM)

```
        |_____|_____|—— Time
      t=-1h                    Measurement at t=0h              Measurement at t=1h
```

Figure II.4 Preparation of fluorescence polarization measurement

160nM XIAP-Bir3 protein was incubated with the test compound in Eppendorf tubes at RT for 1 hour (t=-1h) prior addition of the smac-derived peptide AbuRPFK-(FAM)-NH$_2$ (final concentration 10 nM). The measurement was taken immediately at point 0 (t=0) and after 1 hour (t=1h).

15 Nuclear magnetic resonance analysis

The NMR analysis was performed in collaboration with Anders Frieberg (group of Prof. M. Sattler from the Institute of Structural Biology, Helmholtz Zentrum München and Chair of Biomolecular NMR, Technical University Munich, Germany).

Nuclear magnetic resonance (NMR) spectroscopy is a one of the main techniques to obtain structural data about molecules and their interactions in high resolution. The ^{15}N isotope has a net spin ½ making them suitable for nuclear magnetic resonance and for that reason the protein labeling with this isotope is a common method for NMR experiments.

^{15}N labeled proteins were prepared by growing the bacteria (Rosetta BL21, Novagen, Darmstad, Germany) transformed with appropriate plasmid in the minimal medium (M9) supplemented with 1g/l ^{15}NH$_4$Cl as the sole nitrogen source to produce uniformly ^{15}N-labeled protein [98]. Proteins were purified with nickel-nitrilotriacetic acid columns (Qiagen, Hilden, Germany) and eluted with 330μM imidazole. For measurement elution buffer was exchange into Bir2 buffer (20 mM Tris pH 8.3, 50 μM Zn(Cl)$_2$, 300 mM NaCl, 100 mM 1-methyl-imidazole, 2 mM β-mercaptoethanol) or into Bir3 buffer (20 mM NaP pH 6.8, 50 μM Zn(Cl)$_2$, 300 mM NaCl, 2 mM β-mercaptoethanol). Ligand binding was investigated by aquaring standard ^{1}H^{15}N HSQC experiments after the exchange of H$_2$0 buffer to a buffer containing ^{2}H$_2$O at 298K on a Bruker 600MHz Avance 3 spectrometer (Bruker, Billerica, USA). The spectra were recorded with samples containing 100 μM of ^{15}N labeled Bir2 or Bir3 with test compound (T8 or ABT-11 in DMSO) or without it. Then two spectra were compared to identify the chemical shifts perturbations induced by the additions of the test compound. Chemical shifts are expressed in dimensionless units of parts per million (ppm).

16 Statistics

All experiments were performed at least three times. Results are expressed as mean value ± SEM. Statistical analysis was performed with GraphPad Prism^{TM} version 3.03

using one-way ANOVA with Bonferroni or Dunnett multiple comparison post-test or unpaired two-tailed Student´s T test. P values < 0.05 were considered significant.

For primary cells specific apoptosis was calculated as [(absolute apoptosis of compound-treated cells – absolute apoptosis of untreated cells) / (100 – absolute apoptosis of untreated cells) x 100]. Synergistic effects were determined by analysis of the fractional product [99].

III Results

1 Spongistatin 1
1.1 Spongistatin 1 induces cell death in Jurkat leukemia T cells

To investigate the cytotoxic effects of spongistatin 1 on Jurkat T cells the MTT test was performed. As shown in Figure III.1A spongistatin 1 causes a concentration dependent decrease in cell viability. For a better characterization of the cell death profile of spongistatin 1 the DNA fragmentation assay according to Nicoletti was carried out. After 24 hrs exposure to spongistatin 1 wild type Jurkat showed a dose dependent increase in the DNA fragmentation (Figure III.1B). This feature is significant at the low concentration of 100pM. In comparison, the conventionally used cytotoxic drug etoposide needs an about 10,000 times higher concentration to induce the same effects.
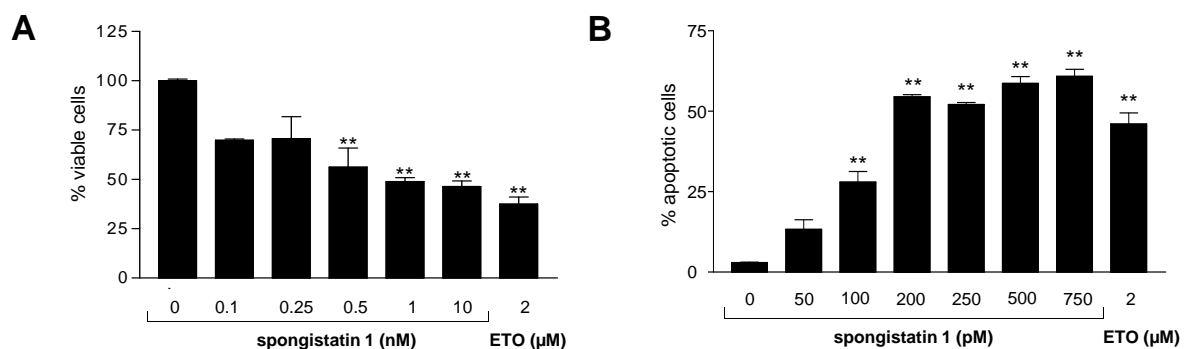
Figure III.1 Spongistatin 1 induces cell death in wild type Jurkat cells

Wild type Jurkat cells were stimulated with increasing concentrations of spongistatin 1 or with 2µM etoposide (ETO) for 24 hrs. A) Cell viability was quantified by MTT assay as described in "Materials and Methods"
B) Apoptotic cells were quantified by flow cytometry as described in "Materials and Methods". All experiments were carried out for three times. Bars, the ± SEM of three independent experiments performed in triplicate (**, P<0.01, ANOVA/Dunnett).

To visualize nuclei fragmentation, cells were treated with the fluorescence dye Hoechst 33342. The nuclei of cells 24 hrs exposed to spongistatin 1 are fragmented and chromatin is strongly condensed (Figure III.2). Both events are typical morphological changes in apoptosis (see also chapter I.5).

Control   spongistatin 1   etoposide
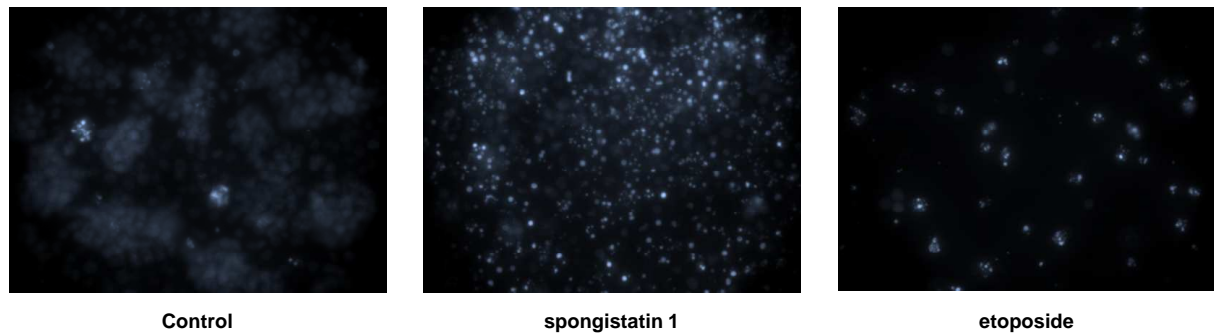
Figure III.2 Spongistatin 1 induces chromatin condensation in wild type Jurkat cells

Fluorescence microscopy pictures of wild type Jurkat cells. Cells were left untreated (control), treated with 200pM spongistatin 1 (spongistatin 1) or treated with 2µM etoposide (etoposide) for 24 hrs. Nuclei were stained with Hoechst 33342.

For the following experiments spongistatin 1 was applied at a concentration of 200pM. In this concentration after 24 hrs stimulation spongistatin 1 caused a DNA fragmentation of about 50 % in wild type Jurkat cells (Figure III.1B).

Next the cells were stimulated with spongistatin 1 for a time course up to 24 hrs. The DNA fragmentation occurred in a time dependent manner and was significant after 16 hrs exposure (Figure III.3).
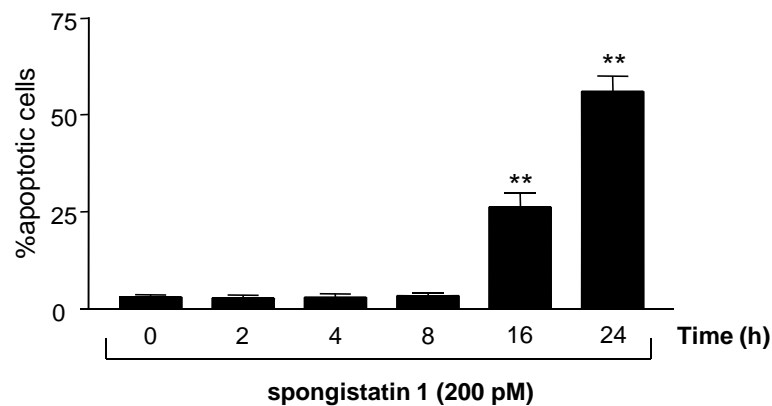

Figure III.3 Spongistatin 1 induces apoptosis in a time dependent manner

Wild type Jurkat cells were stimulated with 200pM spongistatin 1 for the indicated times. Apoptotic cells were quantified by flow cytometry as described in "Materials and Methods". The experiment was carried out for three times. Bars, the ± SEM of three independent experiments performed in triplicate (**, $P<0.01$, ANOVA/Dunnett).
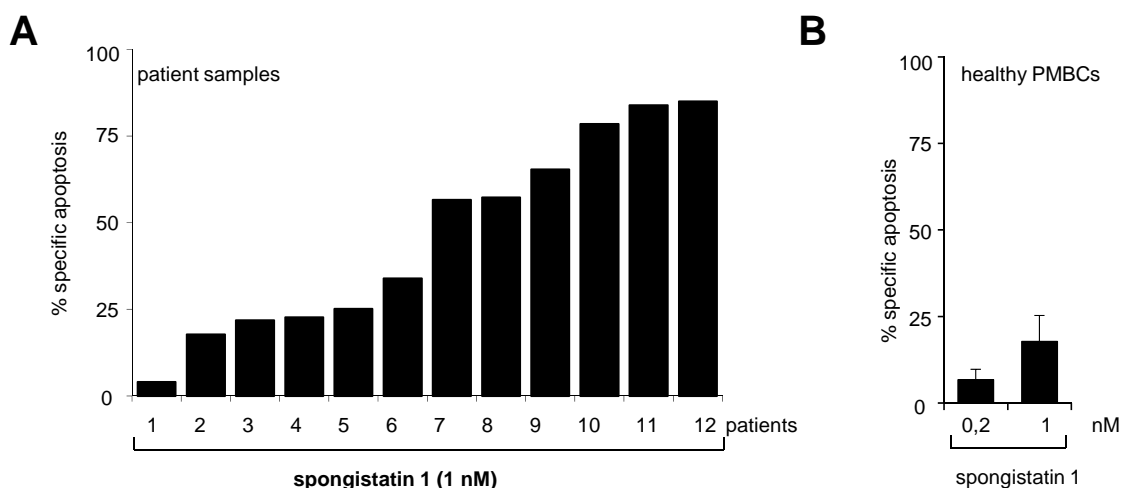
1.2 Spongistatin 1 induces cell death in primary leukemic cells

To examine the clinical relevance of spongistatin 1 in the treatment of acute leukemia the substance was tested on primary tumor cells obtained from children suffering from acute

leukemia. This part of the work was done in cooperation with the group of PD Dr. Irmela Jeremias (Department of Gene Vectors, Helmholz Center, Munich, Germany). To compare different primary cells, specific apoptosis was calculated as described in "Material and Methods" (chapter 16).

After 48 hrs spongistatin 1 at a concentration of 1 nM induced cell death in 11 out of 12 (91.7 %) samples (Figure III.4A). Most importantly, spongistatin 1 shows a minor toxicity on peripheral mononuclear blood cells (PMBCs) pointing to a rather selective effect on tumor cells.

Figure III.4 Spongistatin 1 induces cell death in primary leukemic cells but is low toxic for peripheral mononuclear cells

Samples were analyzed for percentage of apoptotic cells using forward/side scatter in FACScan A) Primary leukemia cells of 12 children with acute leukemia were isolated from bone marrow and incubated with spongistatin 1 for 48 hrs. Each bar represents data obtained from one patient. B) Peripheral mononuclear blood cells were isolated as described in "Materials and Methods" and stimulated with spongistatin 1 as indicated for 48 hrs. *Bars*, the mean ± SEM of three independent experiments performed in triplicate.

To show the extraordinary potency of spongistatin 1, other conventionally used cytotoxic drugs were tested in parallel (Figure III.5). *In vitro* spongistatin 1 was more effective than 8 out of 10 (80 %) drugs. Additionally, spongistatin 1 was used just in nanomolar range, whereas the other cytotoxic drugs were administrated at micromolar concentrations.
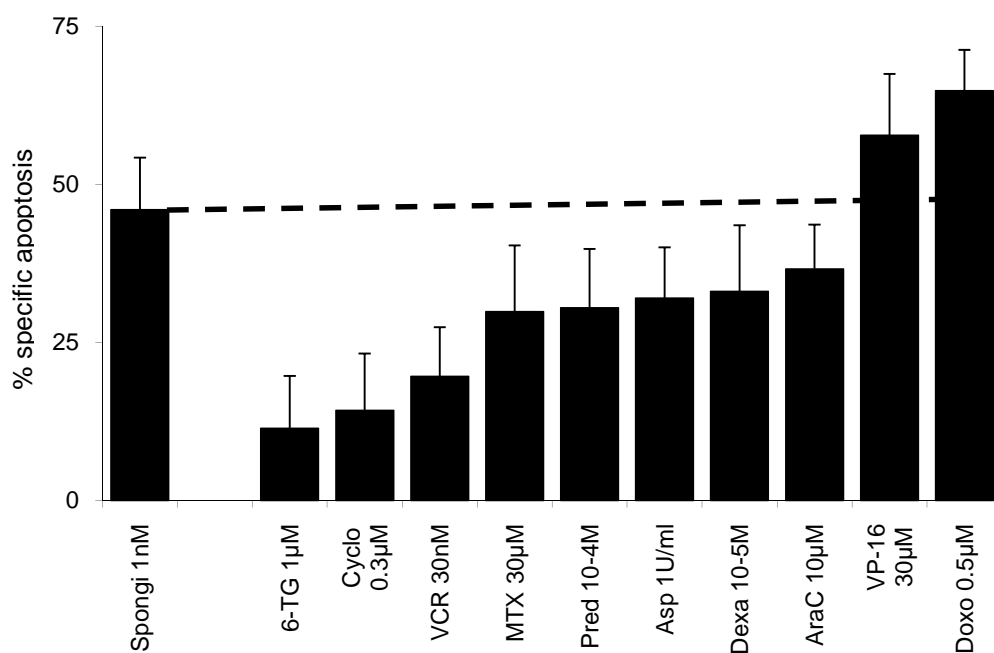
Figure III.5 Spongistatin 1 is more effective than conventional cytotoxic drugs

Primary leukemia cells of 12 children with acute leukemia were isolated from bone marrow and incubated with spongistatin 1 (Spongi, 1 nM) or 6-Thioguanin (6-TG, 1 µM), Cyclophosphamid (Cyclo, 0.3 µM), Vincristin (VCR, 30 nM), Methotrexat (MTX, 30 µM), Prednison (Pred, 10^{-4} M), Asparaginase (Asp 1 U/ml), Dexamethason (Dexa, 10^{-5} M), Cytarabin (AraC, 10 µM), Etoposid (VP-16, 30 µM) or Doxorubicin (Doxo, 0.5 µM) for 48 hrs. Samples were analyzed for percentage of apoptotic cells using forward/side scatter in FACScan. Bars represent mean of 12 samples $\pm$ SEM.

1.3 Spongistatin 1 inhibits clonogenic survival of Jurkat leukemic T cells

For long term analysis of the potency of spongistatin 1 in wild type Jurkat cells, clonogenic assay was performed. After stimulation with spongistatin 1 for just 4 hrs, Jurkat cells showed a strongly reduced ability to form new colonies, indicating chemotherapeutical potential of spongistatin 1 (Figure III.6).
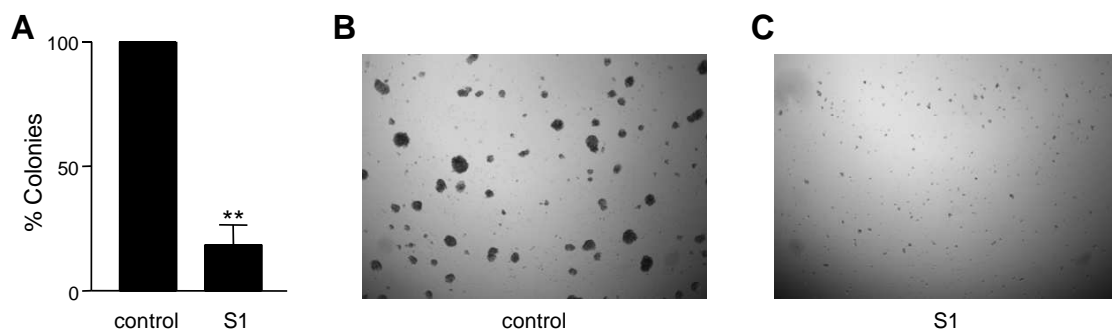
Figure III.6 Spongistatin 1 abrogates clonogenic survival of Jurkat T cells

Jurkat cells were left untreated or stimulated with spongistatin 1 (S1, 200 pM) for 4 hrs and clonogenic survival was analyzed as described in "Materials and Methods". Results are represented as the number of colonies referred to untreated cells (control). *Bars*, the mean ± SEM of three independent experiments performed in triplicate. ** P < 0.001 (ANOVA/Dunnett). Representative pictures of the experiments are shown (B, C).

1.4 Spongistatin 1 induce caspase-dependent apoptosis

Caspase activation is a molecular feature in the execution of the classical apoptotic program. To investigate if spongistatin 1-induced apoptosis is caspase-dependent the broad-range caspase inhibitor zVADfmk was used. Wild type Jurkat cells were pretreated with 25µM caspase inhibitor and stimulated with spongistatin 1 (200pM, 24 hrs) (Figure III.7). Interestingly, caspase inhibition led to an almost complete suppression of spongistatin 1-induced DNA fragmentation, demonstrating the importance of caspases in this apoptotic process.
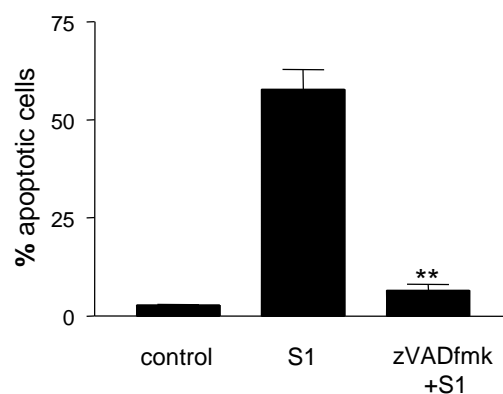
Figure III.7 Spongistatin 1 induced apoptosis is caspase dependent.

Wild type Jurkat were left untreated (control) or pretreated with zVADfmk (25µM, 1h) and incubated with 200pM spongistatin 1 (S1) for 24 hrs. Apoptotic cells were quantified by flow cytometry as described in "Materials and Methods". Bars, the ± SEM of three independent experiments performed in triplicate (**, P<0.001, unpaired two-tailed t-test).

The activation of the respective initiator and effector caspases was elucidated by Western Blot analysis (Figure III.8). The initiator caspases-8 and -9 as well as the effector caspases-3, -7 and -2 were activated 16 hrs after stimulation with 200pM spongistatin 1, as shown by the appearance of the cleavage products.

Poly-ADP-ribose-polymerase (PARP) is an important enzyme supporting the repair of single strand DNA-nicks. PARP cleavage (at 89 kDa) is a common feature of the apoptotic process and could be observed in spongistatin 1 treated cells (Figure III.8).
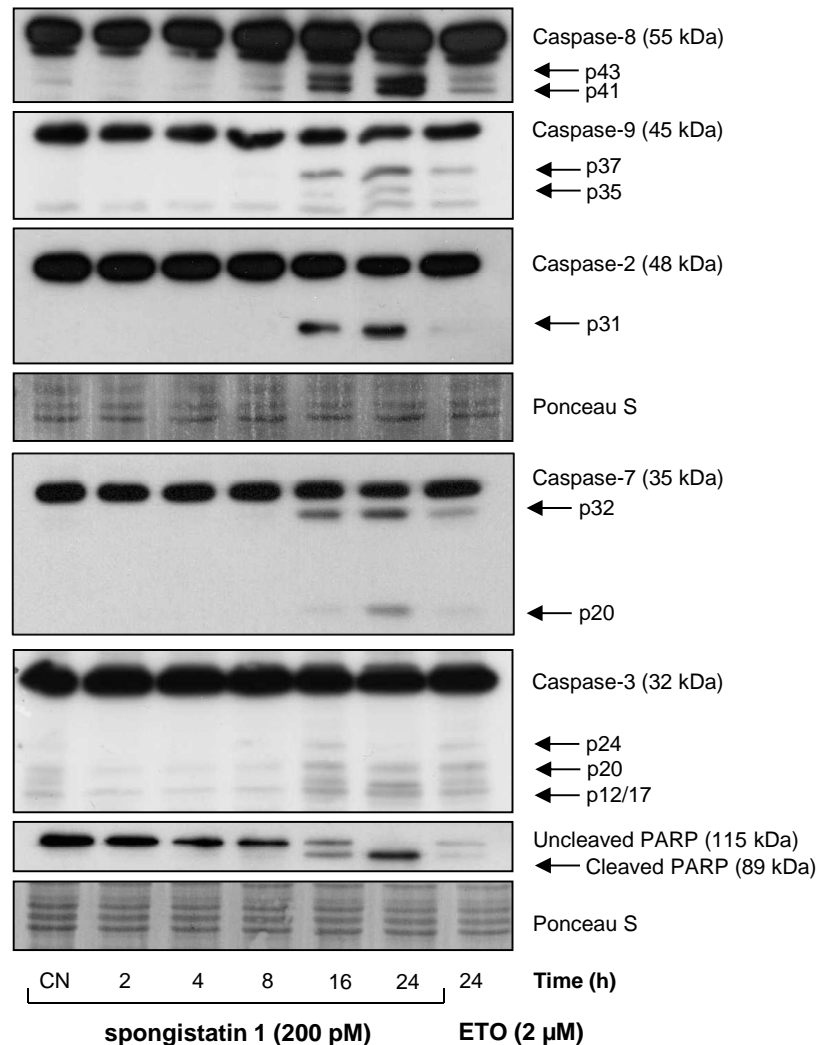
Figure III.8 Spongistatin 1 causes massive caspases activation and PARP cleavage in Jurkat cells

Wild type Jurkat cells were treated with 200pM spongistatin 1 or 2µM etoposide (ETO) for the indicated times. Whole cell lysates were prepared and activation of caspase-8, -9, -2, -3, -2, -7, and PARP cleavage was assessed by Western blot analysis as described in "Materials and Methods". Cleavage products are indicated by arrows. Ponceau S staining was used as loading control. A representative experiment out of three independent experiments is shown.

1.5 The extrinsic apoptotic pathway is not important for spongistatin 1 to induce apoptosis

In order to elucidate the impact of spongistatin 1 on the extrinsic apoptotic pathway, we used Jurkat cells deficient in caspase-8 (caspase-8-/- cells), FADD or CD95, respectively. In caspase-8-/- cells and in FADD (Fas associated death domain) deficient Jurkat cells, no reduction of apoptosis could be detected compared to control cells (Figure III.9A). Moreover, apoptosis was not inhibited in the subclone R-Jurkat cells, which lack the CD95 receptor (Figure III.9B), further supporting the idea that spongistatin 1 acts independent of the classical death-receptor pathway.
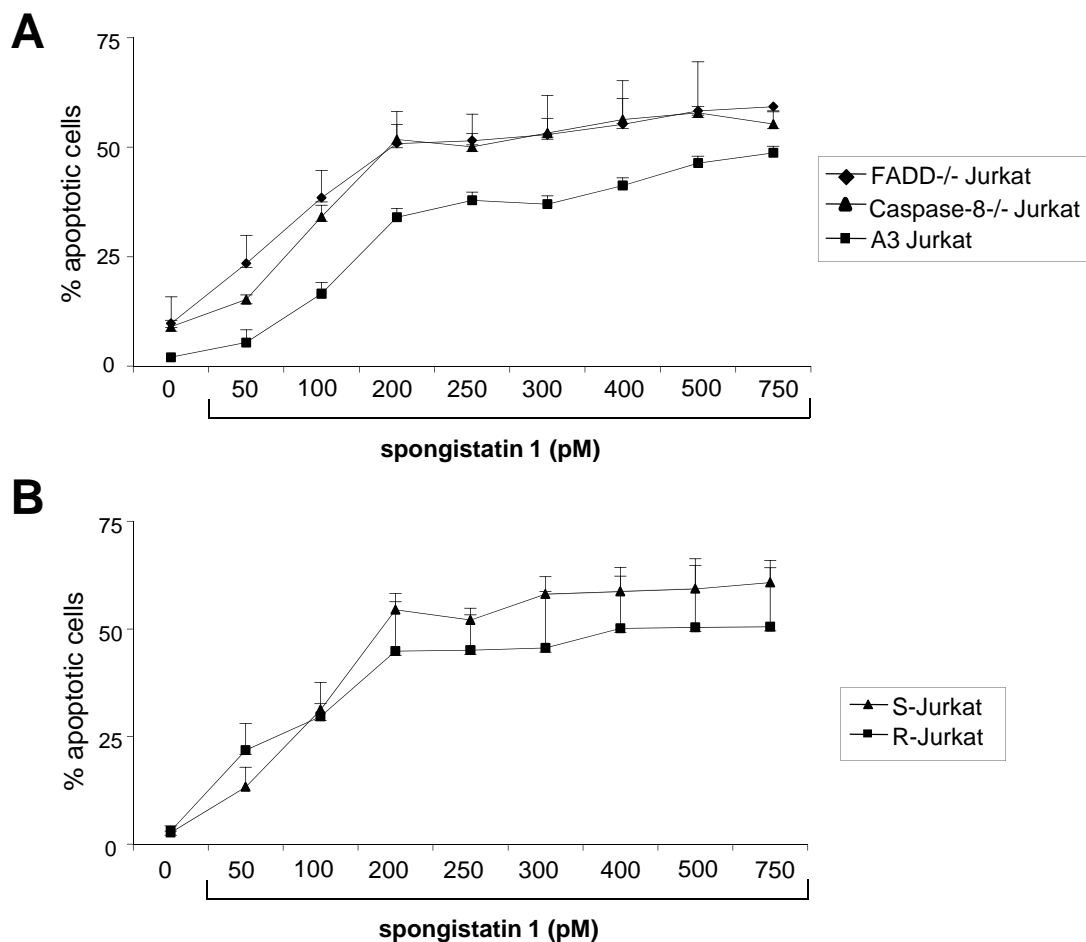
Figure III.9 Spongistatin 1 induces apoptosis independently of the CD95 receptor, the adaptor molecule FADD and caspase-8

Jurkat A3 (control cells), Jurkat caspase-8-/-, Jurkat FADD-/- cells (A) or S-Jurkat and R-Jurkat (lacking the CD95 receptor) (B) were treated with the indicated concentrations of spongistatin 1 for 24 hrs. Apoptotic cells were quantified by flow cytometry as described in "Materials and Methods". All experiments were carried out three times in triplicate. *Data points*, the mean ± SEM of three independent experiments.

1.6 Caspase-9 is essential for spongistatin 1 mediated apoptosis

Besides the extrinsic the intrinsic apoptotic pathway is an important way by which apoptosis can be trigged in cells. Caspase-9 as well as proteins released from mitochondria represents the central elements in this pathway (see also chapter I.128).

To investigate the impact of caspase-9 activation on spongistatin 1 induced apoptosis, caspase-9 deficient Jurkat cells were used. As shown in Figure III.10 caspase-9 deficiency completely inhibited spongistatin 1 induced apoptosis.
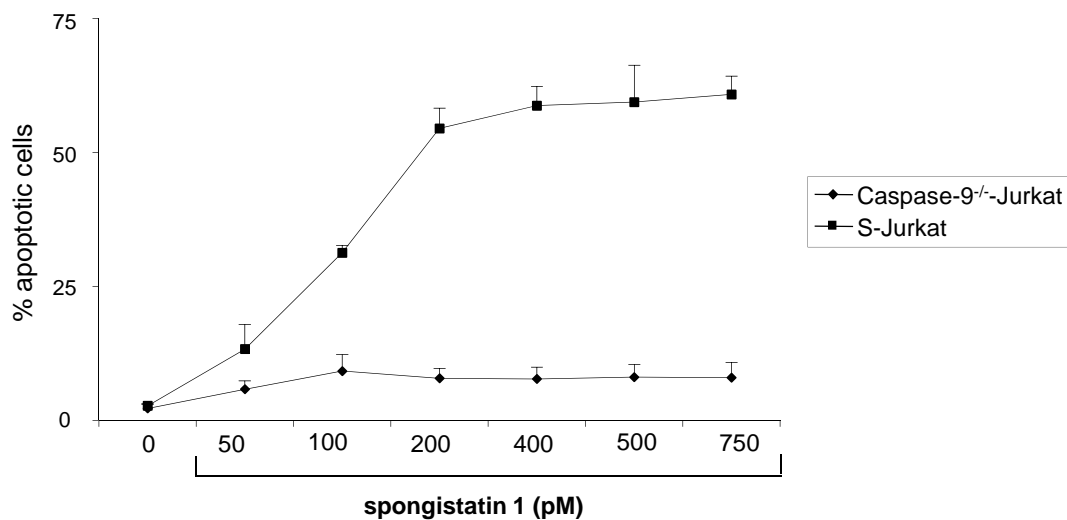
Figure III.10 Spongistatin 1 induced apoptosis is dependent on caspase-9

Control cells (S-Jurkat) and Jurkat caspase-9-/- cells were treated with the indicated concentrations of spongistatin 1 for 24 hrs. Apoptotic cells were quantified by flow cytometry as described in "Materials and Methods". All experiments were carried out three times in triplicate. *Data points*, the mean ± SEM of three independent experiments.

Moreover, in wild type Jurkat cells the activation of effectors caspases-3 and -2 could be observed (Figure III.8), whereas this effect is fully abolished in caspase-9 deficient Jurkat cells (Figure III.11).
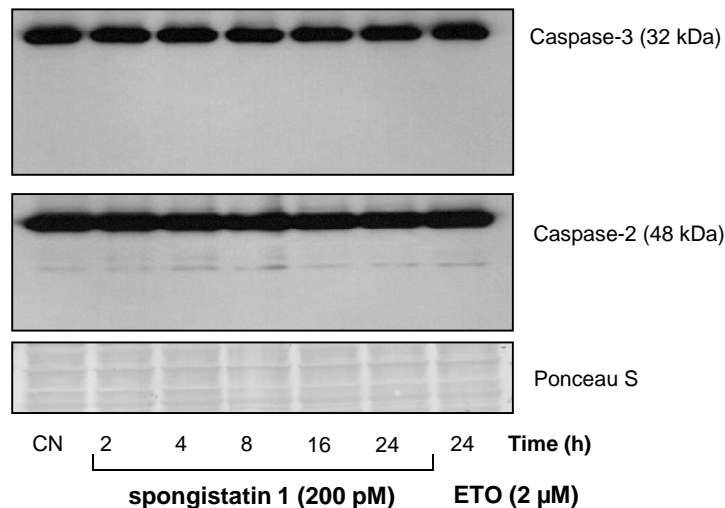
Figure III.11 Caspase-9 is important for the activation of effector caspases

Caspase-9 deficient Jurkat cells were incubated with 200 pM spongistatin 1 for the indicated times or with etoposide (ETO, 2µM, 24 hrs). Caspase-3 and -2 were detected by Western blot analysis as described in "Materials and Methods". A representative experiment out of three independent experiments is shown.

1.7 Mitochondria play a pivotal role in spongistatin 1 induced cell death

Since the intrinsic pathway seems to be important in spongistatin 1 induced apoptosis it was of high interest to investigate the release of proapoptotic proteins from mitochondria. Subcellular fractionation and Western blot analysis for cytochrome c, smac/DIABLO and Omi/HtrA2 was carried out. As shown in Figure III.12 spongistatin 1 induces release of cytochrome c, smac/DIABLO and Omi/HtrA2 from mitochondria into the cytosol after 16 hrs. For control of fractionation quality Western blot membranes were reprobed with cytochrome c oxidase (COX). This enzyme of the respiratory chain is localized to the inner mitochondrial membrane and can be used as a mitochondrial loading control. As expected the COX can be detected just in mitochondrial fraction and in whole cell lysate (Figure III.12) confirming the proper preparation of the fractions.
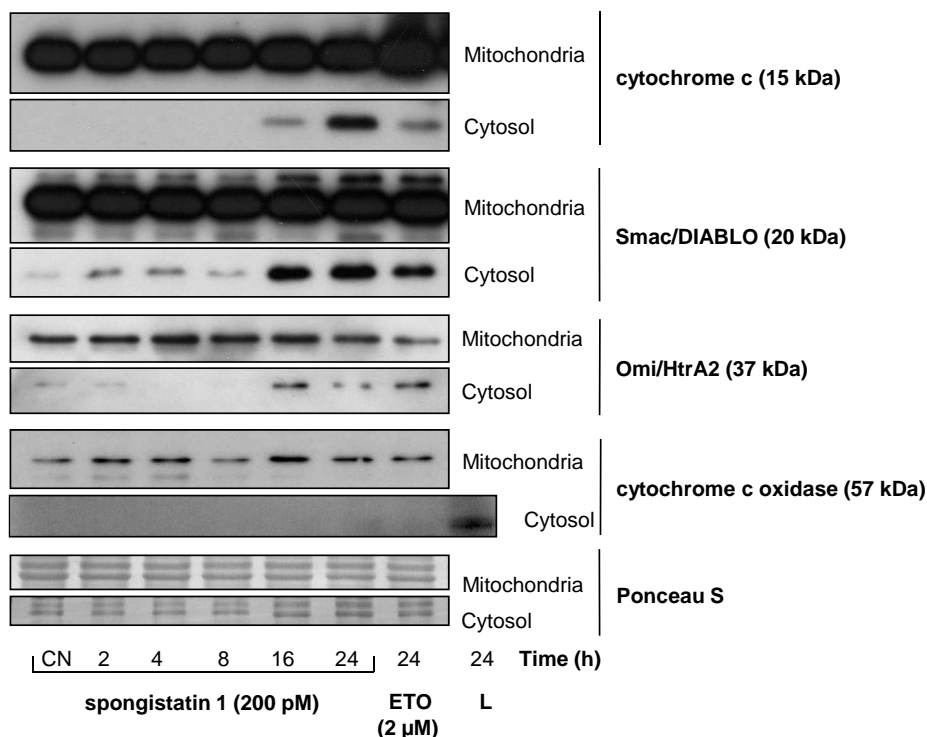
Figure III.12 Spongistatin 1 induces mitochondrial release of cytochrome c, smac/DIABLO and Omi/HtrA2

Jurkat cells were treated with 200pM spongistatin 1 for the indicated times or with etoposide (ETO, 24h, 2 µM). Cytosolic and mitochondrial fractions were prepared as described in "Materials and Methods". Cytochrome c, smac/DIABLO and Omi/HtrA2 were detected by specific antibodies using Western blot analysis. Cytochrome c oxidase served as control for the quality of the extraction procedure and a whole cell lysate (L) was used to control the blotting quality. Ponceau S was used as loading control. A representative experiment out of three independent experiments is shown.

1.8 Bcl-2 and Bcl-xl overexpression saves Jurkat cells from spongistatin 1 induces cell death

Bcl-2 and Bcl-xl are important proteins for saving the mitochondria membrane integrity. These two antiapoptotic members of the Bcl-2 family (see also chapter I.9) inhibit the pore formation in OMM and the release of proapoptotic proteins into the cytosol.

To analyze the role of Bcl-2 and Bcl-xl proteins in spongistatin 1 induced apoptosis, cells overexpressing the respective proteins were used. Figure III.13 shows that Bcl-xl as well as Bcl-2-overexpressing Jurkat cells were protected against spongistatin 1. In contrast, Neo-Jurkat carrying empty vector and serving as control cell line showed concentration dependent increasing apoptosis levels. This further emphasizes the idea that spongistatin 1 induces a mitochondria-dependent pathway of apoptosis.

50
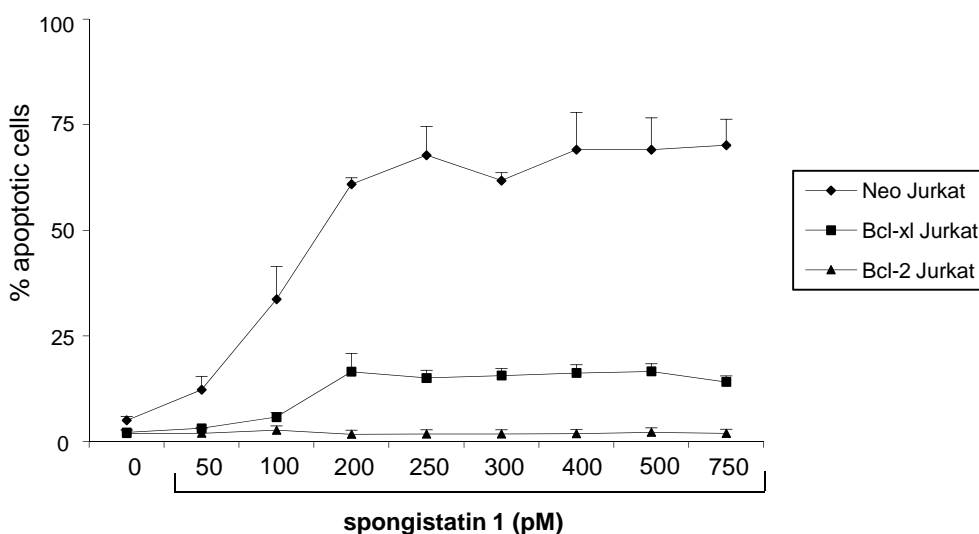
Figure III.13 Bcl-2 and Bcl-xl overexpression protects Jurkat cells from spongistatin 1 induced apoptosis

Neo-Jurkat, Bcl-xl-Jurkat and Bcl-2-Jurkat cells were incubated with the indicated concentrations of spongistatin 1 for 24 hrs. Apoptosis was quantified by flow cytometry as described in "Materials and Methods". *Data points*, the mean ± SEM of three independent experiments.

1.9 Spongistatin 1 induces cell death in XIAP overexpressing Jurkat cells

XIAP is the most potent natural cellular inhibitor of active caspases. Many tumor cells show XIAP overexpression which is discussed as one of the reasons for chemoresistance in cancer cells [100, 101]. Since the spongistatin 1 trigged apoptosis is dependent on caspases (see also chapter III.1.4) it was important to investigate the influence of XIAP overexpression on the efficacy of spongistatin 1 to induce cell death. Interestingly, spongistatin 1 is able to overcome overexpression of XIAP. XIAP overexpressing cells treated with various concentrations of spongistatin 1 for different time points died up to the same percentage as wild type Jurkat cells after 24 hrs treatment. (Figure III.14). In contrast, etoposide, a widely used chemotherapeutic agent failed to induce cell death in XIAP overexpressing cells.
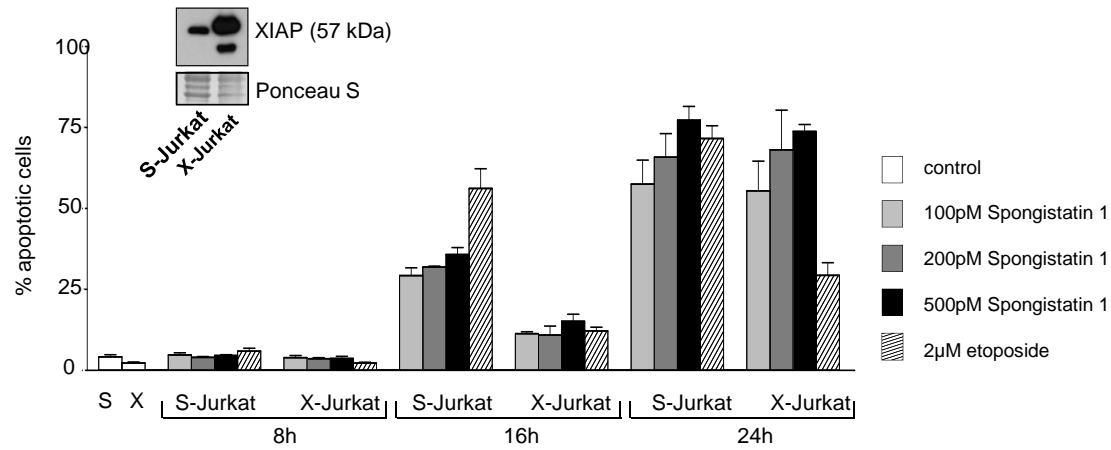
Figure III.14 Spongistatin 1 induces apoptosis in XIAP overexpressing cells

Wild type (S-Jurkat) Jurkat and XIAP overexpressing (X-Jurkat) Jurkat cells were treated with different doses of spongistatin 1 or 2 µM etoposide for different time points. Cell death was evaluated as described in "Materials and Methods". Insert: XIAP levels in S-Jurkat and X-Jurkat cells were analyzed by Western blot. The mean ± SEM of three independent experiments performed in triplicate is shown.

1.10 Spongistatin 1 reduces XIAP protein level

XIAP can be inactivated by different ways. One possibility is a decrease of protein level. Indeed, we observed in both, wild type and XIAP-overexpressing Jurkat cells, that spongistatin 1 leads to XIAP degradation, as shown in Western blot analysis in Figure III.15A. This down-regulation of XIAP could be due to modulation at either the transcriptional or posttranscriptional level. Therefore, analysis of XIAP mRNA levels using reverse transcription RT-PCR was performed. As shown in Figure III.15B spongistatin 1 did not alter XIAP mRNA expression (data by Dr. N. Barth) suggesting a post-transcriptional influence of spongistatin on XIAP level.

A

S-Jurkat							XIAP (57 kDa)
							Ponceau S

CN   2   4   8   16   24 | 24   **Time (h)**

spongistatin 1 (200 pM)   ETO (2 µM)

X-Jurkat							XIAP (57 kDa)
							Ponceau S

CN   2   4   8   16   24   24   **Time (h)**

spongistatin 1 (200 pM)   ETO (2 µM)

B
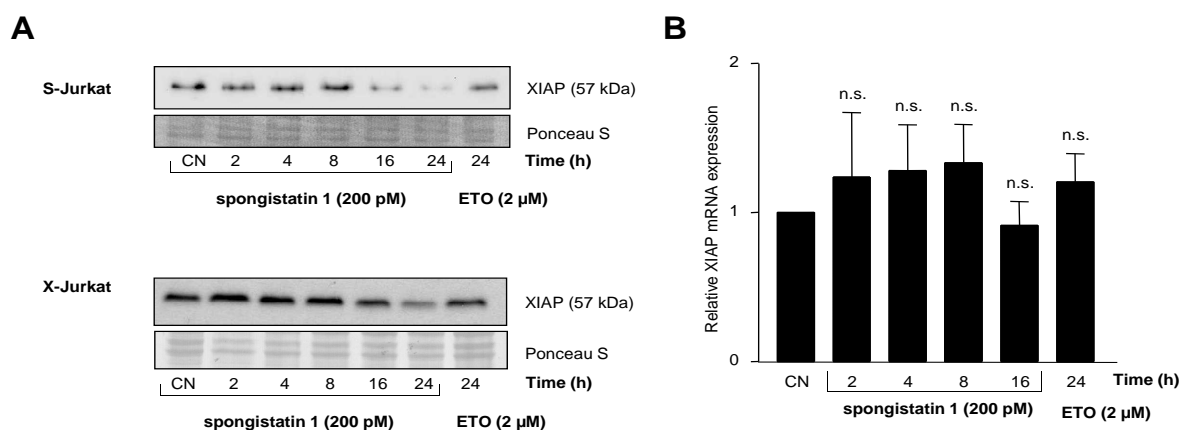
Figure III.15 Spongistatin 1 reduces XIAP protein level

(A) S-Jurkat and X-Jurkat cells were left untreated (CN) or were treated with spongistatin 1 (200 pM) or etoposide (ETO, 2 µM) for the indicated periods of time. XIAP protein degradation was detected by Western blot analysis. (B) Jurkat cells were exposed to 200 pM spongistatin 1 or etoposide (ETO, 2 µM) for the indicated interval, after which expression of XIAP mRNA was monitored by RT-PCR as described in "Materials and Methods". XIAP mRNA was normalized to 18s rRNA levels. *Bars*, the mean ± SEM of three independent experiments performed in duplicate. (ANOVA/Dunnett; *n.s.*, not significant).

1.11 Spongistatin 1 sensitizes Jurkat cells for staurosporine treatment

To overcome the chemoresistance in cancer cells the combination therapy of different drugs is applied. It allows hitting the resistant cells from different sites and is often more effective than the treatment with a single agent. Mostly, the drugs used in such combinations are used at lower concentrations compared to monotherapy but achieve synergistically elevated effects on cell death induction. A further advantage is to minimize toxic side-effects for healthy tissue [102].

Therefore, we investigated, whether spongistatin 1 might enhance the cell death induced by another apoptosis inducing agent such as staurosporine. We treated wild type Jurkat cells with low concentrations of spongistatin 1, staurosporine and a combination of both and quantified apoptosis induction after 24 hrs. As shown in Figure III.16A spongistatin 1 at 50 pM is able to significantly enhance the cell death induced through staurosporine (5 nM). In order to estimate the role of XIAP degradation for the above shown synergistic effect, the chemosensitizing activity was analyzed in XIAP-overexpressing Jurkat cells. Indeed, combination of spongistatin and staurosporine synergistically (synergism was calculated as described in "Materials and Methods") multiplies apoptosis. This cooperative effect is even stronger than in wild type cells, indicating that spongistatin is able to sensitize cells towards apoptosis in XIAP-overexpressing tumor cells.

In terms of therapeutic application we investigated the effect of the combination of both drugs on healthy PMBCs. As shown in Figure III.16B, neither a significant increase nor synergistic

effects of the substances on apoptosis could be detected, suggesting a specific effect on tumor cells.
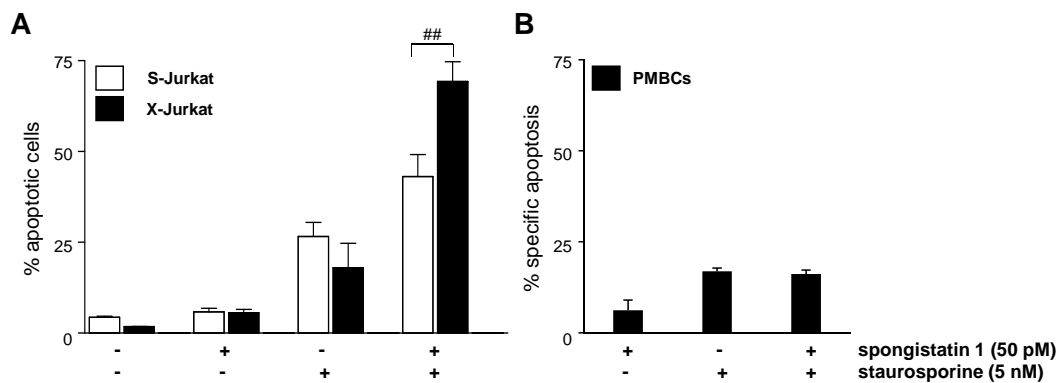
Figure III.16 Spongistatin 1 enhances staurosporine-induced cell death

Wild type (S) and XIAP overexpressing (X) Jurkat cells as well as healthy PMBCs were treated with a low concentration of staurosporine (5 nM), spongistatin 1 (50 pM), or a combination of both for 24 hrs. Cell death was evaluated as described in "Materials and Methods". *Bars*, the mean ± SE of three independent experiments performed in triplicate. ## $P < 0.001$, unpaired two-tailed t-test.

Since we used a very low dose of spongistatin in combination with staurosporine to treat cancer cells we were interested if XIAP is degraded. Although spongistatin is not able to induce DNA-fragmentation in this low concentration, XIAP protein level is still slightly decreased (Figure III.17). In combination with staurosporine more XIAP protein is degraded, suggesting that the increased apoptosis levels are related to this degradation.
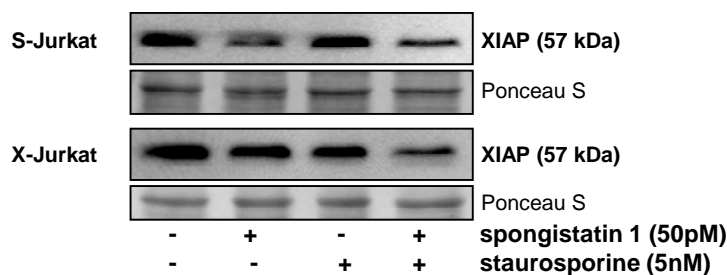
Figure III.17 Spongistatin in combination with staurosporine reduces XIAP protein level

Wild type (S) and XIAP overexpressing (X) Jurkat cells were treated with a low concentration of staurosporine (5 nM), spongistatin 1 (50 pM), or a combination of both for 24 hrs and XIAP protein degradation was analyzed by Western blot. Ponceau S was used as loading control. A representative experiment out of three independent experiments is shown.

2 Search for XIAP inhibitors

As mentioned above it is known from literature that XIAP overexpression confers resistance to apoptotic stimuli. We also could show that XIAP overexpressing cells are resistant towards etoposide (Figure III.14). Interestingly, spongistatin is able to overcome XIAP overexpression, most likely because this natural compound directly targets XIAP (Figure III.15). Therefore, it would be of high interest for therapeutic applications to find substances that directly interact with XIAP. Since random selection of compounds and subsequent testing in cell culture is a little promising approach the virtual screening technique was applied.

2.1 Virtual search for XIAP inhibitors – the pharmacophore model

A pharmacophore model, Hypo2-1TFQexcludvolumes7 based on the interaction of an antagonist of the XIAP - caspase-9 - interaction complex to the Bir3 domain was built (see Figure II.1; data by the group of Prof. H. Stuppner from the Institute of Pharmacy, Pharmacognosy at the University of Innsbruck, Austria). It consists of two donor features describing the ligand's peptide nitrogens which are supposed to bind to the enzyme's Thr308 and Gly306, respectively. Furthermore, a hydrogen acceptor function was localized from the Trp323 to the ligand's N-terminal peptide oxygen. The three hydrophobic features mimic the bulky tert-butyl residue of the ligand, its proline ring, and its 1,2,3,4-tetrahydronaphthalene, respectively. Additionally excluded volume spheres representing side chains of the protein and therefore inaccessible areas were included to the model. The data were implemented into the pharmacophore model using the Catalyst Software 4.9 (Accelrys Inc., San Diego, USA) as shown in Figure III.18.
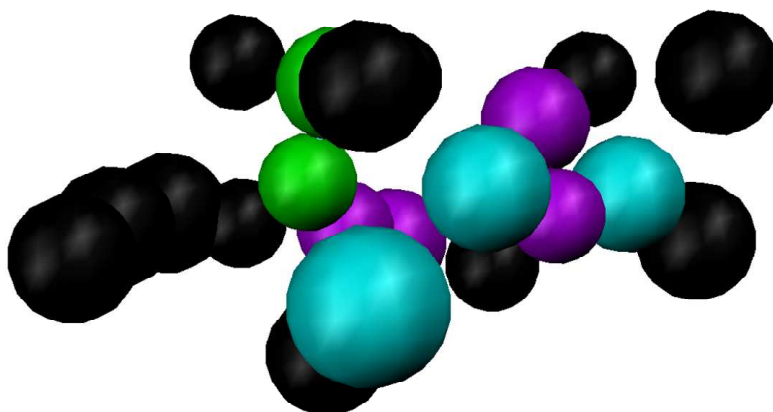
Figure III.18 Pharmacophore hypothesis from Catalyst software.

Pharmacophore model hypothesis: green: H-bond acceptor function; violet: H-bond donor function; turquoise: hydrophobic spheres; black: excluded volume spheres.

The pharmacophore model was validated in a self made database of 30 compounds well known to inhibit XIAP-Bir3 interaction. To retrieve a limited number of virtual hits, a consensus screening was applied using the GRID-based pharmacophore model Hyp3-1G3F previously published by Ortuso et al. [84] and the validated pharmacophore model Hypo2-1TFQexcludvolumes7. Consensus hits obtained by virtual screening filtering experiments of various databases resulted in hit rates in between 0.05 and 1.57 % (see Table 6). Out of the obtained virtual consensus hits some compounds were selected according to the previously mentioned criteria (see chapter II.2) and tested in cell culture models.

Table 6 Consensus hits of virtually screened databases

Database	Amount of compounds	Number of consensus hits	Virtual hits in %
Asinex Platinum 1104	114652	489	0.43 %
Asinex Gold 1104	224371	129	0.06 %
Specs 1104	216823	106	0.05 %
Maybridge 2004	59652	31	0.05 %
Derwent WDI_2003	63307	997	1.57 %
NCI	123219	144	0.12 %

2.2 Cellular models for the *in vitro* validation of virtual screening hits

For validating the results from virtual screening, selected hit substances were tested in cell culture models. To create a rapid cellular screening method, four Jurkat clones were used, characterized by different XIAP levels as shown in Figure III.19. S-Jurkat cells (wild type Jurkat) and pBabe (empty vector Jurkat cells) served as the control cells. XIAP overexpressing Jurkat cells (X-Jurkat) as well as Bir3- and RING- overexpressing Jurkat cells (Bir3/RING-Jurkat) were used to verify the first virtual screening derived evidence for the XIAP-Bir3 to be a major target of the compound.

To prove the relevance of XIAP-Bir3 inhibitors, the testing was extended beyond leukemia to other cancer cell lines including the prostate cancer cell line LNCAP, the breast carcinoma cell line MDA-MB-231 and two pancreatic cell lines: PancTu1 and high invasive L3.6pl cell line. All cell lines were verified to express XIAP, as shown in Figure III.19.
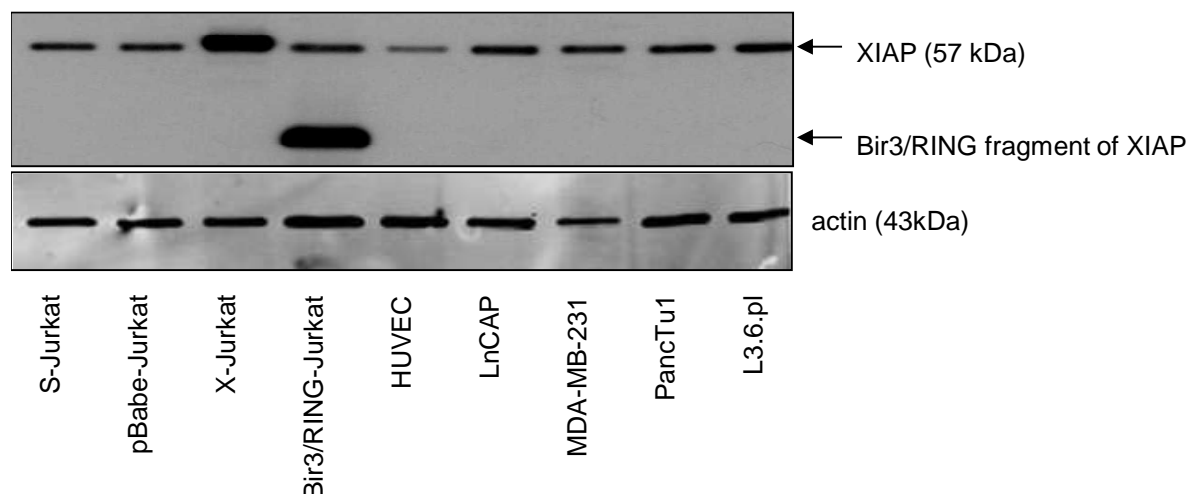
Figure III.19 XIAP expression in different cell lines

Cell lysates from wild type Jurkat cells (S-Jurkat), empty vector Jurkat cells (pBabe-Jurkat), XIAP overexpressing Jurkat cells (X-Jurkat), Bir3/Ring overexpressing Jurkat cells, Human umbilical vein endothelial cells (HUVECs), LNCAP, MDA-MB-231, PancTu1 and L3.6pl cells were prepared and XIAP level was analyzed by Western blot. Actin was used as loading control. The upper arrow denotes full length XIAP, the lower one indicates Bir3/RING fragment of XIAP. A representative experiment out of three independent experiments is shown.

2.3 The synthetic compound T8 as XIAP inhibitor

During the virtual screening of the available databases, compound T8 was recognized as virtual hit and was chosen for further pharmacological tests. In order to derive a structure activity relationship for T8, analogues of T8 were searched. As shown in Figure III.20 twenty structures of the resulting hits were selected for testing according to their high value of similarity and their different substitution patterns.

III Results
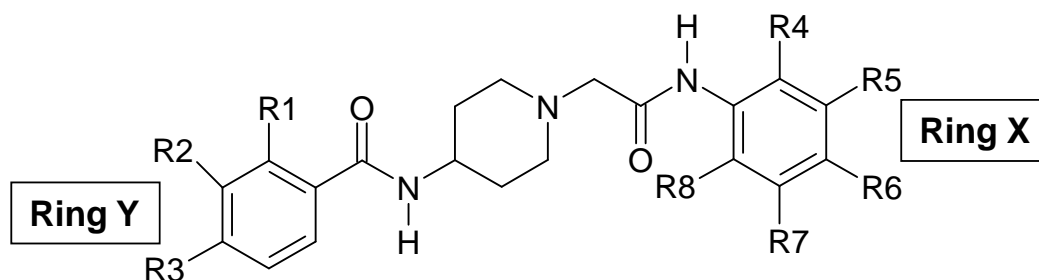
Internal number	R1	R2	R3	R4	R5	R6	R7	R8
T8	H	F	H	Et	H	H	H	Et
T8-1	H	F	H	Me	H	H	Me	H
T8-2	Br	H	H	Et	H	H	H	Et
T8-3	H	F	H	H	Me	H	Me	H
T8-4	Br	H	H	Et	H	H	H	H
T8-5	Me	H	H	H	F	H	H	H
T8-6	H	F	H	H	Cl	H	H	H
T8-7	H	H	t-Bu	H	F	H	H	H
T8-8	Me	H	H	Me	H	H	H	Me
T8-9	H	H	Me	Me	H	Me	H	Me
T8-10	H	H	H	H	H	F	H	H
T8-11	H	F	H	OMe	H	H	H	OMe
T8-12	Me	H	H	H	Cl	H	H	H
T8-13	H	OMe	H	Me	H	Me	H	Me
T8-14	H	F	H	OEt	H	H	OEt	H

T8-15	T8-16	T8-17
T8-18	**T8-19**	**T8-20**
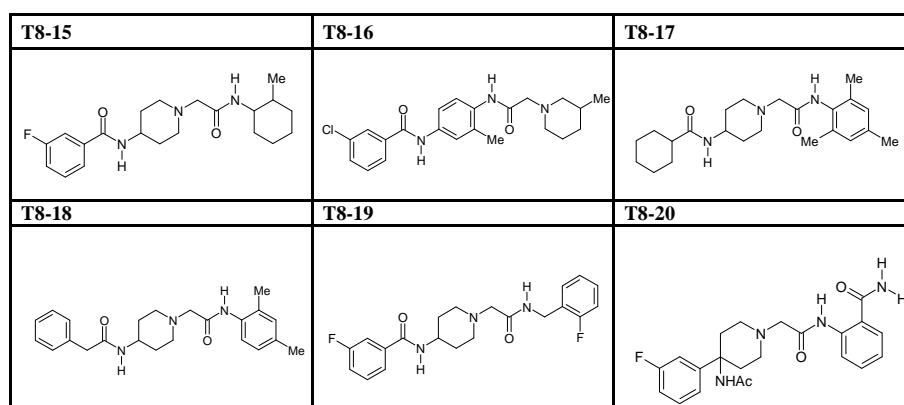
Figure III.20 Structure of T8 and T8 analogues

T8 and its analogues (T8-1 – T8-20) were obtained from Asinex Ltd (Moscow, Russia). T8 was furthermore synthesized and kindly provided by the group of Prof. K. T. Wanner.

2.3.1 T8 sensitizes different Jurkat cell lines for etoposide treatment

T8 was tested in the different XIAP-Jurkat cell lines on its ability to induce apoptosis in combination with a low dose of etoposide. As shown in Figure III.21 T8 alone is not toxic for Jurkat cells but in the combination with low dose of etoposide significantly induce apoptosis in all four Jurkat clones.
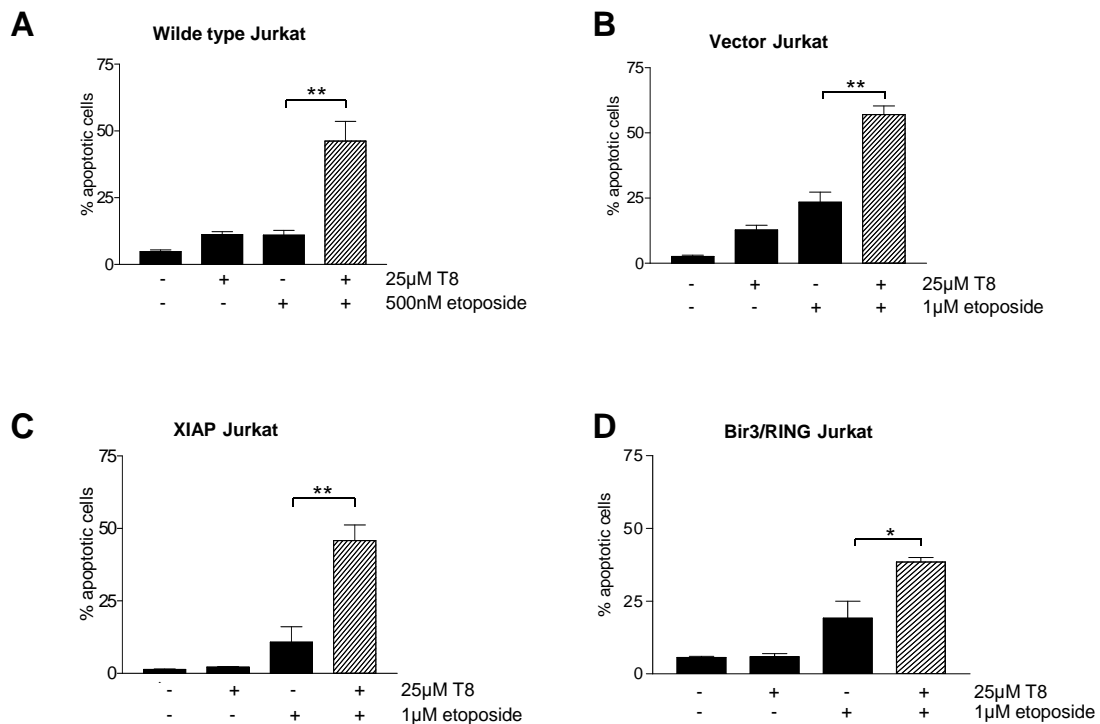
Figure III.21 T8 sensitized different Jurkat cell lines towards etoposide-induced apoptosis

T8 was tested in wild type human leukemia Jurkat T cells (S-Jurkat), as well as in Jurkat cells stably transfected with empty vector (pBabe-Jurkat), full-length XIAP overexpressing cells (X-Jurkat) or the Bir3/Ring domain overexpressing Jurkat cells (Bir3/RING-Jurkat). Cell death was evaluated as described in "Materials and Methods". *Bars*, the mean ± SEM of three independent experiments performed in triplicate. * P<0.05, ** P<0.01, unpaired two-tailed t-test.

2.3.2 T8 in combination with etoposide inhibits clonogenic growth of Jurkat cells

To analyze the long term effects of T8 on Jurkat cells, the clonogenic assay was performed. Cells were stimulated for just 4 hrs with T8, etoposide or the combination of both agents. Subsequently, cells were washed with PBS, replaced at the defined cell number in medium and allowed to grow for seven days. This experiment investigates if the new agents are able to affect growth of all cells in the population or if a part of cells is able to form new colonies after removing the agents, a sign of chemoresistance. Based on the relatively short exposition to the drugs the assay is also closer to the therapy situation where cytostatic drugs are applied just in short time.

T8 in combination with etoposide is able to inhibit the formation of new colonies (Figure III.22D). In comparison to etoposide alone, colony number in the combination is significantly reduced and the single cells look damaged.
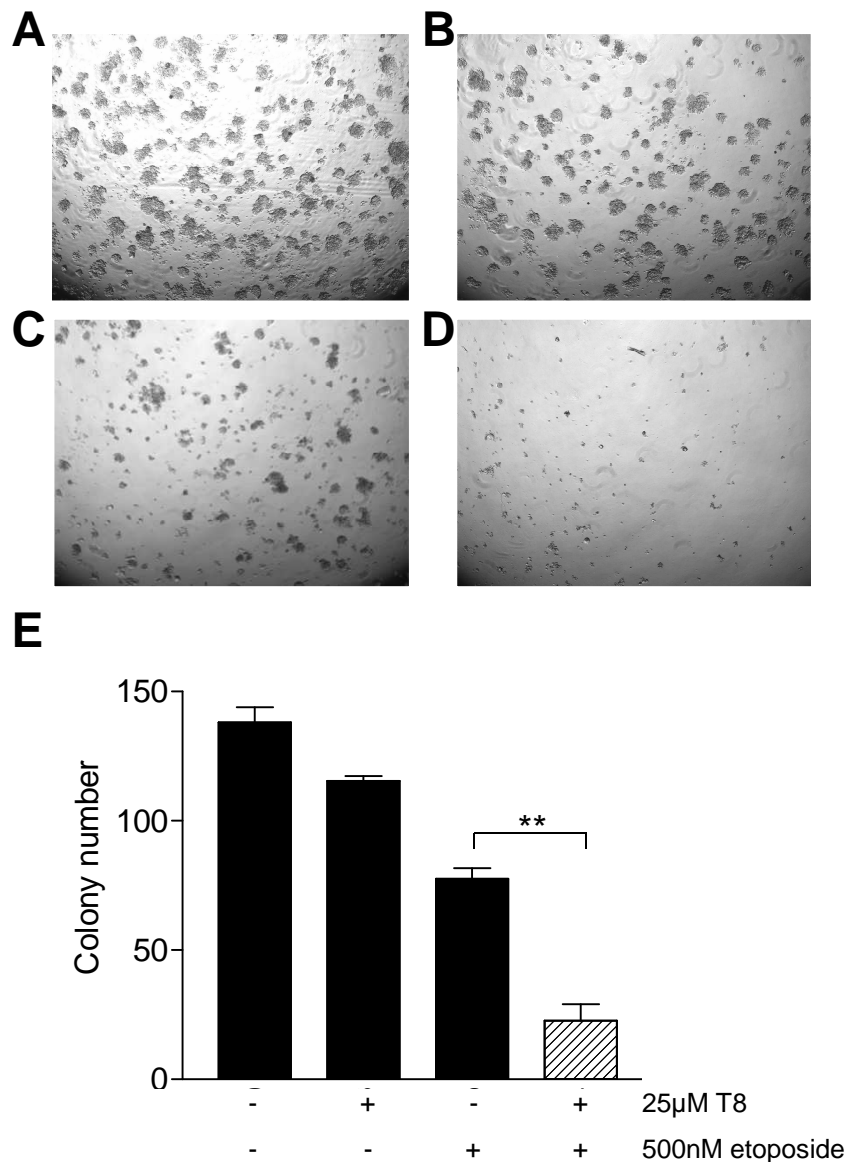
Figure III.22 T8 in combination with etoposide strongly inhibits clonogenic survival of Jurkat cells

Wild type Jurkat cells were left untreated (A) or treated for 1 h with 25μM T8 (B), 500nM etoposide (C) or a combination of both, respectively (D). After 7 days of cultivation, colonies were counted. T8 in combination with a subtoxic dose of etoposide significantly reduced clonogenic growth of the cells (E). Bars, the ± SEM of three independent experiments performed in triplicate. ** $P<0.01$ unpaired two-tailed t-test.

2.3.3 T8 derivatives

Because T8 revealed the best test results, a structure activity relationship (SAR) study was performed (by the group of Prof. H. Stuppner from the Institute of Pharmacy, Pharmacognosy

at the University of Innsbruck, Austria). In order to derive a structure activity relationship for T8, analogues of T8 were searched using the Tanimoto similarity search function of the SciFinder program [SciFinder Scholar 2006; Help tool]. Twenty structures of the resulting similarity hits were selected for further testing (see also Figure III.20). Interestingly, 16 out of the 20 analogues were able to map with all the set features of both pharmacophore models.

T8 derivatives were tested for their ability to induce apoptosis in combination with etoposide using Nicoletti assay. As shown in Figure III.23 some of them were not able to induce apoptosis by themselves, but show more than an additive effect on apoptosis levels in combination with etoposide (mostly T8-18, T8-2). T8-14 induced apoptosis alone in about 30 % of the cell population but in combination with etoposide this effect still can be elevated.
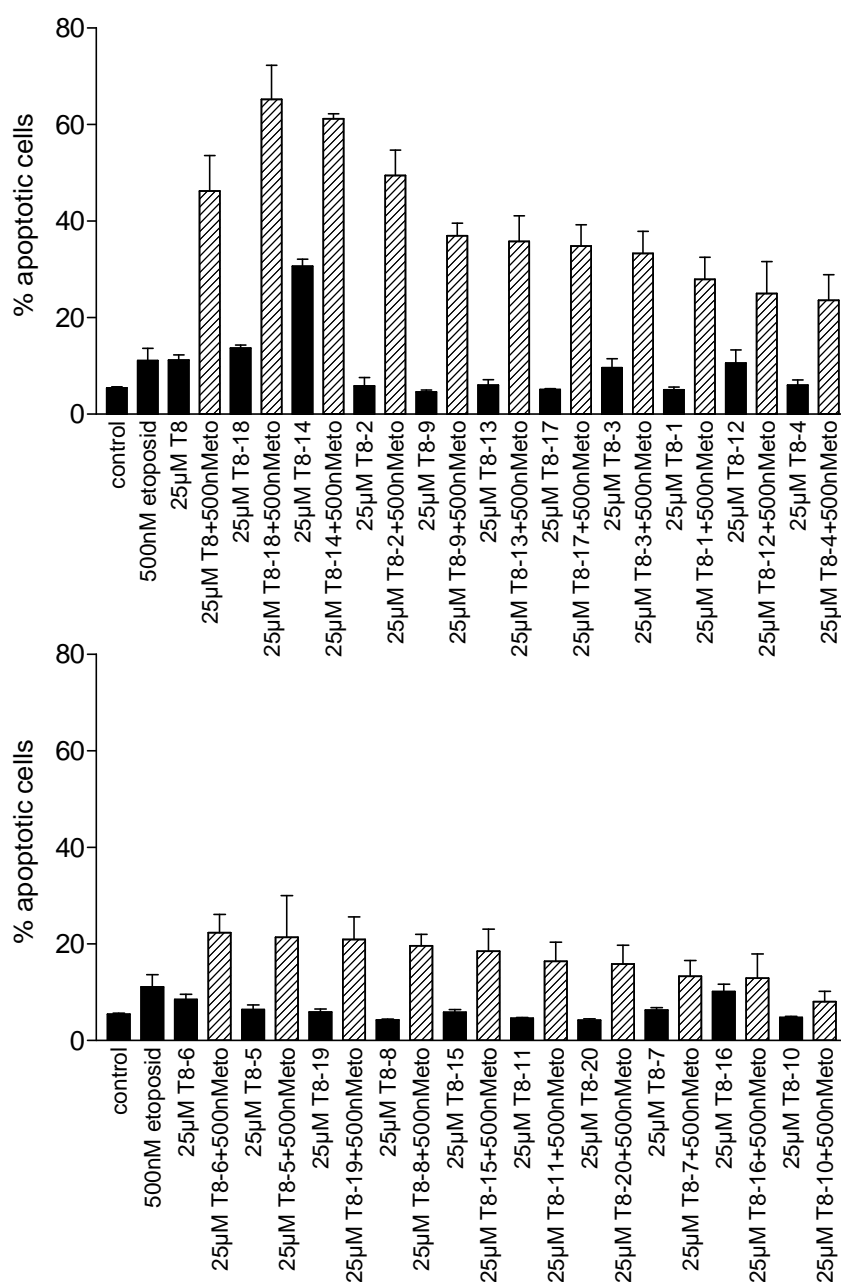
Figure III.23 T8 derivatives sensitized Jurkat cells for etoposide treatment

Cells were left untreated (control) or treated with 500nM etoposide, 25µM of the respective derivatives or a combination of both. Cell death was evaluated by Nicoletti assay as described in "Materials and Methods". Bars, the ± SEM of three independent experiments performed in triplicate. ***<0.001, ** P<0.01, * P<0.05, unpaired two-tailed t-test.

According to its strong effects in Nicoletti assay, T8-18 was also tested for ability to inhibit the clonogenic growth of the cells in clonogenic assay. Jurkat cells were treated with T8-18, 500nM etoposide or combination of both for 1 hour and then replaced into fresh medium for further seven days. After colony counting, T8-18 in combination with 500nM etoposide

showed significant decrease in clonogenic survival of wild type Jurkat cells in comparison to etoposide alone (Figure III.24).
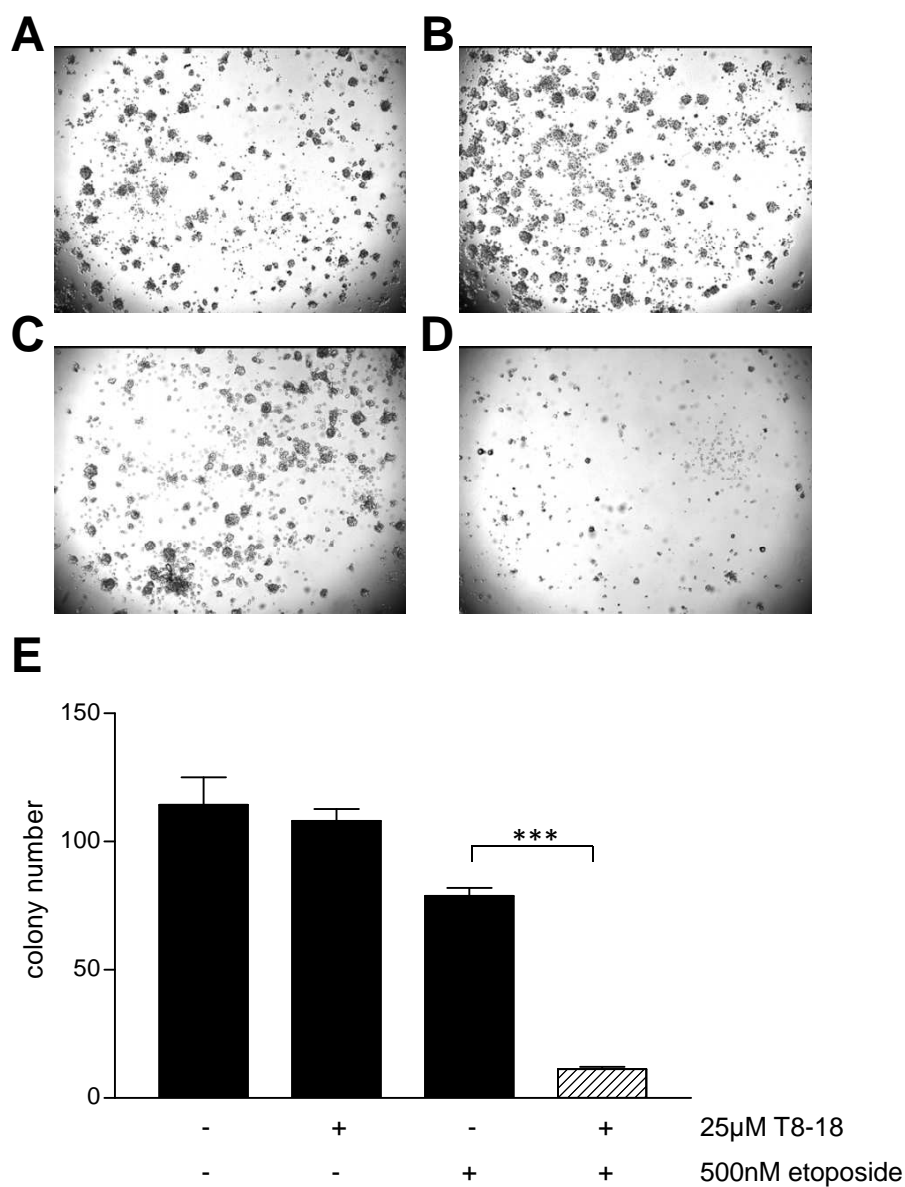
Figure III.24 T8-18 in combination with etoposide strongly inhibits clonogenic survival of Jurkat cells

Wild type Jurkat cells were left untreated (A) or treated for 1 h with 25µM T8-18 (B), 500nM etoposide (C) or a combination of both, respectively (D). After replacement into fresh methylcellulose medium, cells were incubated for seven days, afterwards colonies were counted. T8-18 in combination with a subtoxic dose of etoposide significantly reduced clonogenic growth of the cells (E). Bars, the ± SEM of two independent experiments performed in triplicate. *** P<0.01 unpaired two-tailed t-test.

Since T8 was the structure originally found by virtual screening all further experiments were done with T8.

2.3.4 T8 sensitizes different cancer cells for doxorubicin treatment

To investigate if the chemosensitizing effect of T8 is limited to leukemia cells and works only in combination with etoposide, additional experiments were performed. The prostate cancer cell line LNCAP and the breast adenocarcinoma cell line MDA-MB-231 were treated with 25µM T8 and 500nM or 600nM doxorubicin, respectively, for 48 hrs. Afterwards DNA fragmentation was assessed using Nicoletti assay.

As shown in Figure III.25 T8 sensitized both cell lines for treatment with doxorubicin. Moreover, this effect is significant in the LNCAP cell line.
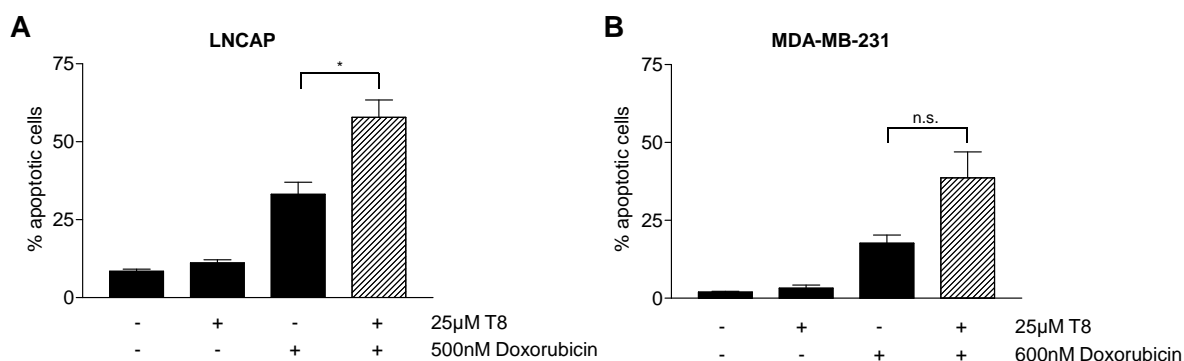
Figure III.25 T8 sensitizes different tumor cells to low dose of doxorubicin

T8 was tested in prostate cancer cells LNCAP (**A**) or breast carcinoma cells MDA-MB-231 (**B**) for 48 hrs in combination with 500nM or 600nM doxorubicin, respectively. *% apoptotic cells*, percentage of cells with subdiploid DNA content. *Bars*, the mean ± SEM of three independent experiments.

2.3.5 T8 sensitizes PancTu1 cells for TRAIL treatment

In order to investigate the influence of T8 on different cancer cells and different stimuli, the pancreatic PancTu1 cell line and tumor necrosis factor-related apoptosis-inducting ligand (TRAIL) was chosen, since it has been reported that XIAP knockdown sensitizes pancreatic carcinoma cells for TRAIL treatment [103]. We can confirm these data by showing that after six days of cultivation the formation of new colonies is reduced in samples simultaneously treated with T8 and TRAIL.
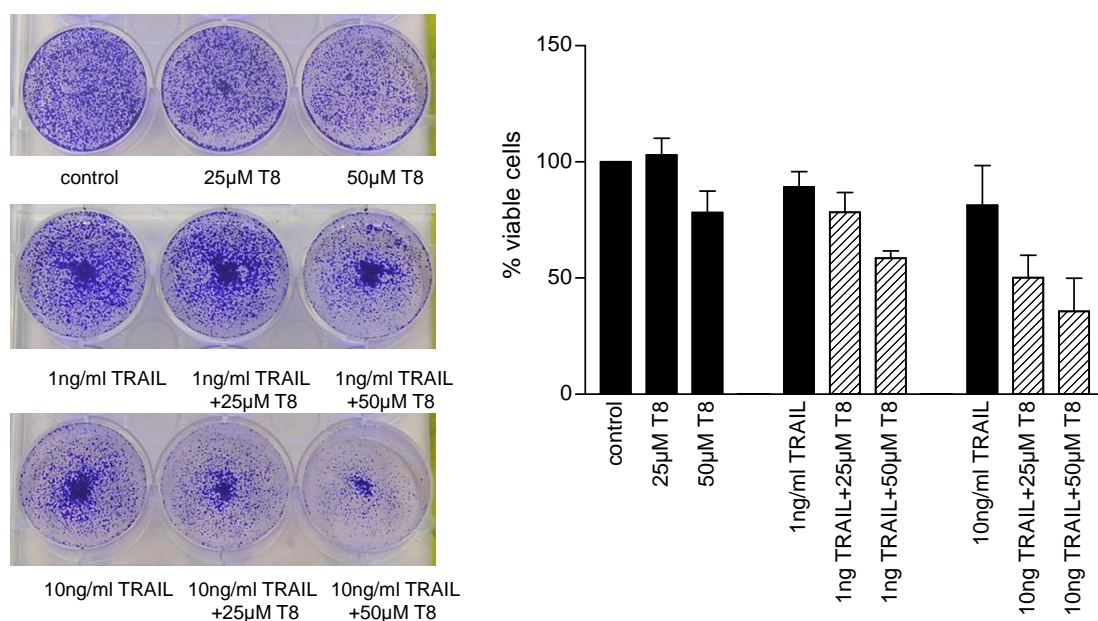
Figure III.26 T8 sensitizes PancTu1 carcinoma cells for TRAIL treatment

PancTu1 pancreas cancer cells were left untreated or were stimulated for 24 hrs with T8 and TRAIL as indicated. Afterwards, cells were washed with PBS, replaced in new medium and allowed to grow for further six days. The cells were incubated with crystal violet as described in "Materials and Methods". Pictures were taken and the intracellular crystal violet was dissolved with destaining solution. The absorption was measured and untreated cells were set at 100 % viability. *Bars*, the mean ± SEM of two independent experiments performed in duplicates.

2.3.6 T8 in combination with etoposide decreases clonogenic survival of pancreas cancer cells

To investigate the long-term effects of T8 in combination with etoposide on the high invasive pancreatic cancer cell line L3.6pl clonogenic assay was performed. L3.6pl was derived from the human pancreatic adenocarcinoma cell line COLO 357 by injection into the pancreas of nude mice. Afterwards the spontaneous hepatic metastases were harvested and reinjected into the pancreas of another set of nude mice. This selection cycle was repeated three times. In these cells increased cell motility and expression of matrix metalloproteinase 9 (MMP-9) was detected [88], facts that are in line with the high metastatic profile of L3.6pl cell line.

As shown in Figure III.27 T8 is able to sensitize the L3.6pl to etoposide treatment. After treatment for 1 h with the respective drugs and subsequent replacement of the cells in new medium for further six days, the number of cells treated with a combination of T8 and etoposide is strongly decreased. Moreover, 25µM and 50µM T8 alone have no effects on the cell viability.
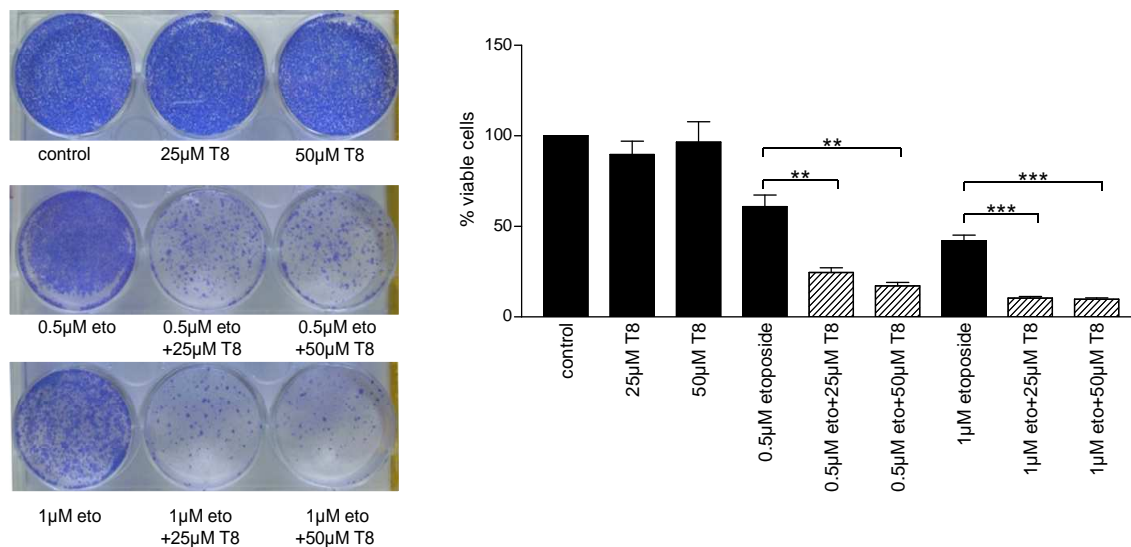
Figure III.27 T8 in combination with etoposide reduces clonogenic survival of pancreas cancer cells

L3.6pl cells were left untreated (control) or were stimulated for 24 hrs with T8 and etoposide (eto) as indicated. Afterwards, cells were washed with PBS, replaced in new medium and allowed to grow for further six days. The cells were incubated with crystal violet as described in "Materials and Methods". Pictures were taken and the intracellular crystal violet was dissolved with destaining solution. The absorption was measured and untreated cells were set at 100 % viability. *Bars*, the mean ± SEM of three independent experiments. ***<0.001, ** P<0.01, unpaired two-tailed t-test.

2.3.7 T8 in combination with cytotoxic drugs is not toxic for HUVECs

Finally, to investigate if T8 in combination with etoposide induce apoptosis selectively in cancer cells or affects also non-cancer cells, HUVECs (Human Umbilical Vein Cells) were used. As shown in Figure III.28 T8 in combination with 2µM etoposide or 600nM doxorubicin showed just slight toxicity in the MTT assay in HUVECs.
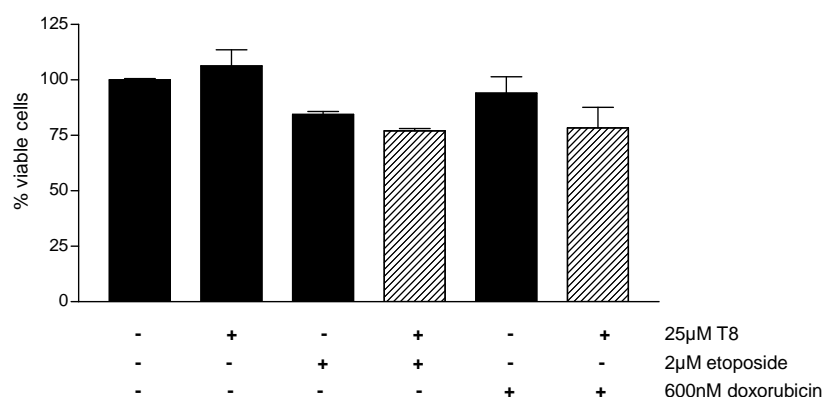
Figure III.28 T8 with the same combination of the drugs as for tumor cells is not toxic for primary endothelial cells (HUVECs)

HUVECs were left untreated or stimulated for 48 hrs with substances as indicated. Cell viability was quantified by MTT assay as described in "Materials and Methods". Bars, the ± SEM of three independent experiments performed in triplicate.

2.3.8 T8 reduces XIAP protein level

Having clearly shown that the chemosensitizing effect of T8 is neither restricted to a single cell type nor to a single chemotherapeutic and importantly is rather selective for cancer cells, we were interested if XIAP is targeted by T8. To investigate the effect of T8 on XIAP protein expression in cells, Western blot analysis was performed. As shown in Figure III.29 T8 alone and in combination with etoposide reduces the XIAP protein level in both wild type and XIAP overexpressing Jurkat cells in a so far unknown process.

A

B
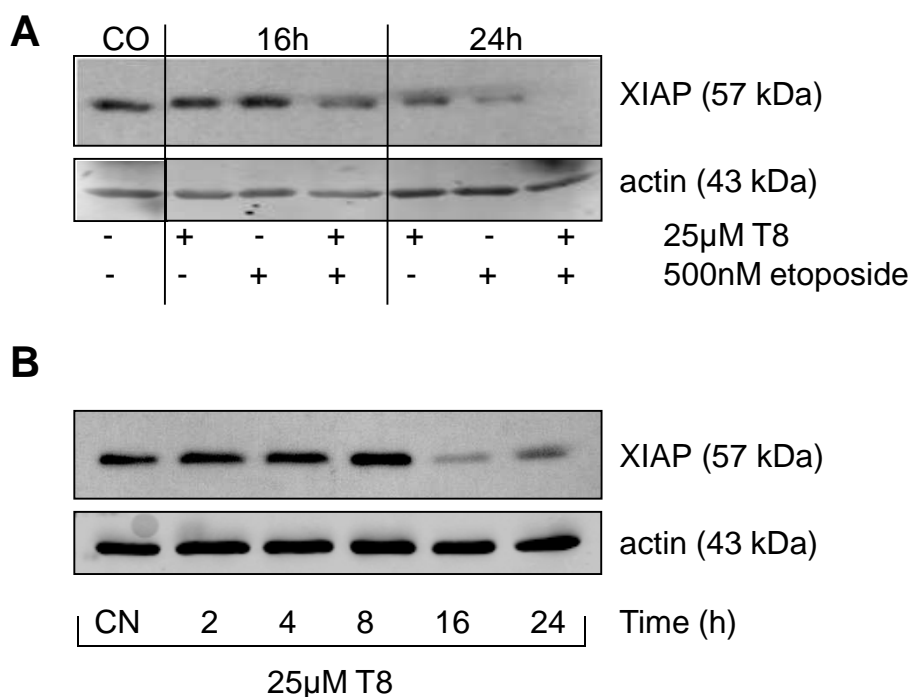
Figure III.29 T8 alone and in combination with etoposide reduces XIAP protein level

S-Jurkat cells were treated with T8 (25 µM), a low concentration of etoposide (500 nM), or a combination of both (A) and XIAP overexpressing Jurkat were incubated with 25µM T8 (B) for indicated time points. XIAP protein degradation was analyzed by Western blot as described in "Materials and Methods". Actin was used as loading control. A representative experiment out of three independent experiments is shown.

2.3.9 T8 enhances etoposide induced caspase-dependent apoptosis

We were further interested in the underlying signaling mechanisms leading to apoptosis induced by the combination of T8 and etoposide in Jurkat cells. To investigate if T8-induced apoptosis is caspase-dependent the broad-range caspase inhibitor zVADfmk was used. Wild type Jurkat cells were stimulated with T8 (25µM), 500nM etoposide or combination of both. Cells treated with the combination of T8 and etoposide, additionally were pretreated with 25µM of zVADfmk. The almost complete suppression of T8 and etoposide-induced DNA fragmentation showed the importance of caspase in this cell death process (Figure III.30A).

T8 was found in the virtual screening to be able to bind to Bir3. Since caspase-9 selectively binds to the Bir3 domain, T8 should lead to the release of free caspase from the inhibition complex. Subsequently, treatment with etoposide could initiate the caspase cascade. Thus, if indeed XIAP is affected caspase-9 should play a central role in the apoptosis induction by T8. Therefore, cells were pretreated with cell permeable caspase-9 inhibitor zLEHDfmk. Interestingly, inhibition of caspase-9 led to a suppression of the T8 and etoposide induced apoptosis to control level (Figure III.30B).

A

B
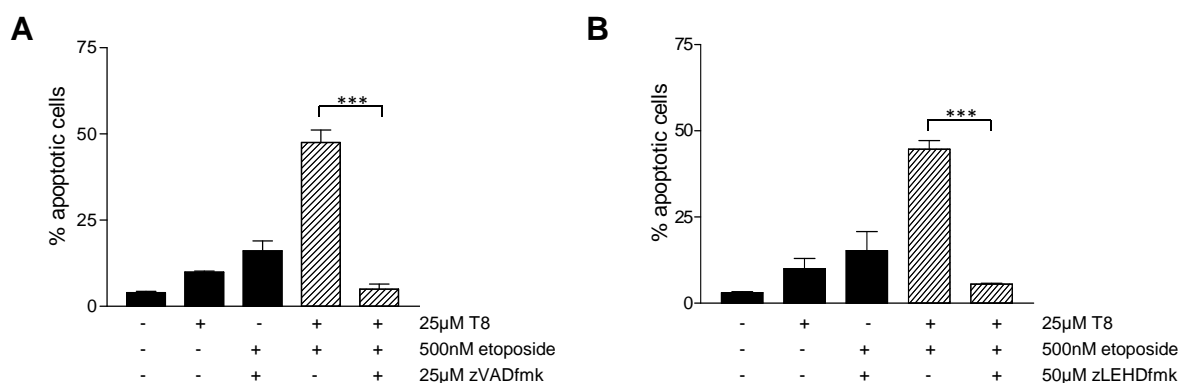
Figure III.30 T8 in combination with etoposide induces caspase-dependent apoptosis. Caspase-9 plays central role in this process

Wild type Jurkat cells were left untreated (Co) or pretreated for 1 h with 25µM zVADfmk (A) or 50µM zLEHDfmk (B) and subsequently incubated with 25µM T8, 500nM etoposide or a combination of both for 24 hrs. Apoptotic cells were quantified by flow cytometry as described in "Materials and Methods". Bars, the ± SEM of three (A) and two (B) independent experiments performed in triplicate (***, P<0.001, unpaired two-tailed t-test).

2.3.10 T8 in combination with etoposide increase caspase activity

To examine the effects of T8 on caspase activity the fluorescence based caspase activity assay was performed. It is based on the ability of activated caspase to cleave specific substrates in the cell lysate. The whole procedure also allows to test the caspase activity independently of pharmacological inhibitors and to exclude its possible side effects on the cells.

As expected for a XIAP inhibitor, caspase activities induced by a subtoxic dose of etoposide are significantly increased by T8 co-treatment. As shown in Figure III.31A the initiator caspase-9 activity is 1.5-fold higher as in comparison to control cells. Since caspase-3 is activated by caspase-9 also this effector caspase activity was increased as shown in Figure III.31B. After 16 hrs of stimulation, the caspase-3 activity is 13.5-fold higher as in the control cells.
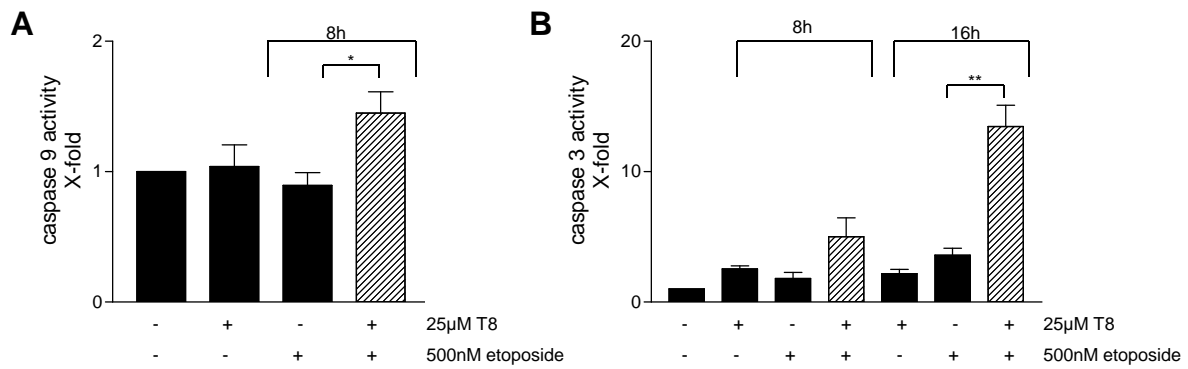
Figure III.31 T8 increases initiator and effector caspase activity

Wild type Jurkat cells were left untreated or treated with 25µM T8, 500nM etoposide or a combination of both agents for the indicated time periods. Fluorescence measurements of caspase-9 (A) and caspase-3 (B) activities were performed as described in "Material and Methods". Protein concentration was used for normalization. Bars, the ± SEM of three independent experiments performed in triplicate. ** $P<0.01$, * $P<0.05$, unpaired two-tailed t-test.

2.3.11 T8 in combination with etoposide activates the intrinsic caspase cascade

The activation of the respective initiator and effector caspases was elucidated by Western Blot analysis. As shown in Figure III.32 T8 in combination with etoposide caused an activation of the initiator caspase-9 as well as the effector caspase-3 after 16 hrs. At this time point etoposide alone does not affect the cleavage of caspases. Furthermore, PARP cleavage at 89 kDa can be detected after stimulation for 16 hrs with a combination of both compounds.
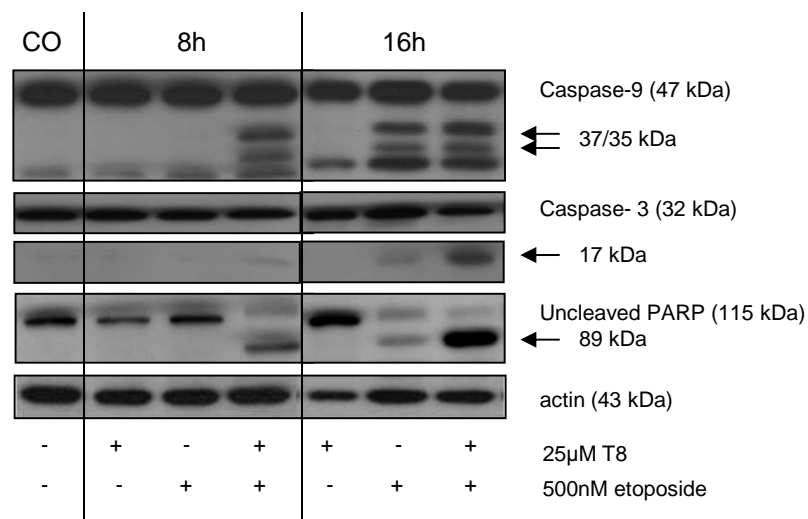
Figure III.32 T8 in combination with etoposide activates caspases and induces PARP cleavage in Jurkat cells

Wild type Jurkat cells were treated with 25µM T8 or 0.5µM etoposide or a combination of both for the indicated times. Whole cell lysates were prepared and activation of caspase-9, -3, and PARP cleavage was assessed by Western blot analysis as described in "Materials and Methods". Cleavage products are indicated by arrows. Actin was used as loading control. A representative experiment out of three independent experiments is shown.

2.3.12 Fluorescence polarization assay

The fact that T8 is able to sensitize chemoresistant XIAP overexpressing cells to etoposide induced apoptosis and that this apoptosis is dependent on caspase-9 are strong signs of T8 being a XIAP -binding and -inhibiting compound. In order to assure this assumption and to prove the virtual screening concept, fluorescence polarization experiments were performed. These assays were done in collaboration with Martin Gräber in the group of Dr. Thorsten Berg from the Department of Molecular Biology at the Max Planck Institute of Biochemistry, Martinsried, Germany.

The substance ABT-11 is a validated XIAP-Bir3 inhibitor [81] and served as a positive control in the experimental setting. As shown in Figure III.33A ABT-11 is able to displace the fluorescein labeled smac-derived peptide AbuRPFK-(FAM)-NH_2 from the Bir3 domain in a dose dependent manner with the IC_{50} of approximately 50 nM after one hour.

Unexpectedly, T8 showed no changes in the binding between Bir3 and the fluorescein labeled peptide AbuRPFK-(FAM)-NH_2 (Figure III.33B). These findings implicate that Bir3 is not the primary target of T8.
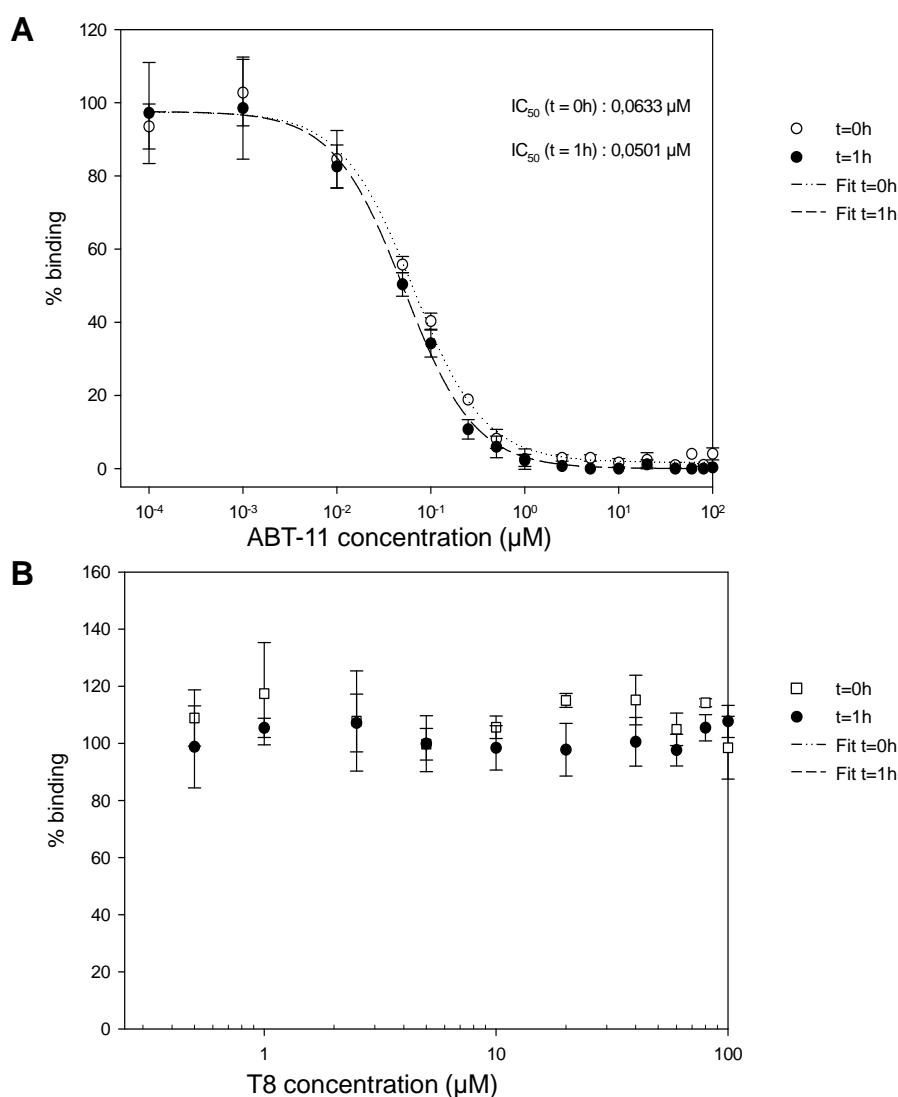
Figure III.33 Effect of ABT-11 (A) and T8 (B) on binding of AbuRPFK-(FAM)-NH$_2$ to Bir3 measured by fluorescence polarization assay

Serial dilutions of ABT-11 (A) and T8 (B) were prepared in assay buffer. Smac-derived peptide AbuRPFK-(FAM)-NH$_2$ and Bir3 was added, and the % binding of the AbuRPFK-(FAM)-NH$_2$ to Bir3 was assessed at the start point of measurement (t=0h) and after 1h (t=1h), respectively. Error bars represent SD.

2.3.13 NMR analysis

To confirm the data from the fluorescence polarization assay and to obtain additional information about T8 targets, NMR analysis was performed. The analysis was done in collaboration with Anders Frieberg (group of Prof. M. Sattler) from the Institute of Structural Biology, Helmholtz Zentrum München and Chair of Biomolecular NMR, Technical University Munich, Germany.

Bir3 and Bir2 proteins were labeled with ^{15}N and the spectrum of free protein and protein with ABT-11 (positive control) and T8, respectively was collected at the Bruker 600 Mhz

III Results

Avance 3 spectroscope (Bruker, Billerica, USA). Overlay of two ^{1}H^{15}N HSQC spectra of the Bir3 domain with ABT-11 (green) and without it (red) is shown in Figure III.34A. Several residues in XIAP-Bir3 protein were affected by the binding of ABT-11 (chemical shift perturbations in the spectrum of free protein and protein incubated with ABT-11). As shown in Figure III.34B T8 does not affect the Bir3 domain of XIAP.
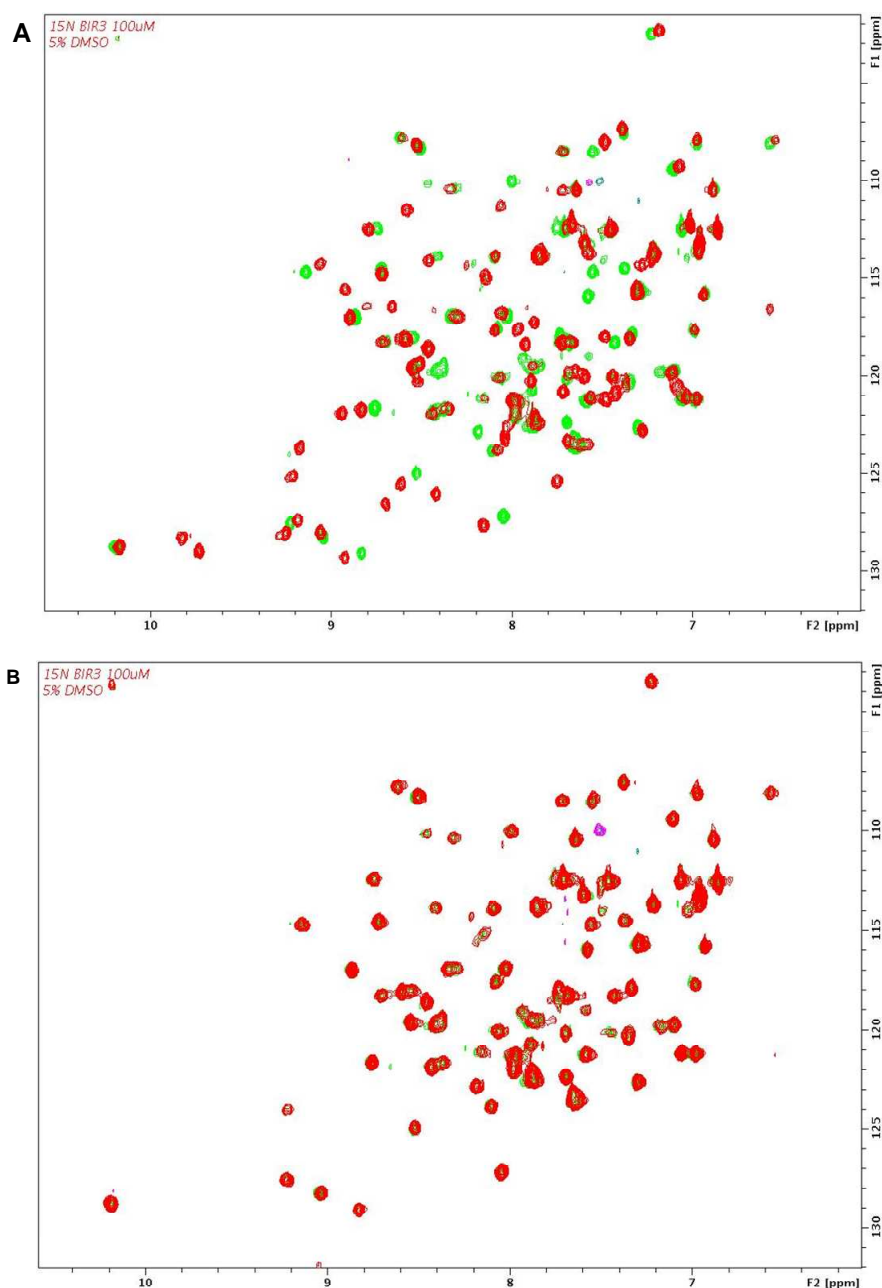
Figure III.34 NMR spectrum from Bir3 domain with ABT-11 and T8

Overlay of ^{1}H^{15}N-HSQC spectra of free XIAP Bir3 (100µM, red) and upon addition of equal amount of ABT-11 (A, green) or seven fold molar excess of T8 (B, green), respectively.

III Results

Since the Bir3 and Bir2 share nearly 40 % identity [54] we performed additional NMR experiments using the Bir2 domain of XIAP. As shown in Figure III.35A ABT-11 binds to the Bir2 domain of XIAP. The chemical shift perturbations in many residues (red versus green) of this domain identify ABT-11 as a strong binding partner of Bir2 domain. In comparison, the overlay of two spectra from Bir2 domain with (green) and without T8 (red) (Figure III.35B) did not show any chemical shifts perturbations, showing that T8 is not a Bir2 domain binding compound.
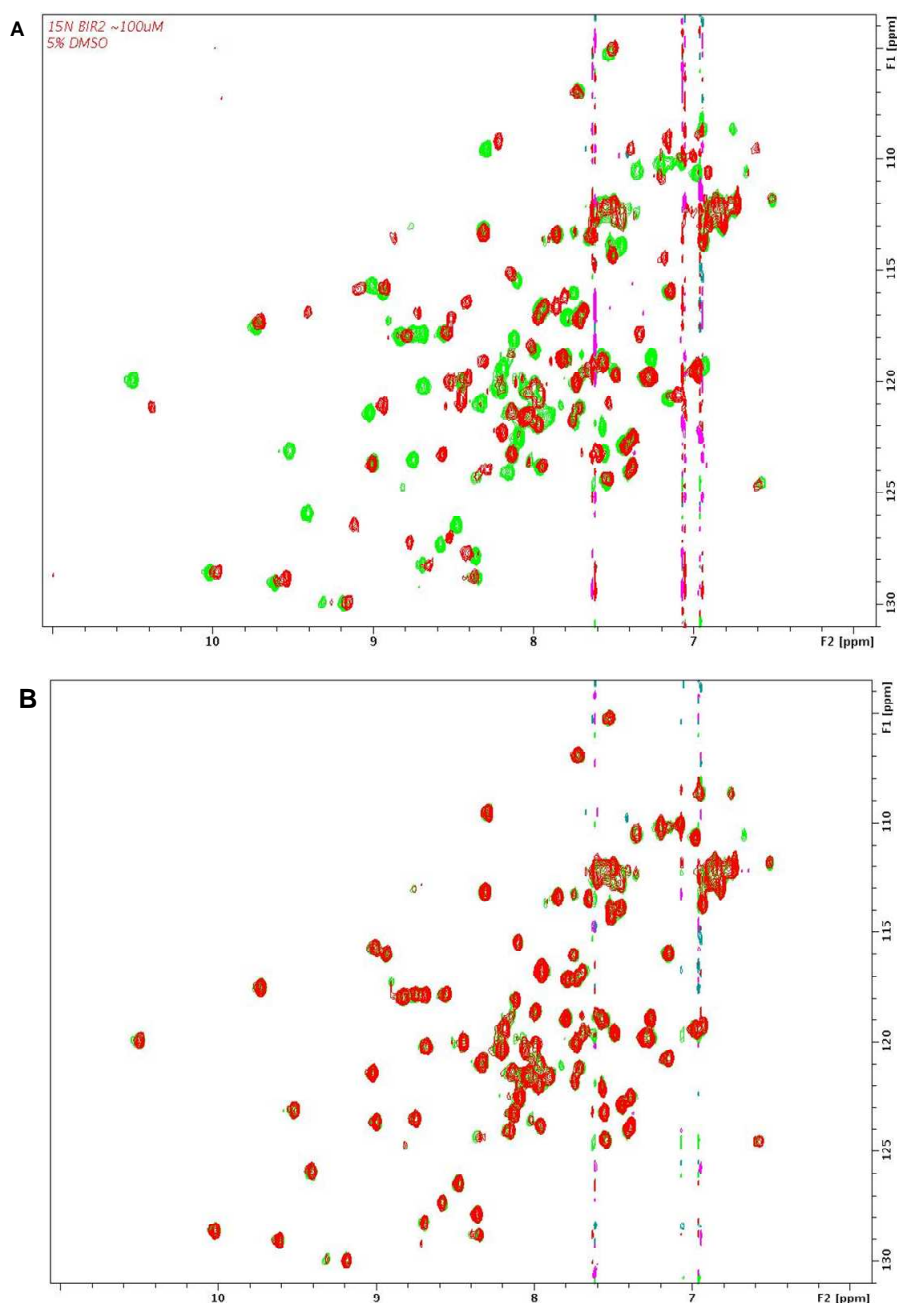
Figure III.35 NMR spectrum from Bir2 domain with ABT-11 and T8

Overlay of ^{1}H^{15}N-HSQC correlation spectra of free Bir2 domain (100µM, red) and upon addition of the equal amount of ABT-11 (A, green) or T8 (B, green), respectively.

2.3.14 T8 inhibits NF-κB activation

Although T8 is not able to bind either isolated Bir3 or Bir2 domains it shows the same biological activities as other XIAP inhibitors *in vitro* [104, 105]. Therefore, we were interested in the impact of T8 on the other XIAP domains. It is known that XIAP dimerization induces the recruitment and activation of TAB1 to Bir1 domain. TAB1 is an upstream adapter for the activation of the TAK1 kinase linked to the NF-κB pathway. Smac/DIABLO indirectly is able to disrupt this assembly [67].

As shown in Figure III.36 TNFα (1ng/ml) induces an increase of NF-κB activity which dose-dependently was reduced by pretreatment with T8. Moreover, 100μM T8 reduced the NF-κB activity to the same level as the positive control, pyrrolidine dithiocarbonate (PDTC, 50μM).
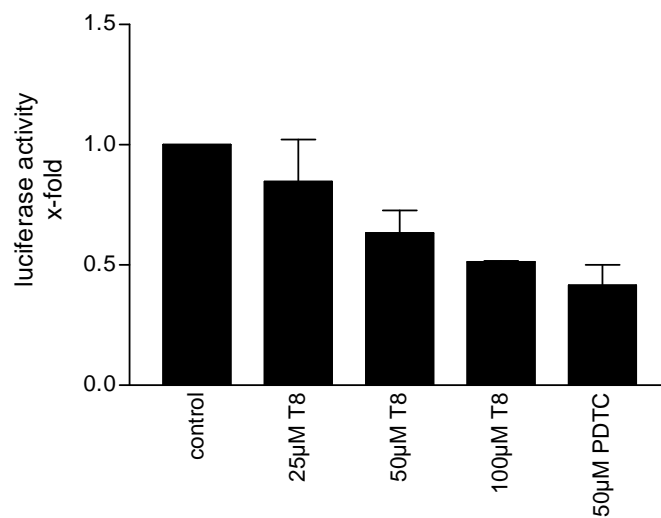
Figure III.36 T8 inhibits NF-κB promoter activity

HEK-293 cells transfected with NF-κB promoter driving a luciferase reporter gene were left untreated (control) or stimulated with increasing concentrations of T8 as indicated. After 0.5 hrs, 1ng/ml TNFα was added to the culture and cells were left for further 5.5 hrs. Cells were lysed and analyzed for luciferase activity as described in "Materials and Methods". β-galactosidase was used for normalizing the luciferase activity. *Bars*, the mean ± SEM of three independent experiments performed in triplicate. ** P<0.01, * P<0.05, unpaired two-tailed t-test.

IV Discussion
1 Spongistatin 1

Natural compounds play a major role as a source for the discovery of new anticancer agents [3]. Currently a significant number of marine compounds is evaluated in clinical trials [106]. Spongistatin 1 is a new marine compound which shows extraordinary potency in the NCI cancer cell line panel [13]. In this work spongistatin 1 was examined in the treatment of leukemia. Although there is some progress in therapy of leukemia which leads to an increase of the survival rates of the patients, more effective treatments are still needed [107]. Thus, spongistatin 1 can be a promising novel therapeutic agent for the treatment of leukemia.

1.1 Spongistatin 1 is a potent new anticancer agent

This work identifies spongistatin 1, a marine natural product, as a powerful anti-leukemic compound. Spongistatin 1 induces apoptosis in Jurkat T leukemia cells already in the picomolar range. Additionally this compound shows long term effects on leukemic cells as it significantly reduces clonogenic survival.

Most importantly, spongistatin 1 is also active in patient leukemic cells. Spongistatin 1 induces apoptosis in 11 out of 12 primary tumor cell samples of children suffering from acute leukemia. As no *in vivo* data concerning spongistatin 1 toxicity exist so far, the maximal tolerable plasma concentration of spongistatin 1 remains elusive. Spongistatin 1 is even more potent than 8 out of 10 already clinically applied cytotoxic drugs (such as 6-thioguaninin, methotrexate, etoposide or AraC). Moreover, spongistatin 1 only slightly affects healthy peripheral mononuclear blood cells.

All these aspects together with the successfully completed synthesis [108] make spongistatin 1 an exceptional new natural drug and a promising anticancer agent.

1.2 Spongistatin 1 induces caspase dependent cell death in leukemic cells

As shown by using the caspase inhibitor zVADfmk, spongistatin 1 induced cell death depends on caspases. In detail, we found that caspase-9 deficient cells are resistant to spongistatin 1, whereas the lack of caspase-8 has no impact on the spongistatin 1-induced apoptosis. In this context, for spongistatin 1 the intrinsic apoptotic cell death pathway seems to be more important than the extrinsic one. Moreover, the results show a strong involvement of mitochondria in the apoptotic process. Spongistatin 1 triggers apoptosis via the release of mitochondrial factors such as cytochrome c, smac/DIABLO or Omi/HtrA2 and the subsequent activation of caspases. Overexpression of Bcl-2 or Bcl-xl rescues cells from spongistatin 1 induced death, additionally confirming the relevance of the intrinsic pathway.

1.3 Spongistatin 1 overcomes XIAP caused resistance

Apoptosis is essential in maintaining tissue homeostasis. Therefore, dysfunctions in this process lead to disorders such as cancer. At a fundamental level, cancer occurs or progresses because malignant cells fail to undergo apoptosis either spontaneously or in response to chemotherapy. As caspases play the central role in the execution of apoptosis, the barrier in the activation of caspases leads to apoptosis resistance [109]. The most potent caspase inhibitor from the IAP family, X chromosome-linked IAP (XIAP) prevents both, the activation of the initiator caspase-9 as well as the activation of the effector caspases-3 and -7. [63, 110, 111]. XIAP is highly expressed in several classes of cancer [112, 113] and correlates with poor survival in childhood de novo acute myeloid leukemia [8]. Therefore, the blockade of XIAP function is an attractive strategy for restoring apoptosis sensitivity in neoplasia. Consequently, a variety of small molecule inhibitors of XIAP have been developed such as polyphenylurea derivatives, the natural compound embelin and others [5, 114].

This work introduces spongistatin 1 as a highly promising experimental drug in this context. Spongistatin, in contrast to other chemotherapeutics such as etoposide, is able to induce cell death in XIAP overexpressing Jurkat cells. After treatment with spongistatin 1 XIAP overexpressing cells show slower, time dependent DNA fragmentation in comparison to wild type Jurkat cells, but after 24 hrs the levels of the fragmented DNA is comparable in both clones. In contrast XIAP overexpressing Jurkat cells stimulated with etoposide show just a minor response to the treatment in comparison to wild type cells. We can show that spongistatin 1 had no effect on XIAP mRNA level, hence the reduced XIAP protein level is most likely the result of enhanced posttranscriptional degradation. XIAP is effectively degraded at the protein level in spongistatin 1 treated wild type and XIAP overexpressing Jurkat T cells. This indicates XIAP to be the possible target of spongistatin 1 in leukemia cells. Spongistatin 1 could be involved in XIAP autoubiquitination and proteasomal degradation of XIAP [66]. However, the indirect XIAP degradation induced by spongistatin 1-mediated release of smac/DIABLO, Omi/HtrA2 from mitochondria as well as the activation of caspases or cathepsins is also possible [70, 72, 73, 115]. The exact mechanism for XIAP degradation after spongistatin 1 treatment has to be elucidated.

1.4 Spongistatin 1 sensitizes leukemic cells for staurosporine treatment

The most important feature in terms of a therapeutic benefit of spongistatin 1 is the sensitization of leukemic cells for other chemotherapeutics. The synergistic interactions between anticancer agents applied in combination provide a greater benefit than the additive effects of each agent applied alone. Beside improved efficacy there is also the hope to minimize side effects of the chemotherapeutics [102]. It is proven that XIAP targeting in addition to conventional treatment improves cancer therapy. The XIAP antisense AEG35156 is already evaluated in a clinical phase I/II in combination with carboplatin and paclitaxel in patients suffering from advanced non-small cell lung cancer [116].

IV Discussion

In this work we are presenting that spongistatin 1 at a very low concentration sensitizes leukemic cells towards staurosporine-induced apoptosis. The combination of the two agents shows high synergistic effects. Interestingly, the extent of cooperative effect of spongistatin and staurosporine was much more pronounced in XIAP-overexpressing cells in compare to wild type Jurkat cells. Spongistatin 1 is able to decrease the XIAP level in wild type Jurkat cells and the combination with staurosporine leads to a significant degradation of XIAP in XIAP overexpressing cells, being in line with increased apoptosis levels in X-Jurkat cells after treatment with the combination of these two substances. These facts indicate that XIAP degradation is a possible underlying mechanism for the synergistic effects of spongistatin 1 and staurosporine. The healthy blood cell experiments indicate that the combination of both agents does not have any additional negatives effects on the cells in comparison to monotherapy with staurosporine.

However, regarding the attractivity of XIAP as a drug target overcoming chemoresistance it is of note that XIAP regulates apoptosis in a context-dependent manner: XIAP inhibition has been shown to fail to sensitize leukemia cells treated with etoposide [117] or in breast carcinoma cells upon treatment with carboplatin or doxorubicin [118]. Spongistatin 1 showed only a synergistic effect on leukemic cell death when cells were treated with low dose of staurosporine, but not with etoposide (data not shown). This may be due to the different mode of action of the both agents: etoposide activates the apoptosis via the mitochondrial pathway whereas staurosporine is a protein kinase inhibitor. Furthermore, spongistatin 1 as well as etoposide activates the mitochondria-mediated apoptotic pathway. This possibly causes the overlapping of the cytotoxic effects and finally results in just additive or even antagonistic results. The same ineffective results were found in the diffuse large B-cell lymphomas (DLBCLs) where caspase-9 is constitutively activated [119]. After combination of the experimental XIAP inhibitor 1396-12 with etoposide there was no significant increase in apoptosis levels, because the intrinsic pathway was already activated and could not further get activated by etoposide [120]. The same situation occurs in spongistatin 1 treatment. Mitochondria and intrinsic apoptotic pathway already are activated by spongistatin 1 and thus etoposide treatment is irrelevant for the apoptotic effects. Staurosporine in contrast, as a protein kinase inhibitor, induces apoptosis by multiple pathways in leukemia cells [121] which can contribute to the synergistic effects observed after treatment with spongistatin 1.

1.5 Concluding remarks and future directions

The present work has demonstrated that spongistatin 1 is a potent new compound in the treatment of leukemia, whereas toxicity on normal blood cells is low. Spongistatin 1 induces apoptosis in primary tumor cells of children suffering from acute leukemia. When used in low nanomolar concentrations, spongistatin causes apoptosis more efficiently than most of clinically used, cytotoxic drugs applied with 300–10,000 times higher concentrations.

Spongistatin 1 induces apoptosis in leukemia Jurkat T cells and inhibits long time survival of these cells. The induced apoptosis involves the mitochondrial pathway and is caspase dependent. Spongistatin 1 kills XIAP-overexpressing, apoptosis resistant, leukemic cells and

degrades XIAP protein which might be the reason for its sensitizing effect when combined with staurosporine. Three major questions remain to be answered and require further studies:

(i)   Is XIAP the primary target of spongistatin 1 and if so, in which way does this natural compound degrade XIAP?

(ii)   Is there a correlation between the XIAP levels in patient samples and the treatment outcome?

(iii)   Are there other cytotoxic drugs which in combination with spongistatin 1 lead to synergistic apoptosis elevation? Are there criteria which can predict a good outcome of combination?

2   T8 as a XIAP inhibitor

XIAP overexpression frequently is observed in cancer chemoresistance and leads to poor patient's outcome [8, 112, 113]. For this reason, approaches antagonizing XIAP haven´t lost their attractivity in search for potent antitumor strategies. XIAP antisense oligonucleotides as well as ectotopic expression of smac/DIABLO, an endogeneous inhibitor of IAPs provided the proof of principle by enhancing the efficacy of chemo-and/or radiotherapy of cancer [81, 122-125]. Consequently a variety of small molecule inhibitors of XIAP have been developed such as polyphenylurea derivatives [114], the natural compound embelin and others [5, 114] which have been shown to directly induce apoptosis of tumor cell lines in culture and sensitize cancer cells to chemotherapeutic drugs.

The Bir3 domain of the XIAP is involved in the inhibition of caspase-9 activation [63]. This interaction of Bir3 and caspase-9 was the basis for the pharmacophore model generation. During the virtual screening of the available databases, molecules that fulfill set features in the pharmacophore model were recognized as virtual hits and evaluated in the *in vitro* screen comprising wild type Jurkat, empty vector, XIAP overexpressing and Bir3/RING overexpressing Jurkat leukemia T cells. From the panel of substances T8 was chosen as the most promising one and analyzed in detail.

2.1 T8 in combination with etoposide significantly increases cell death in leukemia cells

T8 alone is not toxic for leukemia Jurkat T cells but in combination with a subtoxic dose of etoposide significantly increases apoptosis in all four Jurkat clones (wild type, empty vector, XIAP overexpressing and Bir3/RING overexpressing Jurkat). The sensitizing effect in XIAP and Bir3/RING overexpressing clones support first evidence that Bir3 is a major target for T8. As XIAP inhibitor, T8 is not expected to be cytotoxic by itself as shown for other XIAP

inhibitors such as LBW242 or smac peptides [104, 105]. For this reason etoposide treatment serves as inducer for the apoptotic events. In combination with etoposide T8 is able to decrease the clonogenic growth of wild type Jurkat cells in the long term assay.

2.2 T8 analogues

In order to find the optimal chemical structure for XIAP inhibition a structure activity relationship (SAR) study was performed. Twenty analogues of T8 were tested for their ability to induce apoptosis in leukemic cells. T8-18 and T8-2 were the most potent compounds in this panel. In combination with etoposide they caused even more apoptosis in Jurkat cells than the parental T8. Also in long term clonogenic assay T8-18 shows comparable effects with T8.

It seems that elongation of the T8 molecule by a methylene group between the piperidine ring and ring Y (as seen in T8-18) results in a distinct increase of apoptotic activity. Furthermore a halogen in ring X seems rather not desirable since the most potent compounds do not exhibit such substituent. Exchange of the F atom (T8) by a Br moiety (T8-2) in ring Y has rather no effect. Additional information about analogues solubility or pharmacokinetic attributes like membrane permeability are required to explain the different sensitizing effects of the respective compounds.

2.3 T8 sensitizes different cancer cells for cytotoxic drugs

As shown in this work T8 also sensitized other cancer cell lines for various cytotoxic drugs. There were reports concerning the sensitizing effects of XIAP suppression and DNA intercalating doxorubicin treatment [126, 127]. The two cell lines LNCAP prostate cancer cells and MDA-MB-231 breast carcinoma cells show an increase in apoptosis level after treatment with the combination of T8 and doxorubicin in comparison to doxorubicin alone. As reported in the past XIAP plays a pivotal role in the chemoresistance of LNCAP to chemotherapy [128]. This fact correlates with the significant increase in apoptosis level after treatment with XIAP inhibitor T8 and doxorubicin.

The expression of XIAP protein in pancreatic cancer cells is elevated in comparison to non-malignant pancreas tissue. Furthermore, pancreatic cancer is one of the most aggressive human tumors with poor survival prognosis [129]. Thus, the inhibition of XIAP has become a very promising approach in pancreas cancer therapy [103, 130].

We can show that the pancreas cancer cell line PancTu1 is sensitized for Tumor Necrosis Factor Related Apoptosis Inducing Ligand (TRAIL) upon co-treatment with our XIAP inhibitor. T8 enhances TRAIL-induced inhibition of proliferation in the long term clonogenic assay. Our findings agree with earlier studies where stable downregulation of XIAP in PancTu1 cells induced TRAIL-mediated apoptosis [87], or where smac mimetics sensitized for TRAIL induced apoptosis in breast cancer cells [103, 125, 131]. Furthermore, in the long

term clonogenic assay, the high invasive pancreas cancer cell line L3.6pl [88] shows a significant reduction of new colonies formation after T8 and etoposide treatment.

2.4 T8 is not toxic for the healthy cells

T8 alone is not toxic for Human Umbilical Vein Endothelial Cells (HUVECs) as evaluated in cytotoxicity assays. XIAP expression is frequently elevated in cancer cells [100, 112] making it a good target for cancer therapy with low side effects for the healthy tissue. T8 even in the same combination with the cytotoxic drugs (etoposide and doxorubicin) as for tumor cell treatment shows just slight toxic effect in HUVEC cells. Due to these data T8 seems to be a target- specific compound which affects cancer cells. Low cytotoxic effects in healthy cells make T8 a new attractive chemosensitizing agent.

2.5 T8 reduces XIAP protein level and contributes to caspase dependent apoptosis

T8 alone and in combination with etoposide reduces the XIAP protein level both in wild type and XIAP overexpressing Jurkat cells via a so far unknown process. Caspases, calpains and smac/DIABLO could be involved in XIAP degradation or ubiquitination [70, 72, 73] and XIAP level also could be regulated at the transcriptional level. To explore the exact mechanism for XIAP degradation after T8 treatment additional experiments have to be performed.

As shown in this work T8 in combination with non toxic doses of etoposide induces caspase dependent cell death in leukemic cell. After pretreatment with the broad spectrum caspase inhibitor no apoptotic cell death can be detected. Pretreatment with the specific caspase-9 inhibitor also completely reduces apoptosis. The measurement of the caspase activity shows that caspase-9 as well as caspase-3 is strongly increased upon stimulation with T8 and etoposide. The same effects can be confirmed by Western blot analysis. Additionally the cleavage of DNA-repair associated nuclear enzyme poly-(ADP-ribose)-polymerase (PARP), a common feature of the apoptotic process [132], can be observed. T8 alone is not able to induce apoptosis. It seems that etoposide is required for the initial activation of caspase-9 after T8 induced XIAP inactivation. There exist various other reports describing XIAP inhibitors to enhance caspases activation and PARP cleavage. XIAP knockdown using antisense AEG35156 or short-hairpin RNA (shRNA) increases TRAIL-mediated caspase activation [103, 116, 118] and small molecule smac-mimics enhance etoposide-mediated caspase activation [131]. These data correlate well with our results.

2.6 T8 does not bind to Bir3 or Bir2 domains of XIAP

In order to prove if T8 binds to Bir3 domain of XIAP, a sensitive and quantitative fluorescence polarization-based assay was performed. The known XIAP-Bir3 inhibitor ABT-11 was used as a positive control [81]. Unexpectedly, T8 does not show direct binding affinity to the Bir3 domain, whereas ABT-11 concentration dependently was able to bind to the Bir3 domain of XIAP (IC_{50} 0.05µM).

This data was supported by experiments using nuclear magnetic resonance (NMR) heteronuclear single quantum coherence spectroscopy (HSQC). Upon T8 incubation no changes in the Bir3 domain could be observed whereas ABT-11 strongly affected Bir3.

Since the Bir3 and Bir2 share nearly 40 % identity [54] we performed additional experiments showing that Bir2 was affected by ABT-11 but not by T8.

In summary it was unexpected that T8 does not directly bind to either the Bir3 or the Bir2 domain, although the pharmacophore modeling and virtual screening predicted T8 to fit into Bir3. In addition, in cellular assays T8 shows a strong chemosensitizing effect correlating very well with published data from other XIAP inhibitors. These effects could result from indirect binding of T8 to the Bir2 or Bir3 domain, e.g. to the XIAP surface close to both domains in such a way which excludes the binding between XIAP and caspase-9 or -3 or which changes the XIAP conformation. It is also possible that XIAP is not the target of T8, but T8 inhibits other proteins upstream of XIAP e.g. the protein kinase Akt. Akt is shown to protect XIAP ubiquitination [133]. If Akt is inhibited by T8, XIAP can be degraded in the proteasome. To verify these hypotheses additional experiments with full length XIAP have to be performed.

2.7 T8 reduces NF-κB activation

XIAP is involved in the modulation of diverse signaling pathways such as cell motility or copper homeostasis [51, 52]. The XIAP-NF-κB pathways connection was discovered in the late '90s in endothelial cells [76], but only recently the detailed mode of NF-κB activation through XIAP has been elucidated [67]. It involves the Bir1 domain dimerization and its interaction with TAB1. Smac/DIABLO can negatively affect the NF-κB activation by interaction with the Bir2 and the Bir3 domains. According to these facts we were interested in the impact of T8 on NF-κB activation. In this work we present that in fact T8 negatively regulates this pathway. It was shown that inhibition of NF-κB sensitized carcinoma cells to apoptosis induced by etoposide, doxorubicin or TRAIL [134, 135]. We could also observe sensitizing effects of T8 in combination with etoposide, doxorubicin or TRAIL, which suggests a connection between XIAP - NF-κB pathways. Although smac/DIABLO does not directly interact with Bir1, it antagonizes Bir1/TAB1 interaction by steric exclusion. T8 could act in a similar way and hinder Bir1/TAB1 complex formation. NF-κB inhibition might be a mechanism responsible for the sensitizing effects of T8 treatment. Up to now this is highly speculative and has to be confirmed in future experiments.

2.8 Concluding remarks and future directions

T8 was chosen from the hit entities of a pharmacophore-based virtual screening as a promising new agent to overcome the XIAP caused chemoresistance of cancer cells. In cellular assays, T8 induces significant enhancement of apoptosis in combination with cytotoxic drugs such as etoposide, doxorubicin or TRAIL. The triggered cell death is caspase dependent with caspase-9 which activates the effector caspase-3 and the cleavage of DNA repair enzyme PARP playing a major role. T8 also inhibits NF-κB activation which might be a result of Bir1/TAB1 complex disruption. Moreover, T8 does not show any toxic effects on healthy HUVEC cells.

The hypothesis of T8 to be a compound that binds to the Bir3 domain could not be supported by fluorescence polarization assays and NMR analysis.

Three major questions remain to be answered and require further studies:

(i)   What is the cellular target of T8? Is it XIAP or do other proteins play a pivotal role? To what extent does NF-κB inhibition contribute to the sensitizing effects of T8?

(ii)   Which upstream proteins lead to the activation of caspases?

(iii)   Are the *in vitro* effects of T8 also relevant *in vivo*?

Up to now we can say that T8 is a promising new agent to overcome XIAP caused chemoresistance in combination with other cytotoxic drugs. Furthermore T8 is not toxic per se, making it an appropriate agent in multi-drug chemotherapy.

V Summary

This work presents two new agents: spongistatin 1 and T8 as potent compounds to overcome XIAP caused chemoresistance in different cancer cells.

SPONGISTATIN 1

The natural marine compound spongistatin 1 is a potent new agent to induce cell death in primary tumor cells of children suffering from acute leukemia. It is even more potent as 8 out of 10 clinically applied cytotoxic drugs. Most importantly, it shows selectivity towards cancer cells since it does not affect healthy mononuclear blood cells.

Based on the presented data we propose the mechanism of spongistatin 1 induced cell death as illustrated in Figure V.1. Spongistatin 1 induces caspase-9 dependent cell death which involves the release of cytochrome c, smac/DIABLO and Omi/HtrA2 from mitochondria. Overexpression of Bcl-2 or Bcl-xl saves leukemia cells from spongistatin 1 induced apoptosis. Moreover, spongistatin 1 proves beneficial to overcome the XIAP related chemoresistance in leukemia cancers and is a promising new agent for the treatment of cancer cells in combination with other cytotoxic drugs.
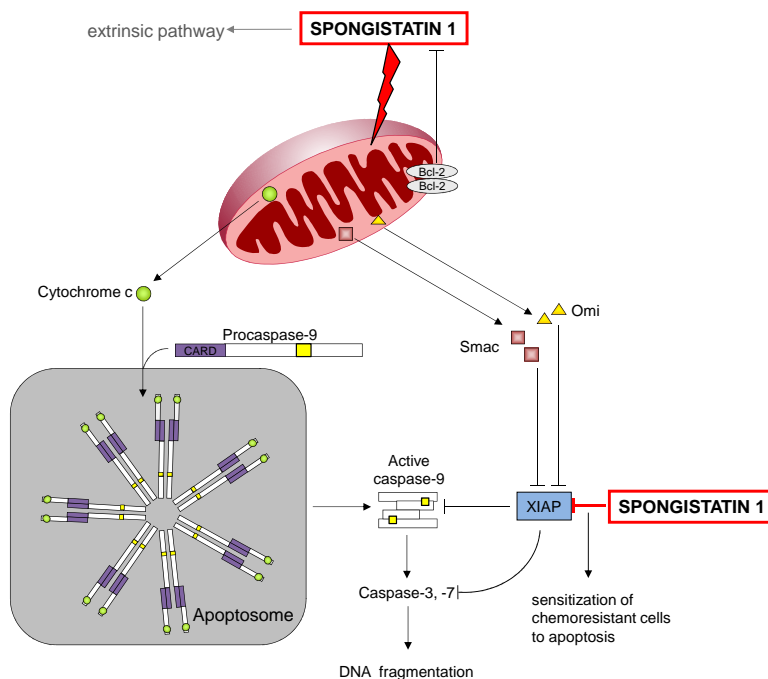
Figure V.1 Proposed mechanism of spongistatin 1-induced apoptosis

T8 AS A XIAP INHIBITOR

T8 is a synthetic compound found by virtual screening for XIAP-Bir3 inhibitors. Indeed T8 is able to restore the ability of etoposide to induce apoptosis in XIAP and Bir3/RING overexpressing chemoresistant Jurkat T cells. As shown in Figure V.2 T8 enhances etoposide-mediated caspase activation. T8 activity is not limited to leukemia cells, this chemosensitizing agent is also active in breast, prostate and pancreas cancer cells in combination with etoposide, doxorubicin or TRAIL.

Although T8 shows benefits in XIAP overexpressing cancer cells, neither Bir2 nor Bir3 seem to be a main direct targets of T8. Interestingly, T8 is able to suppress NF-κB activation, a process connected to the Bir1 domain of XIAP. Further studies will elucidate molecular targets responsible for T8 biological activity.
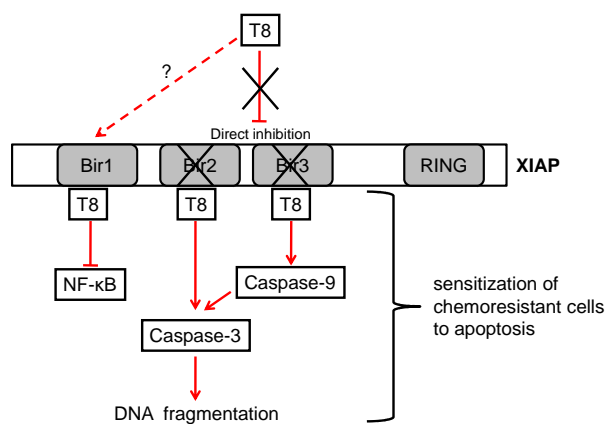
Figure V.2 Schematic illustration of T8 mode of action

VI References

1. WHO. *The global burden of disease: 2004 update* 2004; Available from: http://www.who.int/healthinfo/global_burden_disease/2004_report_update/en/index.html.

2. Dy, G.K. and A.A. Adjei, *Systemic cancer therapy: evolution over the last 60 years.* Cancer, 2008. **113**(7 Suppl): p. 1857-1887.

3. Newman, D.J. and G.M. Cragg, *Natural products as sources of new drugs over the last 25 years.* J.Nat.Prod., 2007. **70**(3): p. 461-477.

4. Shoemaker, R.H., *The NCI60 human tumour cell line anticancer drug screen.* Nat.Rev.Cancer, 2006. **6**(10): p. 813-823.

5. Nikolovska-Coleska, Z., et al., *Discovery of embelin as a cell-permeable, small-molecular weight inhibitor of XIAP through structure-based computational screening of a traditional herbal medicine three-dimensional structure database.* J.Med.Chem., 2004. **47**(10): p. 2430-2440.

6. Rollinger, J.M., et al., *Discovering COX-inhibiting constituents of Morus root bark: activity-guided versus computer-aided methods.* Planta Med, 2005. **71**(5): p. 399-405.

7. Symonds, H., et al., *p53-dependent apoptosis suppresses tumor growth and progression in vivo.* Cell, 1994. **78**(4): p. 703-11.

8. Tamm, I., et al., *Expression and prognostic significance of IAP-family genes in human cancers and myeloid leukemias.* Clin.Cancer Res., 2000. **6**(5): p. 1796-1803.

9. Pettit, G.R., *Isolation and structure of Spongistatin 1.* The Journal of Organic Chemistry, 1993. **58**(6): p. 1302-1304.

10. Kobayashi, M. *Altohyrtin A, a Potent Anti-tumor Macrolide from the Okinawan Marine Sponge Hyrtios altum.* Tetrahedron Letters 1993 1993 [cited 34 17]; 2795-2798].

11. Dafni, J., *http://www.dafni.com/corals/Black%20sponge.jpg>.* 2009.

12. Thoms, C. 2009; Available from: http://www.carsten-thoms.net/sponges/ecology/2_zentr.html.

13. Boyd M. R., P.K.D., *Some practical considerations and applications of the National Cancer Institute in vitro anticancer drug discovery screen.* Drug Development Research, 1995. **34**: p. 91-109.

14. Bai, R., et al., *Spongistatin 1, a highly cytotoxic, sponge-derived, marine natural product that inhibits mitosis, microtubule assembly, and the binding of vinblastine to tubulin.* Mol.Pharmacol., 1993. **44**(4): p. 757-766.

15. Ovechkina, Y.Y., et al., *Unusual antimicrotubule activity of the antifungal agent spongistatin 1.* Antimicrob Agents Chemother, 1999. **43**(8): p. 1993-9.

16. Mohammad, R.M., et al., *Clonal preservation of human pancreatic cell line derived from primary pancreatic adenocarcinoma.* Pancreas, 1999. **19**(4): p. 353-61.

17. Wermuth, C.G., et al., *Glossary of terms used in medicinal chemistry (IUPAC Recommendations 1997).* Annu. Rep. Med. Chem., 1998. **33**: p. 385-395.

18. Rollinger, J.M., T. Langer, and H. Stuppner, *Integrated in silico tools for exploiting the natural products' bioactivity.* Planta Med, 2006. **72**(8): p. 671-8.

19. Berman, H.M., et al., *The Protein Data Bank.* Nucleic Acids Res, 2000. **28**(1): p. 235-42.

20. Wolber, G. and T. Langer, *LigandScout: 3-D pharmacophores derived from protein-bound ligands and their use as virtual screening filters.* J Chem Inf Model, 2005. **45**(1): p. 160-9.

21. Smith, A., *Screening for drug discovery: the leading question.* Nature, 2002. **418**(6896): p. 453-9.

22. Kroemer, G., et al., *Classification of cell death: recommendations of the Nomenclature Committee on Cell Death 2009.* Cell Death.Differ., 2008.

VI References

23. Fadeel, B. and S. Orrenius, *Apoptosis: a basic biological phenomenon with wide-ranging implications in human disease.* J.Intern.Med., 2005. **258**(6): p. 479-517.
24. Thornberry, N.A., et al., *A novel heterodimeric cysteine protease is required for interleukin-1 beta processing in monocytes.* Nature, 1992. **356**(6372): p. 768-774.
25. Cerretti, D.P., et al., *Molecular cloning of the interleukin-1 beta converting enzyme.* Science, 1992. **256**(5053): p. 97-100.
26. Yuan, J., et al., *The C. elegans cell death gene ced-3 encodes a protein similar to mammalian interleukin-1 beta-converting enzyme.* Cell, 1993. **75**(4): p. 641-652.
27. Shi, Y., *Mechanisms of caspase activation and inhibition during apoptosis.* Mol.Cell, 2002. **9**(3): p. 459-470.
28. Salvesen, G.S. and V.M. Dixit, *Caspase activation: the induced-proximity model.* Proc.Natl.Acad.Sci.U.S.A, 1999. **96**(20): p. 10964-10967.
29. Bao, Q. and Y. Shi, *Apoptosome: a platform for the activation of initiator caspases.* Cell Death.Differ., 2007. **14**(1): p. 56-65.
30. Srinivasula, S.M., et al., *Autoactivation of procaspase-9 by Apaf-1-mediated oligomerization.* Mol.Cell, 1998. **1**(7): p. 949-957.
31. Chao, Y., et al., *Engineering a dimeric caspase-9: a re-evaluation of the induced proximity model for caspase activation.* PLoS.Biol., 2005. **3**(6): p. e183.
32. Timmer, J.C. and G.S. Salvesen, *Caspase substrates.* Cell Death.Differ., 2007. **14**(1): p. 66-72.
33. Fischer, U., R.U. Janicke, and K. Schulze-Osthoff, *Many cuts to ruin: a comprehensive update of caspase substrates.* Cell Death.Differ., 2003. **10**(1): p. 76-100.
34. Gross, A., et al., *Caspase cleaved BID targets mitochondria and is required for cytochrome c release, while BCL-XL prevents this release but not tumor necrosis factor-R1/Fas death.* J.Biol.Chem., 1999. **274**(2): p. 1156-1163.
35. Schreiber, V., et al., *Poly(ADP-ribose): novel functions for an old molecule.* Nat.Rev.Mol.Cell Biol., 2006. **7**(7): p. 517-528.
36. Walczak, H. and P.H. Krammer, *The CD95 (APO-1/Fas) and the TRAIL (APO-2L) apoptosis systems.* Exp.Cell Res., 2000. **256**(1): p. 58-66.
37. Fulda, S. and K.M. Debatin, *Signaling through death receptors in cancer therapy.* Curr.Opin.Pharmacol., 2004. **4**(4): p. 327-332.
38. Reed, J.C., *Proapoptotic multidomain Bcl-2/Bax-family proteins: mechanisms, physiological roles, and therapeutic opportunities.* Cell Death.Differ., 2006. **13**(8): p. 1378-1386.
39. Martinou, J.C. and D.R. Green, *Breaking the mitochondrial barrier.* Nat.Rev.Mol.Cell Biol., 2001. **2**(1): p. 63-67.
40. Saelens, X., et al., *Toxic proteins released from mitochondria in cell death.* Oncogene, 2004. **23**(16): p. 2861-2874.
41. Susin, S.A., et al., *Molecular characterization of mitochondrial apoptosis-inducing factor.* Nature, 1999. **397**(6718): p. 441-446.
42. Li, L.Y., X. Luo, and X. Wang, *Endonuclease G is an apoptotic DNase when released from mitochondria.* Nature, 2001. **412**(6842): p. 95-99.
43. Goodford, P.J., *A computational procedure for determining energetically favorable binding sites on biologically important macromolecules.* J.Med.Chem., 1985. **28**(7): p. 849-857.
44. Youle, R.J. and A. Strasser, *The BCL-2 protein family: opposing activities that mediate cell death.* Nat Rev Mol Cell Biol, 2008. **9**(1): p. 47-59.
45. Crook, N.E., R.J. Clem, and L.K. Miller, *An apoptosis-inhibiting baculovirus gene with a zinc finger-like motif.* J.Virol., 1993. **67**(4): p. 2168-2174.

VI References

46. Xue, D. and H.R. Horvitz, *Inhibition of the Caenorhabditis elegans cell-death protease CED-3 by a CED-3 cleavage site in baculovirus p35 protein.* Nature, 1995. **377**(6546): p. 248-251.

47. Bump, N.J., et al., *Inhibition of ICE family proteases by baculovirus antiapoptotic protein p35.* Science, 1995. **269**(5232): p. 1885-1888.

48. Roy, N., et al., *The gene for neuronal apoptosis inhibitory protein is partially deleted in individuals with spinal muscular atrophy.* Cell, 1995. **80**(1): p. 167-178.

49. Duckett, C.S., et al., *A conserved family of cellular genes related to the baculovirus iap gene and encoding apoptosis inhibitors.* EMBO J., 1996. **15**(11): p. 2685-2694.

50. Yang, Y., et al., *Ubiquitin protein ligase activity of IAPs and their degradation in proteasomes in response to apoptotic stimuli.* Science, 2000. **288**(5467): p. 874-877.

51. Mufti, A.R., et al., *XIAP Is a copper binding protein deregulated in Wilson's disease and other copper toxicosis disorders.* Mol Cell, 2006. **21**(6): p. 775-85.

52. Dogan, T., et al., *X-linked and cellular IAPs modulate the stability of C-RAF kinase and cell motility.* Nat Cell Biol, 2008. **10**(12): p. 1447-55.

53. Knauer, S.K., W. Mann, and R.H. Stauber, *Survivin's dual role: an export's view.* Cell Cycle, 2007. **6**(5): p. 518-21.

54. Srinivasula, S.M. and J.D. Ashwell, *IAPs: what's in a name?* Mol.Cell, 2008. **30**(2): p. 123-135.

55. Shin, S., et al., *An anti-apoptotic protein human survivin is a direct inhibitor of caspase-3 and -7.* Biochemistry, 2001. **40**(4): p. 1117-1123.

56. Ekert, P.G., J. Silke, and D.L. Vaux, *Caspase inhibitors.* Cell Death.Differ., 1999. **6**(11): p. 1081-1086.

57. Maier, J.K., et al., *The neuronal apoptosis inhibitory protein is a direct inhibitor of caspases 3 and 7.* J.Neurosci., 2002. **22**(6): p. 2035-2043.

58. Kasof, G.M. and B.C. Gomes, *Livin, a novel inhibitor of apoptosis protein family member.* J.Biol.Chem., 2001. **276**(5): p. 3238-3246.

59. Lagace, M., et al., *Genomic organization of the X-linked inhibitor of apoptosis and identification of a novel testis-specific transcript.* Genomics, 2001. **77**(3): p. 181-188.

60. Bartke, T., et al., *Dual role of BRUCE as an antiapoptotic IAP and a chimeric E2/E3 ubiquitin ligase.* Mol.Cell, 2004. **14**(6): p. 801-811.

61. Deveraux, Q.L., et al., *X-linked IAP is a direct inhibitor of cell-death proteases.* Nature, 1997. **388**(6639): p. 300-4.

62. Chai, J., et al., *Structural basis of caspase-7 inhibition by XIAP.* Cell, 2001. **104**(5): p. 769-80.

63. Shiozaki, E.N., et al., *Mechanism of XIAP-mediated inhibition of caspase-9.* Mol.Cell, 2003. **11**(2): p. 519-527.

64. Sun, C., et al., *NMR structure and mutagenesis of the inhibitor-of-apoptosis protein XIAP.* Nature, 1999. **401**(6755): p. 818-822.

65. Sun, C., et al., *NMR structure and mutagenesis of the third Bir domain of the inhibitor of apoptosis protein XIAP.* J Biol Chem, 2000. **275**(43): p. 33777-81.

66. Shin, H., et al., *Identification of ubiquitination sites on the X-linked inhibitor of apoptosis protein.* Biochem J, 2003. **373**(Pt 3): p. 965-71.

67. Lu, M., et al., *XIAP induces NF-kappaB activation via the BIR1/TAB1 interaction and BIR1 dimerization.* Mol Cell, 2007. **26**(5): p. 689-702.

68. Chai, J., et al., *Structural and biochemical basis of apoptotic activation by Smac/DIABLO.* Nature, 2000. **406**(6798): p. 855-62.

69. Martins, L.M., et al., *The serine protease Omi/HtrA2 regulates apoptosis by binding XIAP through a reaper-like motif.* J Biol Chem, 2002. **277**(1): p. 439-44.

VI References

70. Srinivasula, S.M., et al., *Inhibitor of apoptosis proteins are substrates for the mitochondrial serine protease Omi/HtrA2.* J Biol Chem, 2003. **278**(34): p. 31469-72.
71. Liston, P., et al., *Identification of XAF1 as an antagonist of XIAP anti-Caspase activity.* Nat Cell Biol, 2001. **3**(2): p. 128-33.
72. Kobayashi, S., et al., *Calpain-mediated X-linked inhibitor of apoptosis degradation in neutrophil apoptosis and its impairment in chronic neutrophilic leukemia.* J.Biol.Chem., 2002. **277**(37): p. 33968-33977.
73. Deveraux, Q.L., et al., *Cleavage of human inhibitor of apoptosis protein XIAP results in fragments with distinct specificities for caspases.* EMBO J., 1999. **18**(19): p. 5242-5251.
74. Lewis, S.M. and M. Holcik, *For IRES trans-acting factors, it is all about location.* Oncogene, 2008. **27**(8): p. 1033-5.
75. Harlin, H., et al., *Characterization of XIAP-deficient mice.* Mol Cell Biol, 2001. **21**(10): p. 3604-8.
76. Hofer-Warbinek, R., et al., *Activation of NF-kappa B by XIAP, the X chromosome-linked inhibitor of apoptosis, in endothelial cells involves TAK1.* J Biol Chem, 2000. **275**(29): p. 22064-8.
77. Winsauer, G., et al., *XIAP regulates bi-phasic NF-kappaB induction involving physical interaction and ubiquitination of MEKK2.* Cell Signal, 2008. **20**(11): p. 2107-12.
78. Srinivasula, S.M., et al., *A conserved XIAP-interaction motif in caspase-9 and Smac/DIABLO regulates caspase activity and apoptosis.* Nature, 2001. **410**(6824): p. 112-6.
79. Suzuki, Y., Y. Nakabayashi, and R. Takahashi, *Ubiquitin-protein ligase activity of X-linked inhibitor of apoptosis protein promotes proteasomal degradation of caspase-3 and enhances its anti-apoptotic effect in Fas-induced cell death.* Proc Natl Acad Sci U S A, 2001. **98**(15): p. 8662-7.
80. MacFarlane, M., et al., *Proteasome-mediated degradation of Smac during apoptosis: XIAP promotes Smac ubiquitination in vitro.* J Biol Chem, 2002. **277**(39): p. 36611-6.
81. Oost, T.K., et al., *Discovery of potent antagonists of the antiapoptotic protein XIAP for the treatment of cancer.* J.Med.Chem., 2004. **47**(18): p. 4417-4426.
82. Kipp, R.A., et al., *Molecular targeting of inhibitor of apoptosis proteins based on small molecule mimics of natural binding partners.* Biochemistry, 2002. **41**(23): p. 7344-7349.
83. Park, C.M., et al., *Non-peptidic small molecule inhibitors of XIAP.* Bioorg.Med.Chem.Lett., 2005. **15**(3): p. 771-775.
84. Ortuso, F., T. Langer, and S. Alcaro, *GBPM: GRID-based pharmacophore model: concept and application studies to protein-protein recognition.* Bioinformatics., 2006. **22**(12): p. 1449-1455.
85. Peter, M.E., et al., *APO-1 (CD95)-dependent and -independent antigen receptor-induced apoptosis in human T and B cell lines.* Int.Immunol., 1995. **7**(11): p. 1873-1877.
86. Sprick, M.R., et al., *FADD/MORT1 and caspase-8 are recruited to TRAIL receptors 1 and 2 and are essential for apoptosis mediated by TRAIL receptor 2.* Immunity., 2000. **12**(6): p. 599-609.
87. Vogler, M., et al., *Regulation of TRAIL-induced apoptosis by XIAP in pancreatic carcinoma cells.* Oncogene, 2007. **26**(2): p. 248-257.
88. Bruns, C.J., et al., *In vivo selection and characterization of metastatic variants from human pancreatic adenocarcinoma by using orthotopic implantation in nude mice.* Neoplasia., 1999. **1**(1): p. 50-62.

89. Marin, V., et al., *Endothelial cell culture: protocol to obtain and cultivate human umbilical endothelial cells.* J.Immunol.Methods, 2001. **254**(1-2): p. 183-190.

90. Mosmann, T., *Rapid colorimetric assay for cellular growth and survival: application to proliferation and cytotoxicity assays.* J Immunol Methods, 1983. **65**(1-2): p. 55-63.

91. Available from: http://www.cyto.purdue.edu/class/e-lectures/jpr1/jpr1.html.

92. Nicoletti, I., et al., *A rapid and simple method for measuring thymocyte apoptosis by propidium iodide staining and flow cytometry.* J Immunol Methods, 1991. **139**(2): p. 271-9.

93. Bradford, M.M., *A rapid and sensitive method for the quantitation of microgram quantities of protein utilizing the principle of protein-dye binding.* Anal Biochem, 1976. **72**: p. 248-54.

94. Laemmli, U.K., *Cleavage of structural proteins during the assembly of the head of bacteriophage T4.* Nature, 1970. **227**(5259): p. 680-5.

95. Owicki, J.C., *Fluorescence polarization and anisotropy in high throughput screening: perspectives and primer.* J.Biomol.Screen., 2000. **5**(5): p. 297-306.

96. Schust, J. and T. Berg, *A high-throughput fluorescence polarization assay for signal transducer and activator of transcription 3.* Anal.Biochem., 2004. **330**(1): p. 114-118.

97. Nikolovska-Coleska, Z., et al., *Development and optimization of a binding assay for the XIAP BIR3 domain using fluorescence polarization.* Anal Biochem, 2004. **332**(2): p. 261-73.

98. Cai, M., et al., *An efficient and cost-effective isotope labeling protocol for proteins expressed in Escherichia coli.* J Biomol NMR, 1998. **11**(1): p. 97-102.

99. Webb, J.L., ed. *Effect of more than one inhibitor, antagonism, summation, and synergism.* Enzyme and Metabolic Inhibitors. Vol. 1. 1963, Academic Press: New York. 488-512.

100. Nakagawa, Y., et al., *IAP family protein expression correlates with poor outcome of multiple myeloma patients in association with chemotherapy-induced overexpression of multidrug resistance genes.* Am J Hematol, 2006. **81**(11): p. 824-31.

101. Li, J., et al., *Human ovarian cancer and cisplatin resistance: possible role of inhibitor of apoptosis proteins.* Endocrinology, 2001. **142**(1): p. 370-80.

102. Dancey, J.E. and H.X. Chen, *Strategies for optimizing combinations of molecularly targeted anticancer agents.* Nat Rev Drug Discov, 2006. **5**(8): p. 649-59.

103. Vogler, M., et al., *Targeting XIAP bypasses Bcl-2-mediated resistance to TRAIL and cooperates with TRAIL to suppress pancreatic cancer growth in vitro and in vivo.* Cancer Res, 2008. **68**(19): p. 7956-65.

104. Ziegler, D.S., et al., *Resistance of human glioblastoma multiforme cells to growth factor inhibitors is overcome by blockade of inhibitor of apoptosis proteins.* J Clin Invest, 2008. **118**(9): p. 3109-22.

105. Fulda, S., et al., *Smac agonists sensitize for Apo2L/TRAIL- or anticancer drug-induced apoptosis and induce regression of malignant glioma in vivo.* Nat Med, 2002. **8**(8): p. 808-15.

106. Newman, D.J. and G.M. Cragg, *Marine natural products and related compounds in clinical and advanced preclinical trials.* J Nat Prod, 2004. **67**(8): p. 1216-38.

107. Kantarjian, H., et al., *Therapeutic advances in leukemia and myelodysplastic syndrome over the past 40 years.* Cancer, 2008. **113**(7 Suppl): p. 1933-52.

108. Paterson, I., et al., *The stereocontrolled total synthesis of altohyrtin A/spongistatin 1: fragment couplings, completion of the synthesis, analogue generation and biological evaluation.* Org Biomol Chem, 2005. **3**(13): p. 2431-40.

109. Fulda, S. and K.M. Debatin, *Modulation of apoptosis signaling for cancer therapy.* Arch.Immunol.Ther.Exp.(Warsz.), 2006. **54**(3): p. 173-175.

VI References

110. Huang, Y., et al., *Structural basis of caspase inhibition by XIAP: differential roles of the linker versus the BIR domain.* Cell, 2001. **104**(5): p. 781-790.

111. Shi, Y., *Caspase activation, inhibition, and reactivation: a mechanistic view.* Protein Sci, 2004. **13**(8): p. 1979-87.

112. Krajewska, M., et al., *Elevated expression of inhibitor of apoptosis proteins in prostate cancer.* Clin.Cancer Res., 2003. **9**(13): p. 4914-4925.

113. Ferreira, C.G., et al., *Expression of X-linked inhibitor of apoptosis as a novel prognostic marker in radically resected non-small cell lung cancer patients.* Clin.Cancer Res., 2001. **7**(8): p. 2468-2474.

114. Schimmer, A.D., et al., *Small-molecule antagonists of apoptosis suppressor XIAP exhibit broad antitumor activity.* Cancer Cell, 2004. **5**(1): p. 25-35.

115. Martins, L.M., *The serine protease Omi/HtrA2: a second mammalian protein with a Reaper-like function.* Cell Death Differ, 2002. **9**(7): p. 699-701.

116. LaCasse, E.C., et al., *Preclinical characterization of AEG35156/GEM 640, a second-generation antisense oligonucleotide targeting X-linked inhibitor of apoptosis.* Clin Cancer Res, 2006. **12**(17): p. 5231-41.

117. Wilkinson, J.C., et al., *Upstream regulatory role for XIAP in receptor-mediated apoptosis.* Mol.Cell Biol., 2004. **24**(16): p. 7003-7014.

118. McManus, D.C., et al., *Loss of XIAP protein expression by RNAi and antisense approaches sensitizes cancer cells to functionally diverse chemotherapeutics.* Oncogene, 2004. **23**(49): p. 8105-8117.

119. Cillessen, S.A., et al., *Inhibition of the intrinsic apoptosis pathway downstream of caspase-9 activation causes chemotherapy resistance in diffuse large B-cell lymphoma.* Clin Cancer Res, 2007. **13**(23): p. 7012-21.

120. Cillessen, S.A., et al., *Small-molecule XIAP antagonist restores caspase-9 mediated apoptosis in XIAP-positive diffuse large B-cell lymphoma cells.* Blood, 2008. **111**(1): p. 369-75.

121. Stepczynska, A., et al., *Staurosporine and conventional anticancer drugs induce overlapping, yet distinct pathways of apoptosis and caspase activation.* Oncogene, 2001. **20**(10): p. 1193-202.

122. Lacasse, E.C., et al., *Application of XIAP antisense to cancer and other proliferative disorders: development of AEG35156/ GEM640.* Ann.N.Y.Acad.Sci., 2005. **1058**: p. 215-234.

123. Schimmer, A.D., et al., *Targeting XIAP for the treatment of malignancy.* Cell Death.Differ., 2006. **13**(2): p. 179-188.

124. Giagkousiklidis, S., et al., *Sensitization of pancreatic carcinoma cells for gamma-irradiation-induced apoptosis by XIAP inhibition.* Oncogene, 2007.

125. Li, L., et al., *A small molecule Smac mimic potentiates T.* Science, 2004. **305**(5689): p. 1471-1474.

126. Bilim, V., et al., *Role of XIAP in the malignant phenotype of transitional cell cancer (TCC) and therapeutic activity of XIAP antisense oligonucleotides against multidrug-resistant TCC in vitro.* Int J Cancer, 2003. **103**(1): p. 29-37.

127. Gagnon, V., et al., *Akt and XIAP regulate the sensitivity of human uterine cancer cells to cisplatin, doxorubicin and taxol.* Apoptosis, 2008. **13**(2): p. 259-71.

128. Nomura, T., et al., *The X-linked inhibitor of apoptosis protein inhibits taxol-induced apoptosis in LNCaP cells.* Urol Res, 2003. **31**(1): p. 37-44.

129. Lopes, R.B., et al., *Expression of the IAP protein family is dysregulated in pancreatic cancer cells and is important for resistance to chemotherapy.* Int J Cancer, 2007. **120**(11): p. 2344-52.

VI References

130. Karikari, C.A., et al., *Targeting the apoptotic machinery in pancreatic cancers using small-molecule antagonists of the X-linked inhibitor of apoptosis protein.* Mol Cancer Ther, 2007. **6**(3): p. 957-66.

131. Bockbrader, K.M., M. Tan, and Y. Sun, *A small molecule Smac-mimic compound induces apoptosis and sensitizes TRAIL- and etoposide-induced apoptosis in breast cancer cells.* Oncogene, 2005. **24**(49): p. 7381-8.

132. Shah, G.M., R.G. Shah, and G.G. Poirier, *Different cleavage pattern for poly(ADP-ribose) polymerase during necrosis and apoptosis in HL-60 cells.* Biochem Biophys Res Commun, 1996. **229**(3): p. 838-44.

133. Dan, H.C., et al., *Akt phosphorylation and stabilization of X-linked inhibitor of apoptosis protein (XIAP).* J Biol Chem, 2004. **279**(7): p. 5405-12.

134. Arlt, A., et al., *Inhibition of NF-kappaB sensitizes human pancreatic carcinoma cells to apoptosis induced by etoposide (VP16) or doxorubicin.* Oncogene, 2001. **20**(7): p. 859-68.

135. Jeremias, I., et al., *Inhibition of nuclear factor kappaB activation attenuates apoptosis resistance in lymphoid cells.* Blood, 1998. **91**(12): p. 4624-31.

VII Appendix

1 Abbreviations

AIF   Apoptosis inducing factor

ANOVA   Analysis of variance between groups

Apaf-1   Apoptotic protease-activating factor-1

APS   Ammonium persulfate

ATP/dATP   Adenosine-5´-triphosphate/2´-desoxyadenosine-5´-triphosphate

Bcl   B-cell lymphoma

BH   Bcl-2 homology

BIR   Baculoviral IAP repeats

BSA   Bovine serum albumin

CAD   Caspase-activated DNase

CARD   Caspase recruitment domain

CED   Cell death abnormality

cIAP   Cellular inhibitor of apoptosis

CPRG   Chlorophenol Red-β-D-galactoside

DD   Death domain

DED   Death effector domain

DIABLO   Direct IAP binding protein with low pI

DISC   Death inducing signaling complex

DMSO   Dimethyl sulfoxide

DNA   Deoxyribonucleic acid

DR   Death receptor

DTT   Dithiothreitol

ECL   Enhanced chemoluminescence

EDTA   Ethylene diamintetraacetic acid

EGTA   Ethylene glycol-bis(2-aminoethylether) tetraacetic acid

EndoG   Endonuclease G

ER   Endoplasmic reticulum

FACS	Fluorescence activated cell sorter
FADD	Fas-associated death domain
FasL	Fas ligand
FCS	Fetal calf serum
FL	Fluorescence
FP	Fluorescence polarization
GI	Growth inhibition
HEK	Human embryonic kidney
HEPES	N-(2-hydroxyethyl)piperazine-N'-(2-ethanesulfonic acid)
HFS	Hypotonic fluorochrome solution
HRP	Heteronuclear single quantum coherence spectroscopy
HSQC	Heteronuclear single quantum coherence spectroscopy
HtrA2	High temperature requirement protein A2
HUVEC	Human umbilical vein cell
IAP	Inhibitor of apoptosis protein
IBM	IAP-binding motif
ICE	Interleukin-1β converting enzyme
IL	Interleukin
IMM	Inner mitochondrial membrane
IRES	Internal ribosome entry site
JNK	c-Jun N-terminal kinase
kDa	Kilo Dalton
k_i	Inhibitory constant
LB	Lennox L Broth Base
LRR	leucine-rich repeats
ML-IAP	melanoma IAP
MMP	Mitochondrial membrane permeabilization
MMP-9	Matrix metalloproteinase 9
mRNA	Messenger RNA
MTT	3-(4,5-dimethylthiazol-2-yl)-2,5-diphenyl tetrazolium bromide
NAIP	Neuronal apoptosis inhibitory protein
NCCD	Nomenclature Committee on Cell Death

NCI	National Cancer Institute
NF-κB	Nuclear Factor-κB
NMR	Nuclear magnetic resonance
NOD	nucleotide-binding oligomerization domain
OMM	Outer mitochondrial membrane
PAA	Polyacrylamide
PARP	Poly(ADP-ribose) polymerase
PBS	Phosphate buffered saline
PCD	Programmed cell death
PDB	Protein Data Bank
PDTC	Pyrrolidine dithiocarbamate
PI	Propidium iodide
PIDD	p53 inducible protein with a death domain
PMSF	Phenylmethylsulphonylfluoride
ppm	parts per milion
PS	Phosphatidylserine
RING	Really interesting new gene
ROS	Reactive oxygen species
RT	Room temperature
SDS	Sodium dodecyl sulfate
SDS-PAGE	Sodium dodecyl sulfate polyacrylamide gel electrophoresis
SE	Standard error
SEM	Standard error mean
shRNA	short-hairpin RNA
Smac	Second mitochondria derived activator of caspases
SSC	Sideward scatter
TAB1	TAK 1-binding protein 1
TAK1	TGF-β-activated kinase 1
TBS-T	Tris buffered saline with tween
TEMED	N, N, N' N' tetramethylethylene diamine
TG	Transglutaminase
TNF	Tumor necrosis factor

TNF-R1	TNF receptor 1
TRAIL	TNF-related apoptosis inducing ligand
UBC	ubiquitin-conjugation
VDAC	Voltage dependent anion channel
WB	Western blot
XAF1	XIAP associated factor 1
XIAP	X-chromosome linked IAP
zVADfmk	N-benzyloxycarbonyl-Val-Ala-Asp(OMe)-fluoromethylketone
ΔΨ$_m$	Mitochondrial transmembrane potential

TNF-R1   TNF receptor 1

TRAIL   TNF-related apoptosis inducing ligand

2 Alphabetical list of companies

Abbott Laboratories	Abbott Park, Illinois, USA
Agfa	Cologne, Germany
Alexis	Grünberg, Germany
Amaxa	Cologne, Germany
Ambion	Hamburg, Germany
Amersham Bioscience	Freiburg, Germany
Amersham Pharmacia Biotech	Uppsala, Sweden
Applichem	Darmstadt, Germany
Applied Biosystems	Foster City, CA, USA
Assinex Ltd.	Moscow, Russland
Axxora Deutschland GmbH	Lörrach, Germany
Bachem	Bubendorf, Germany
BD Biosciences	Heidelberg, Germany
BD PharMingen	Heidelberg, Germany
Beckman Coulter	Krefeld, Germany
Becton Dickinson	Heidelberg, Germany
Berthols detection Systems	Pforzheim, Germany
Biochrom AG	Berlin, Germany
Biomol	Hamburg, Germany
BioRad	Munich, Germany
Biotrend Chemikalien GmbH	Cologne, Germany
Biozol	Eching, Germany
Calbiochem	Schwalbach, Germany
Canon	Krefeld, Germany
Cayman Chemical	Ann Arbor, USA
Cell Signaling	Frankfurt, Germany
Clontech	Mountain View, USA
Dharmacon	Lafayette, CO, USA
Dianova	Hamburg, Germany
Fuji	Düsseldorf, Germany

Gerhard	Königswinter, Germany
Gibco/Invitrogen	Karlsruhe, Germany
Immunotech	Marseille, France
Invitrogen	Karlsruhe, Germany
Kodak	Rochester, USA
Li-COR Biosciences GmbH	Bad Homburg, Germany
MBI-Fermentas	St. Leon-Rot, Germany
Merck Biosciences	Darmstadt, Germany
Millipore	Schwalbach, Germany
Molecular Probes/Invitrogen	Karlsruhe, Germany
Novagen	Darmstad, Germany
Olympus Optical	Hamburg, Germany
PAA Laboratories	Cölbe, Germany
PAN Biotech	Aidenbach, Germany
Peqlab Biotechnologie GmbH	Erlangen, Germany
Perkin Elmer	Überlingen, Germany
Peske	Aindling-Arnhofen, Germany
Promega	Mannheim, Germany
Promocell	Heidelberg, Germany
R&D Systems	Minneapolis, USA
Roche	Mannheim, Germany
Roth GmbH	Karlsruhe, Germany
Santa Cruz	Heidelberg, Germany
SERVA Electrophoresis GmbH	Heidelberg, Germany
Sigma-Aldrich	Taufkirchen, Germany
StemCell Technologien Inc.	Vancouver, Canada
Stratagene	La Jolla, USA
Tecan	Crailsheim, Germany
TILL Photonics	Gräfelfing, Germany
TPP	Trasadingen, Switzerland
Upstate	Lake Placid, NY, USA
Zeiss	Oberkochen, Germany

3 Publications

ORIGINAL PUBLICATIONS:

L Schyschka, A Rudy, I Jeremias, N Barth, GR Pettit and AM Vollmar. Spongistatin 1: a new chemosensitizing marine compound that degrades XIAP. Leukemia 2008 Sep; 22(9):1737-45

L Schyschka, A Rudy, J Rollinger, H Stuppner, KT Wanner, M Gräber, T Berg, A Frieberg, M Sattler, AM Vollmar. T8, new chemosensitizing agent for the cancer treatment. *In preparation.*

POSTERS:

Schyschka, L., Barth, N., Bliem, C., Stuppner, H., Vollmar, A.M.(2006): Search by virtual screening techniques for XIAP inhibitors which target BIR3 domain. Poster presentation (01.10.2006) at the 14th Euroconference on Apoptosis in Chia, Sardinia, Italy.

Schyschka, L., Rudy, A., Stuppner, H., Vollmar, A.M. (2007): Characterization of novel non-peptidic inhibitors of the anti apoptotic target Bir3. Poster presentation (11.10.2007), Jahrestagung der DPHG in Erlangen, Deutschland.

Schyschka, L., Pfisterer, P.H., Stuppner, H., Vollmar, A.M. (2007): Characterization of novel inhibitors of the apoptosis regulating target XIAP-BIR3. Poster presentation (07.12.2007) at the 1st Life-Science PhD Symposium in Munich, Germany.

U. M. Schneiders, L. Schyschka, N. Barth, A. M. Vollmar. Characterisation of apoptosis signal transduction induced by spongistatin 1 in MCF-7 cells. 48th Spring Meeting of the Deutsche Gesellschaft für experimentelle und klinische Pharmakologie und Toxikologie, March 13-15, 2006, Mainz, Germany. Naunyn-Schmiedeberg's Archieve of Pharmacology, Vol. 375

Bliem, C.B., Schyschka, L., Rollinger, J.M., Langer, T., Vollmar, A.M., Stuppner, H. (2006): Pharmacophore modelling on the apoptosis regulating target XIAP-Bir3. Poster presentation at the 54th Annual Congress on Medicinal Plant Research, August 29th to September 2nd 2006 in Helsinki, Finland. Abstract: Bliem, C.B. et al. (2006) Planta Med 72, P084, 1008.

Pfisterer, P.H., Rollinger, J.M., Schyschka, L., Vollmar, A.M., Stuppner, H. (2008): *In silico* discovery of natural chemosensitizers from *Eriobotrya japonica*. Poster presentation (05.08.2008) at the 7th Joint Meeting of AFERP, ASP, GA, PSE & SIF, August 3rd to 8th 2008 in Athens, Greece. Abstract: Pfisterer, P.H., et al. (2008) Planta Med 74, PG23: 1153.

LECTURES:

Barth, N., Schyschka, L., Rudy, A., López-Antón N., Pettit, G. R. and Vollmar A. M. Spongistatin-1 induces protein degradation of inhibitor of apoptosis and mitochondrial cell death in a CD95/FAS receptor and caspase-8-independent manner in human leukemia Jurkat T cells. 47th Spring Meeting of the Deutsche Gesellschaft für experimentelle und klinische Pharmakologie und Toxikologie, April 4-6, 2006, Mainz, Germany. Naunyn-Schmiedeberg's Archieve of Pharmacology, Vol. 372

VII Appendix

Barth, N., Schyschka, L., Bliem, C., Stuppner, H., and Vollmar A. M. Identification of novel XIAP inhibitors targeting BIR3 by a pharmacophore-based virtual screening. 48th Spring Meeting of the Deutsche Gesellschaft für experimentelle und klinische Pharmakologie und Toxikologie, March 13-15, 2007, Mainz, Germany. Naunyn-Schmiedeberg's Archieve of Pharmacology, Vol. 375

Rudy, A., Schyschka, L., Pfisterer, P., Stuppner, H., and Vollmar AM. T8- a novel inhibitor of the anti-apoptotic protein XIAP. BIOVARIA, Munich, May 08, 2008.

Presenter underlined

4 Curriculum vitae

Personal Data	
Name	Lilianna Schyschka
Date of Birth	September 26th, 1978
Place of Birth	Pyskowice, Poland
Nationality	Polish, German

Academic Education	
01/2005 - 02/2009	Ph.D. Thesis at the Department of Pharmaceutical Biology, LMU Munich, Chair Prof. Dr. A. M. Vollmar
10/1997 - 02/2002	Study of biology at the Silesia University, Diploma

School Education	
9/1993 - 5/1997	Lyzeum, Pyskowice, Poland; Abitur
9/1985 - 5/1993	Primary school, Pyskowice, Poland

Work Experience	
09/2003 - 12/2004	Technician at the Department of Pharmaceutical Biology, LMU Munich, Chair Prof. Dr. A. M. Vollmar
8/2001 – 3/2002	Teacher at the primary school, Katowice, Poland

5 Acknowledgments

First and foremost, I would like to thank Prof. Dr. Angelika M. Vollmar for persuading me to make the Ph.D. study in her laboratory. I am grateful for her support and optimism. Her sentence, "now it is making the whole project much more interesting Mrs. Schyschka", was for me a driving force during the whole time of this work.

Sincere thanks are given to all members of my thesis committee for their time and efforts, especially to Prof. Dr. Frank Böckler for acting as second examiner.

Special thanks go to my fellow workers: Anders Frieberg from Prof. Michael Sattler lab and Martin Gräber and Thorsten Berg from MPI, Martinsried. I have had a great luck to meet you.

I am very thankful group of Prof. Dr. H. Stuppner for virtual screening experiments and group of Prof. Dr. K. T. Wanner for T8 synthesizing. Lots of thanks go to Dr. I. Jeremias for patient probes analyses and the great support with the interpretation of the results and discussion.

Lots of thanks go to the current and former members of my lab for friendly and motivating work atmosphere. Especially I would like to thank Anita for her presence during my whole study as a colleague, supervisor and just friend giving me a great support. I would like to thank also Hanna for her help.

Lots of thanks go to my technical colleagues: Jana, Rita, Mrs. Schnegg, Bianca and Bernadette for their support in experimental work. I have never forgotten where I came from.

Last but not least I would like to thank my family and Krzysiowi for never-ending support and for just being there whenever I needed him.